

Some Approaches to Testing Hypotheses for Multidimensional Stationary Stochastic Processes

DAVID A. SWICK

*Advanced Projects Group
Acoustics Division*

October 2, 1972



NAVAL RESEARCH LABORATORY
Washington, D.C.

Approved for public release; distribution unlimited.

2. ASYMPTOTIC DISTRIBUTION OF THE FINITE FOURIER TRANSFORM OF A ZERO MEAN STATIONARY PROCESS

In this chapter we investigate the asymptotic variances and covariances of discrete finite Fourier transforms (DFT (1.6)) and the bias in the periodogram (1.9) in one and two dimensions. There are no new conceptual problems in considering higher dimensionality; the results can be extended by induction, but the notation required is cumbersome. In anticipation of the tests of hypotheses of later chapters and to clarify the notation, one- and two-dimensional processes will be represented here by $\{n(t), t \in T\}$ and $\{n(x, t), x \in X, t \in T\}$, respectively. Under the null hypothesis of subsequent chapters, the process $\{y(t), t \in T\}$ of Chapter 1, will be the two-dimensional process $\{n(x, t), x \in X, t \in T\}$. Since it will be clear from the context whether the discrete or the continuous transform is intended, the tilde will be dropped from the DFT. The vector λ will be represented by ω in one dimension, and by $(\kappa, \omega)'$ in two dimensions. The letter n in parentheses or as a subscript is an index, and of course not the same as the functions $n(t)$ or $n(x, t)$.

2.1 The One Dimensional Case

Following Shumway [37], we consider a collection $\{n_r(t), t \in T, r = 1, \dots, R\}$ of observations of a zero mean wide-sense stationary time series, where $T = \{0, 1, \dots, N-1\}$. Let the cross correlation functions be represented as

$$\begin{aligned} R_{rr'}(t-t') &= E\{n_r(t)n_{r'}(t')\} \\ &= \delta_{rr'} \frac{1}{2\pi} \int_{-\pi}^{\pi} e^{i\omega(t-t')} f(\omega) d\omega, \end{aligned} \quad (2.1)$$

where the spectral density $f(\omega)$ is a bounded absolutely continuous function. (See (1.1), (1.4), (1.5).) The DFT (1.6) of $n_r(t)$ is given by

$$\epsilon_r(n) = \frac{1}{\sqrt{N}} \sum_{t=0}^{N-1} n_r(t) e^{-i\omega n t}$$

ACKNOWLEDGMENTS

This NRL Report is based on a dissertation submitted to the Graduate School of Arts and Sciences of the George Washington University in partial satisfaction of the requirements for the degree of Doctor of Philosophy, September 30, 1972.

I am sincerely grateful to Prof. Robert Shumway for his guidance and encouragement. To Mr. William Finney of the U.S. Naval Research Laboratory I am deeply indebted for many helpful discussions and continuing support.

TABLE OF CONTENTS

Chapter	Page
ACKNOWLEDGMENTS	i
LIST OF TABLES	v
LIST OF FIGURES	v
ABSTRACT	vii
1 INTRODUCTION AND OUTLINE	1
2 ASYMPTOTIC DISTRIBUTION OF THE FINITE FOURIER TRANSFORM OF A ZERO MEAN STATIONARY PROCESS	6
2.1 The One-Dimensional Case	6
2.2 The Two-Dimensional Case	13
2.3 Lipschitz Conditions and Order of Convergence	19
2.4 The Asymptotic Joint Distribution of Two-Dimensional Periodograms	20
Appendix 2A—Asymptotic Behavior of the Integral of the Modulus of the Dirichlet Kernel	26
Appendix 2B—Numerical Calculations	30
3 APPROXIMATE LIKELIHOOD RATIO TESTS FOR TWO DIMENSIONAL SIGNALS	36
3.1 Signals Common to R Stationary Noise Processes	36
3.2 Plane Wave Signals	39
3.3 Simulated Tests in the Common Signal Case	44
3.4 Signals with Unknown Epochs	50
3.5 Simulated Tests of Signals with Unknown Epochs	55
4 AN AD HOC TEST FOR SIGNALS WITH UNKNOWN EPOCHS	59
4.1 Distribution of the Test Statistic	60
4.2 Simulated Examples	62
5 ANALYSIS OF VARIANCE AND METHODS OF MULTIPLE COMPARISON	68
5.1 The One-Way Layout, Common Signal Case	69
5.2 Robustness of the F-Test	71
5.3 Multiple Comparisons	77
5.4 The Two-Way Layout	81

Chapter		Page
6	SUMMARY AND CONCLUSIONS	82
	GLOSSARY	88
	REFERENCES	90

LIST OF TABLES

Table		Page
3.1	Analysis of Power at Wavenumber κ_m and Frequency ω_n	39
6.1	Comparison of Power of Various Tests	84

LIST OF FIGURES

Figure		Page
2.1	Illustration of $O(1/N)$ Convergence of the Bias due to the Fejér Kernel, $f(Z) = \cos(Z)$	30
2.2	Illustration of $O(1/N)$ Convergence of the Bias due to the Fejér Kernel, $f(Z) = Z\sin Z$	31
2.3	Numerical Integration of the Absolute Value of the Dirichlet Kernel	32
2.4	Numerical Integration of Eq. (2.14) with $f(\omega) = \cos\omega$	33
2.5	Numerical Integration of Eq. (2.14) with $f(\omega) = \omega\sin\omega$	34
2.6	Illustration of $O(1/M) + O(1/N)$ Convergence of the Bias due to the Fejér Kernel in two dimensions	35
3.1	Simulation of Likelihood Ratio Test for Signals Common to R Replications: Results of One Run, White Noise	46
3.2	Simulation of Likelihood Ratio Test for Signals Common to R Replications: Summary of 100 Runs, White Noise	47
3.3	Simulation of Likelihood Ratio Test for Signals Common to R Replications: Results of One Run, Nonwhite Noise	48
3.4	Simulation of Likelihood Ratio Test for Signals Common to R Replications: Summary of 100 Runs, Nonwhite Noise	49
3.5	Simulation of Modified Likelihood Ratio Test: Results of One Run	57
3.6	Simulation of Modified Likelihood Ratio Test: Summary of 100 Runs	58

Figure	Page
4.1 Simulation of Ad Hoc Test: Results of One Run, White Noise	63
4.2 Simulation of Ad Hoc Test: Summary of 100 Runs, White Noise	65
4.3 Simulation of Ad Hoc Test: Results of One Run, Nonwhite Noise	66
4.4 • Simulation of Ad Hoc Test: Summary of 100 Runs, Nonwhite Noise	67
5.1 Empirical Distribution of the Test Statistic with Normal and Chi-square Populations	73
5.2 Power Curves	75
5.3 Power Curves for the case $M=N=2$, $R=4$	76
5.4 Empirical Distribution of the Test Statistic with Normal and Chi-square Populations, Nonwhite Noise	78
5.5 Empirical Distribution of the Test Statistic with Normal and Chi-square Populations, Nonwhite Noise	79

ABSTRACT

The discrete finite Fourier transform of a multidimensional stationary stochastic process transforms a multivariate problem into an asymptotically univariate one. For a one- or two-dimensional process it is shown that, under stated conditions, the correlation between the real and imaginary parts of the transformed variables is

$$\prod_{j=1}^n 0(T_j^{-1}),$$

and that the variance of each is equal to

$$\frac{1}{2} f(\kappa, \omega) + \sum_{j=1}^n 0(T_j^{-1}),$$

where $f(\kappa, \omega)$ is the spectral density, T_j is the number of observations in the j^{th} dimension, and $n = 1$ or 2 . The limiting joint distribution of a collection of two-dimensional periodograms, defined as the squared modulus of the transformed variables, is shown to be that of mutually independent chi-square variates. The discrete finite Fourier transform also concentrates the information for discrimination between hypotheses for a class of processes of interest.

Several techniques for testing hypotheses concerning multidimensional stationary stochastic processes were developed. These were applied to the detection of two-dimensional plane-wave signals imbedded in a collection of independent identically distributed noise processes.

When the signals are common to all realizations, a likelihood ratio test can be applied in the transformed domain. If the signal model includes an unknown epoch or phase which varies from realization to realization, no true replications are possible, and the test must be modified. The modified test has reasonable power at acceptably low test levels. However an ad hoc test, based on the asymptotic distribution of averaged two-dimensional periodograms, is shown to be more powerful than the likelihood ratio test under the conditions considered. It requires, however, that the signal components be isolated from each other in wavenumber and in frequency, since it utilizes data from neighboring cells to eliminate the unknown spectral density.

Analysis of variance and methods of multiple comparison have also been applied in the transformed domain. With the model of signals with unknown phase differences, the analysis is applied to the periodograms. The test is found to be robust to the resulting non-normal (i.e., chi-square) population, at least when the spectral density is constant. Non-constant spectral density results in unequal cell variances. In this case, the test with a chi-square population is robust only to very moderate inequality of cell variances; the test with a normal population is considerably more robust. When there are many signal components, analysis of variance and multiple comparison tests are more powerful than the ad hoc test. The latter, which considers each component independently, is less sensitive to non-constant spectral density.

The results of computer simulation of the various tests considered are presented, as is a table comparing their power at test levels α , with $0.5 \geq \alpha \geq 10^{-6}$.

PROBLEM STATUS

This is an interim report on a continuing problem.

AUTHORIZATION

NRL Problem S02-35
Project RF 52-552-403-6079

Manuscript submitted July 27, 1972.

SOME APPROACHES TO TESTING HYPOTHESES FOR
MULTIDIMENSIONAL STATIONARY STOCHASTIC PROCESSES

UNCLASSIFIED

1. INTRODUCTION AND OUTLINE

To facilitate the discussion of hypothesis testing for multidimensional stationary stochastic processes we consider some definitions. By an *n-dimensional stochastic process (random process)* we mean a finite real-valued random variable $y(t)$ for every fixed t in some n -dimensional parameter set T . We will be primarily concerned with the discrete case, in which $T_i = 0, \pm 1, \pm 2, \dots, i = 1, \dots, n$. For $n = 1$, we have a one-dimensional random function, or *time series*, although the parameter t may indicate ordering according to a spatial or other dimension. (See, for example, Anderson [2], p. 1 or Hannan [15], p. 3). For $n > 1$ the process may be termed a *space-time series*, if these are the parameters and it is desirable to distinguish between them.

The dimensionality of a particular process is sometimes a matter of interpretation. A collection of observations made at discrete points in space and in time, for example, may be considered for some applications as a set of realizations of a one-dimensional time series. For other applications it may be necessary or at least preferable to interpret such a collection as a single realization of a multidimensional process.

The n -dimensional stochastic process $\{y(t), t \in T\}$ is said to be *strictly stationary* if its n -dimensional distribution functions are invariant under parameter translation (Rosenblatt [30], p. 100). The process is said to be *wide-sense stationary* if for each t its mean is a constant (which we take to be zero without loss of generality) and its *covariance function*

$$R(t_1, t_2) = E\{y(t_1)y(t_2)\} \tag{1.1}$$

depends only on the vector difference $\tau = t_1 - t_2$, i.e., $R(t_1, t_2) = R(\tau)$. Such a process is often called a *homogeneous random field* (Yaglom [48], p. 81, Cramér and Leadbetter [6], p. 167) or a *homogeneous random process* (Hannan [15], p. 94). The terms *multidimensional stationary stochastic process*, *homogeneous random field*, *space-time series*, or simply *process* when no confusion can arise, will all be used interchangeably in the sequel, which will deal exclusively with such processes. Examples are given by Cramér and Leadbetter (*ibid.*).

The assumption of stationarity permits the *spectral representation*

$$y(t) = \frac{1}{(2\pi)^n} \int e^{i\lambda \cdot t} dY(\lambda) \quad (1.2)$$

where the range of integration extends over the whole n -dimensional space of $\lambda' = (\lambda_1, \dots, \lambda_n)$ in the continuous parameter case, and is $[-\pi, \pi]$ for each λ_i in the discrete case. (See, for example, Doob [8], p. 481, p. 527). Here $\lambda \cdot t$ indicates the inner product

$$\lambda \cdot t = \lambda_1 t_1 + \dots + \lambda_n t_n .$$

The $Y(\lambda)$ process has orthogonal increments, i.e., $E\{dY(\lambda_1) dY(\lambda_2)\} = 0$, $\lambda_1 \neq \lambda_2$, and

$$E\{|dY(\lambda)|^2\} = dF(\lambda) , \quad (1.3)$$

where $F(\lambda)$ is the *spectral distribution function*, given by

$$R(\tau) = \frac{1}{(2\pi)^n} \int e^{i\lambda \cdot \tau} dF(\lambda) . \quad (1.4)$$

When it exists, the *spectral density* is the derivative of the spectral distribution:

$$f(\lambda) = \frac{\partial^n F(\lambda)}{\partial \lambda_1 \dots \partial \lambda_n} \quad (1.5)$$

Although there is a one-to-one correspondence between $\{y(t)\}$ and $\{Y(\lambda)\}$, in many cases it is advantageous to consider the variables in the transformed space. Measurement, computation, and interpretation of the spectral density rather than the covariance function is often preferable (Blackman and Tukey [3], p. 6), and spectral analysis may be the most relevant analysis (Jenkins [19], Jenkins and Watts [20]). For discrete data, with which we will primarily be concerned, Shumway [36, 37] points out that in most time series applications the number of replicated series is much less than the number of points in each series, so that the sample covariance matrix will have a singular Wishart density and the classical multivariate tests are not applicable. The *discrete finite Fourier transform (DFT)*, defined below, approximately diagonalizes the covariance matrix. In addition, it will be shown in Chapter 3 that for certain models the DFT also concentrates the information for discrimination between hypotheses (Kullback [22], p. 5) in a particular region of the transformed space. Some of the problems involved in estimating spectra from finite length records are

discussed by Parzen [28]. See also Blackman and Tukey [3], Anderson [2], Chapter 9, Hannan [15], Chapter V, and Jenkins and Watts [20], Chapter 6.

Consider a finite set of discrete observations, $\{y(t), t_j = 0, 1, \dots, T_j - 1, j = 1, \dots, n\}$. The n-dimensional DFT of $y(t)$ is defined as

$$\tilde{Y}(\mathbf{m}) = \left[\prod_{j=1}^n T_j^{-1/2} \right] \sum_{t_1=0}^{T_1-1} \dots \sum_{t_n=0}^{T_n-1} y(t) e^{-i\lambda_{\mathbf{m}} \cdot \mathbf{t}}, \quad (1.6)$$

where

$$\begin{aligned} \mathbf{m}' &= (m_{T_1}, \dots, m_{T_n}), \\ \lambda_{\mathbf{m}}' &= (2\pi m_{T_1}/T_1, \dots, 2\pi m_{T_n}/T_n), \end{aligned} \quad (1.7)$$

and

$$\lim_{T_j \rightarrow \infty} 2\pi m_{T_j}/T_j = \lambda_{j0}, j = 1, \dots, n. \quad (1.8)$$

It will be shown in Chapter 2 that for $n = 1$ or 2 , under stated conditions, the variance of

$$\tilde{Y}(\mathbf{m}) \text{ is } f(\lambda) + \sum_{j=1}^n o(T_j^{-1}),$$

where $o(\cdot)$ is defined in the Glossary, that

$$\text{cov}[\tilde{Y}_{\mathcal{R}}(\mathbf{m}), \tilde{Y}_{\mathcal{I}}(\mathbf{m})] = \prod_{j=1}^n o(T_j^{-1}), \text{ and that}$$

$$\text{cov}[\tilde{Y}_{\mathcal{R}}(\mathbf{m}_1), \tilde{Y}_{\mathcal{R}}(\mathbf{m}_2)] \approx \text{cov}[\tilde{Y}_{\mathcal{I}}(\mathbf{m}_1), \tilde{Y}_{\mathcal{I}}(\mathbf{m}_2)] = \prod_{j=1}^n o(T_j^{-1}),$$

for $\mathbf{m}_1 \neq \mathbf{m}_2$. Here \mathcal{R} and \mathcal{I} refer to the real and imaginary parts, respectively. Extension to higher dimensions is, in principle, straightforward but is notationally unwieldy.

On the lattice points (1.7), we define the n -dimensional *periodogram* of $y(t)$ as

$$I_{T,y}(\lambda_m) = |\tilde{Y}(\mathbf{m})|^2, \quad (1.9)$$

where $T' = (T_1, \dots, T_n)$ and $\tilde{Y}(\mathbf{m})$ is given by (1.6). This definition differs by a factor of $1/2$ or 2π from the two most commonly used definitions. It is adopted so that

$$E\{I_{T,y}(\lambda_m)\} = f(\lambda) + \sum_{j=1}^n o(T_j^{-1}).$$

If $\{y(t), t \in T\}$ is a Gaussian process, then $\tilde{Y}(\mathbf{m})$ will have a complex normal distribution (Goodman [11]). Wahba [42] shows that if $\{y(t), t \in T\}$ is a P -variate zero mean Gaussian process, it is possible to construct K sample spectral density matrices based on averages of one-dimensional periodograms which converge jointly in mean square to K independent complex Wishart matrices. (See Goodman [11].) Also considering Gaussian processes, Liggett [24] shows that spectral analysis is asymptotically optimal in the sense that the "expected cost" of a Bayes test based on a class of spectral estimates approaches that of the Bayes test based on the original data.

The distributional properties of the one-dimensional periodogram have been extensively studied. See, for example, Hannan [14], Chapter III. $I_{T,y}(\lambda_m)$ is not a consistent estimator of $f(\lambda)$, since $2I_{T,y}(\lambda_m)/f(\lambda)$ has a limiting chi-square distribution (Anderson [2], p. 474). The usefulness of periodograms lies in construction of spectral estimates from functions of sets of them (Hannan [15], p. 213). Walker [44] discusses the asymptotic distribution of one-dimensional periodograms and of sets of one-dimensional periodograms. Olshen [26] extends some of the results of Hannan [14] and Walker [44]. The processes considered are one-dimensional *moving averages*

$$y(t) = \sum_{j=-\infty}^{\infty} \gamma(j)u(t-j) \quad (1.10)$$

of independent random variables, $u(t)$, which obey a Central Limit Theorem. Further extensions are given by Pagano [27], who discusses the two-dimensional periodogram. Based on the work of these authors, it is shown in Chapter 2 that the joint distribution of a set of two-dimensional periodograms tends to that of a set of mutually independent chi-square variates. This result is used to justify the approximate test statistics employed in subsequent chapters.

The remainder of the dissertation is devoted to applications of these concepts to the detection of two-dimensional signals imbedded in a collection of two-dimensional independent identically distributed noise processes. Two models are considered here. In the first, two-dimensional plane waves are considered to be common to R realizations of the process. Walker [45] discussed parameter estimation for a one-dimensional model, and Hinich and Shaman [17] have recently extended this treatment to a general n -dimensional model with Gaussian errors. In Chapter 3, the approximate likelihood ratio test developed by Shumway [37] is extended to the detection of two-dimensional signals.

The second model considered is probably more realistic for many applications. In it, each signal has an unknown uniformly distributed epoch or phase. Since the phase is different in each realization, no true replications are possible. A modified version of the likelihood ratio test meets with some limited success with this model, but both types of errors are increased.

In Chapter 4 an ad hoc test, based on the asymptotic distribution of $\tilde{Y}(m)$, is developed. Both computations of the distribution and the results of simulated tests are presented to show that this nonlinear test can be more powerful than the likelihood ratio test, at least with extremely small type I errors.

Shumway [36] has applied regression and analysis of variance to the discrete finite Fourier transform of a stationary normal one-dimensional process. In Chapter 5, analysis of variance and methods of multiple comparison are applied to both transformed two-dimensional models. With the second model, "noise" having a chi-square distribution is employed. Monte Carlo methods show that under the null hypothesis the resulting distribution is indistinguishable from the central F distribution, indicating the robustness of the test for type I errors. The power of the simulated test is compared to the power with the normal distribution, both calculated and simulated. The results, with degrees of freedom for both numerator and denominator very large, are at least in qualitative agreement with those of Srivastava [39], Donaldson [7], and Tiku [40] who consider only much smaller degrees of freedom and larger type I errors.

In the final chapter, a comparison of the power of the various tests employed is made, and the results are summarized. Certain terms that are used without definition and theorems that are cited in the text are listed in the Glossary.

.. ASYMPTOTIC DISTRIBUTION OF THE FINITE FOURIER TRANSFORM OF
A ZERO MEAN STATIONARY PROCESS

In this chapter we investigate the asymptotic variances and covariances of discrete finite Fourier transforms (DFT (1.6)) and the bias in the periodogram (1.9) in one and two dimensions. There are no new conceptual problems in considering higher dimensionality; the results can be extended by induction, but the notation required is cumbersome. In anticipation of the tests of hypotheses of later chapters and to clarify the notation, one- and two-dimensional processes will be represented here by $\{n(t), t \in T\}$ and $\{n(x, t), x \in X, t \in T\}$, respectively. Under the null hypothesis of subsequent chapters, the process $\{y(t), t \in T\}$ of Chapter 1, will be the two-dimensional process $\{n(x, t), x \in X, t \in T\}$. Since it will be dropped from the DFT. The vector λ will be represented by ω in one dimension and $(\kappa, \omega)'$ in two dimensions. The letter n in parentheses or as a subscript is of course not the same as the functions $n(t)$ or $n(x, t)$.

2.1 The One Dimensional Case

Following Shumway [37], we consider a collection $\{n_r(t), t \in T, r = 1, \dots, R\}$ of R zero mean wide-sense stationary time series, where $T = \{0, 1, \dots, N-1\}$. The cross correlation functions be represented as

$$\begin{aligned} R_{rr'}(t-t') &= E\{n_r(t)n_{r'}(t')\} \\ &= \delta_{rr'} \frac{1}{2\pi} \int_{-\pi}^{\pi} e^{i\omega(t-t')} f(\omega) d\omega, \end{aligned}$$

where the spectral density $f(\omega)$ is a bounded absolutely continuous function. (1.4), (1.5).) The DFT (1.6) of $n_r(t)$ is given by

$$\epsilon_r(n) = \frac{1}{\sqrt{N}} \sum_{t=0}^{N-1} n_r(t) e^{-i\omega n t}$$

$$= \epsilon_{rR}(n) - i \epsilon_{rI}(n), \quad n = 0, 1, \dots, N-1, \quad (2.2)$$

where

$$\omega_n = 2\pi n/N, \quad \lim_{N \rightarrow \infty} \omega_n = \omega_{n0},$$

$$\epsilon_{rR}(n) = \frac{1}{\sqrt{N}} \sum_{t=0}^{N-1} n_r(t) \cos \omega_n t \quad (2.3)$$

and

$$\epsilon_{rI}(n) = \frac{1}{\sqrt{N}} \sum_{t=0}^{N-1} n_r(t) \sin \omega_n t \quad (2.4)$$

When $r \neq r'$, $\text{cov}(\epsilon_{rR}, \epsilon_{r'R})$, $\text{cov}(\epsilon_{rI}, \epsilon_{r'I})$, and $\text{cov}(\epsilon_{rR}, \epsilon_{r'I})$ all vanish. For $r = r'$, Anderson [2], Theorem 8.2.9, p. 457 shows that (in our notation, dropping the subscript)

$$\begin{aligned} E\{\epsilon_{rR}(n)\epsilon_{rR}(n')\} &= \frac{\cos[(\omega_n - \omega_{n'})(N-1)/2]}{4\pi N} \int_{-\pi}^{\pi} D_N(\omega - \omega_n) D_N(\omega - \omega_{n'}) f(\omega) d\omega \\ &+ \frac{\cos[(\omega_n + \omega_{n'})(N-1)/2]}{4\pi N} \int_{-\pi}^{\pi} D_N(\omega + \omega_n) D_N(\omega - \omega_{n'}) f(\omega) d\omega, \quad (2.5) \end{aligned}$$

$$\begin{aligned} E\{\epsilon_{rI}(n)\epsilon_{rI}(n')\} &= \frac{\cos[(\omega_n - \omega_{n'})(N-1)/2]}{4\pi N} \int_{-\pi}^{\pi} D_N(\omega - \omega_n) D_N(\omega - \omega_{n'}) f(\omega) d\omega \\ &- \frac{\cos[(\omega_n + \omega_{n'})(N-1)/2]}{4\pi N} \int_{-\pi}^{\pi} D_N(\omega + \omega_n) D_N(\omega - \omega_{n'}) f(\omega) d\omega, \quad (2.6) \end{aligned}$$

and

$$\begin{aligned} E\{\epsilon_{rR}(n)\epsilon_{rI}(n')\} &= \frac{\sin[(\omega_{n'} - \omega_n)(N-1)/2]}{4\pi N} \int_{-\pi}^{\pi} D_N(\omega - \omega_n) D_N(\omega - \omega_{n'}) f(\omega) d\omega \\ &+ \frac{\sin[(\omega_n + \omega_{n'})(N-1)/2]}{4\pi N} \int_{-\pi}^{\pi} D_N(\omega + \omega_n) D_N(\omega - \omega_{n'}) f(\omega) d\omega, \quad (2.7) \end{aligned}$$

where

$$D_N(\omega) = \frac{\sin(\omega N/2)}{\sin(\omega/2)}$$

is the Dirichlet kernel. If $n = n'$, we have

$$\begin{aligned} E\{\epsilon_{\mathcal{R}}^2(n)\} &= \frac{1}{4\pi N} \int_{-\pi}^{\pi} F_N(\omega - \omega_n) f(\omega) d\omega \\ &\quad + \frac{\cos \omega_n(N-1)}{4\pi N} \int_{-\pi}^{\pi} D_N(\omega - \omega_n) D_N(\omega + \omega_n) f(\omega) d\omega, \end{aligned} \quad (2.8)$$

$$\begin{aligned} E\{\epsilon_{\mathcal{I}}^2(n)\} &= \frac{1}{4\pi N} \int_{-\pi}^{\pi} F_N(\omega - \omega_n) f(\omega) d\omega \\ &\quad - \frac{\cos \omega_n(N-1)}{4\pi N} \int_{-\pi}^{\pi} D_N(\omega - \omega_n) D_N(\omega + \omega_n) f(\omega) d\omega, \end{aligned} \quad (2.9)$$

and

$$E\{\epsilon_{\mathcal{R}}(n)\epsilon_{\mathcal{I}}(n)\} = \frac{\sin \omega_n(N-1)}{4\pi N} \int_{-\pi}^{\pi} D_N(\omega - \omega_n) D_N(\omega + \omega_n) f(\omega) d\omega, \quad (2.10)$$

where $F_N(\omega) = D_N^2(\omega)$ is the Fejér kernel.

Since

$$\frac{1}{2\pi N} \int_{-\pi}^{\pi} F_N(\omega) d\omega = 1, \quad (2.11)$$

and

$$\lim_{N \rightarrow \infty} \frac{1}{2\pi N} F_N(\omega) = 0, \quad \omega \neq 0 \quad (2.12)$$

(see, e.g., Anderson [2], p. 461, Hannan [15], p. 507), $F_N(\omega)/2\pi N$ approximates the properties of a Dirac delta function. Thus the first terms in (2.8) and (2.9) approximate $f(\omega_n)/2$. Let the bias in this approximation be represented by

$$\begin{aligned}
 b(\omega_n) &= \frac{1}{4\pi N} \int_{-\pi}^{\pi} F_N(\omega - \omega_n) f(\omega) d\omega - \frac{1}{2} f(\omega_n) \\
 &= \frac{1}{4\pi N} \int_{-\pi}^{\pi} F_N(\omega - \omega_n) [f(\omega) - f(\omega_n)] d\omega
 \end{aligned} \tag{2.13}$$

using (2.11). If $f(\omega)$ is a constant ("white noise") then clearly $b(\omega_n) = 0$.

Theorem 2.1. For $|\omega_n| < \pi$, if $f(\omega)$ is continuous on $[-\pi, \pi]$ and differentiable on $(-\pi, \pi)$, then $b(\omega_n) = o(1/N)$.

Proof. We have by the mean value theorem,

$$b(\omega_n) = \frac{K}{N} \int_{-\pi}^{\pi} F_N(\omega - \omega_n) (\omega - \omega_n) d\omega,$$

where $K = f'(v)/4\pi < \infty$ for some $|v| < \pi$. Thus

$$\begin{aligned}
 b(\omega_n) &= \frac{K}{N} \int_{-\pi - \omega_n}^{\pi - \omega_n} F_N(\lambda) \lambda d\lambda \\
 &= \frac{K}{N} \left\{ \int_{-\pi - \omega_n}^{-\eta} + \int_{-\eta}^{\eta} + \int_{\eta}^{\pi - \omega_n} \right\} F_N(\lambda) \lambda d\lambda,
 \end{aligned}$$

where

$$0 < \eta < \pi - \omega_n.$$

Now

$$\begin{aligned}
 \frac{K}{N} \int_{\eta}^{\pi - \omega_n} F_N(\lambda) \lambda d\lambda &= \frac{K}{N} \int_{\eta}^{\pi - \omega_n} \frac{\sin^2(\lambda N/2)}{\sin^2(\lambda/2)} \lambda d\lambda \\
 &\leq \frac{K}{N \sin^2(\eta/2)} \int_{\eta}^{\pi - \omega_n} \lambda d\lambda = o\left(\frac{1}{N}\right).
 \end{aligned}$$

Similarly,

$$\frac{K}{N} \int_{-\pi-\omega_n}^{-\eta} F_N(\lambda) \lambda d\lambda = 0 \left(\frac{1}{N} \right),$$

while

$$\frac{K}{N} \int_{-\eta}^{\eta} F_N(\lambda) \lambda d\lambda = 0,$$

since the integrand is odd. Q.E.D.

This result appears to strengthen that of Hannan [15], p. 286, Rosenblatt [30], p. 171, Shumway [36, 37], and others who indicate $O(\ln N/N)$ convergence. This difference can have serious practical consequences. If, for example, an accuracy of 0.01 in the spectral estimate is required, 100 terms will suffice in one case while over 600 are necessary in the other. The difference is due to the assumptions about $f(\omega)$. I will comment further on it in section 2.3, after considering a numerical check, the second term in (2.8) and (2.9), and the two-dimensional extension.

The result was checked by numerical integration for several functions, $f(\omega)$ and several values of ω_n . Because of the rapid oscillation of the integrand, 2000 functional values were used with the trapezoidal method. The value of

$$\frac{1}{2\pi N} \int_{-\pi}^{\pi} F_N(X-Z) f(X) dX$$

was calculated for $N = 100(100)1000$ and $Z = 0, .35\pi, .6\pi, .95\pi$. The difference between this integral and $f(Z)$ was divided by $1/N$ and by $\ln N/N$. The computer printout of these calculations is shown on pp. 30 and 31. In Fig. 2.1 $f(x) = \cos x$, and in Fig. 2.2 $f(x) = x \sin x$. The numerical results seem to support the $O(1/N)$ bias shown for all functions satisfying the assumptions of Theorem 2.1.

We now consider the second terms in (2.8) and (2.9) and (2.10). If $n = 0$, then $\omega_n = 0$, and these terms are identical to the first terms in (2.8) and (2.9), so that

$$E \{ \epsilon_R^2(0) \} = \frac{1}{2\pi N} \int_{-\pi}^{\pi} F_N(\omega) f(\omega) d\omega = f(0),$$

by a proof similar to that of Theorem 2.1, leading to an odd integrand, and $\epsilon_{\mathcal{L}}(0) = 0$ with probability one.

For $n = N/2$, $\omega_n = \pi$,

$$F_N(\omega - \pi) = \frac{\sin^2[(\omega - \pi)N/2]}{\sin^2[(\omega - \pi)/2]} = \frac{1 - \cos[(\omega - \pi)N]}{1 - \cos(\omega - \pi)} = \frac{1 - (-1)^N \cos(N\omega)}{1 + \cos \omega},$$

and

$$\begin{aligned} \cos [(N-1)\pi] D_N(\omega - \pi) D_N(\omega + \pi) &= (-1)^{N-1} \left[\frac{\cos(N\pi) - \cos(N\omega)}{\cos \pi - \cos \omega} \right] \\ &= \frac{1 - (-1)^N \cos(N\omega)}{1 + \cos \omega} = F_N(\omega - \pi), \end{aligned}$$

so that by a proof similar to that of Theorem 2.1,

$$E\{\epsilon_{\mathcal{R}}^2(N/2)\} = f(\pi) + O(1/N),$$

and $\epsilon_{\mathcal{I}}(N/2) = 0$ with probability one.

For $0 < \omega_n < \pi$,

$$\begin{aligned} \frac{1}{2\pi N} \int_{-\pi}^{\pi} D_N(\omega - \omega_n) D_N(\omega + \omega_n) f(\omega) d\omega &= \frac{1}{2\pi N} \\ &\times \left\{ \int_{-\pi}^{-\omega_n - \eta} + \int_{\omega_n - \eta}^{-\omega_n + \eta} + \int_{-\omega_n + \eta}^0 + \int_0^{\omega_n - \eta} + \int_{\omega_n - \eta}^{\omega_n + \eta} + \int_{\omega_n + \eta}^{\pi} \right\} \\ &\times D_N(\omega - \omega_n) D_N(\omega + \omega_n) f(\omega) d\omega. \end{aligned} \tag{2.14}$$

The magnitude of the first term of (2.14) is

$$\begin{aligned} &\left| \frac{1}{2\pi N} \int_{-\pi}^{-\omega_n - \eta} D_N(\omega - \omega_n) D_N(\omega + \omega_n) f(\omega) d\omega \right| \\ &\leq \frac{K}{2\pi N} \int_{-\pi}^{-\omega_n - \eta} |D_N(\omega - \omega_n)| |D_N(\omega + \omega_n)| d\omega = O\left(\frac{1}{N}\right) \end{aligned}$$

by the second mean value theorem for integrals, where $\inf |f(\omega)| \leq K \leq \sup |f(\omega)|$, with the last equality following from

$$|D_N(\omega)| = \left| \frac{\sin(\omega N/2)}{\sin(\omega/2)} \right| \leq \frac{1}{|\sin(\delta/2)|} \quad \text{for } 0 < \delta < |\omega| < \pi.$$

Similarly the 3rd, 4th, and 6th terms of (2.14) are $O(1/N)$. For the 5th term, we have

$$\begin{aligned} & \left| \frac{1}{2\pi N} \int_{\omega_n - \eta}^{\omega_n + \eta} D_N(\omega - \omega_n) D_N(\omega + \omega_n) f(\omega) d\omega \right| \\ & \leq \frac{K}{2\pi N} \int_{-\eta}^{\eta} |D_N(\omega)| |D_N(\omega + 2\omega_n)| d\omega \\ & \leq \frac{K'}{2\pi N} \int_{-\pi}^{\pi} |D_N(\omega)| d\omega = O\left(\frac{\ln N}{N}\right), \end{aligned} \quad (2.15)$$

where $\inf |f(\omega)| \leq K \leq \sup |f(\omega)|$, and $K' \leq K/\sin(\delta/2)$ for $0 < \delta < \omega_n$. The last equality follows from Appendix 2A at the end of this chapter.

The 2nd term is similar, so that for $0 < \omega_n < \pi$,

$$\frac{1}{2\pi N} \left| \int_{-\pi}^{\pi} D_N(\omega - \omega_n) D_N(\omega + \omega_n) f(\omega) d\omega \right| = O\left(\frac{\ln N}{N}\right). \quad (2.16)$$

Numerical integration of (2.15), illustrated in Fig. 2.3, seems to imply $o(\ln N/N)$ dependence, not merely $O(\ln N/N)$, but clearly not $O(1/N)$. (Minor discrepancies in this and subsequent calculations can be attributed to the inaccuracies of the numerical integration.) Numerical integration of (2.14) for various $f(\omega)$ and various $\omega_n \in (0, \pi)$ implies $O(1/N)$ dependence, however. This is illustrated in Fig. 2.4 for $f(\omega) = \cos \omega$ and in Fig. 2.5 for $f(\omega) = \omega \sin \omega$. Since $O(1/N)$ clearly implies $O(\ln N/N)$, these numerical results do not violate (2.16). Analytic verification of $O(1/N)$ dependence follows from Lemma 8.3.4 of Anderson [2], p. 471. The left hand side of (2.15) vanishes since the integrand is bounded and η can be arbitrarily small.

2.2 The Two-Dimensional Case

Consider a collection $\{n_r(x, t), x \in X, t \in T, r = 1, \dots, R\}$ of observations of a two-dimensional zero mean wide-sense stationary stochastic process, where $X = \{0, 1, \dots, M-1\}$, and $T = \{0, 1, \dots, N-1\}$. Let the cross correlation functions be represented as

$$\begin{aligned} R_{r,r'}(x-x', t-t') &= E\{n_r(x, t)n_{r'}(x', t')\} \\ &= \delta_{r,r'} \frac{1}{(2\pi)^2} \int_{-\pi}^{\pi} \int_{-\pi}^{\pi} e^{i[\kappa(x-x')+\omega(t-t')]} f(\kappa, \omega) d\kappa d\omega, \end{aligned} \quad (2.17)$$

where the two-dimensional spectral density $f(\kappa, \omega)$ is a bounded absolutely continuous function with continuous first partial derivatives for $\kappa, \omega \in [-\pi, \pi]$. If x and t are space and time variables, $k = \kappa/2\pi$ may represent wavenumber and $f = \omega/2\pi$ may represent frequency.

The two-dimensional DFT (1.6) of $n_r(x, t)$ is given by

$$\begin{aligned} \epsilon_r(m, n) &= \frac{1}{\sqrt{MN}} \sum_{x=0}^{M-1} \sum_{t=0}^{N-1} n_r(x, t) e^{-i(\kappa_m x + \omega_n t)} \\ &= \epsilon_{r,R}(m, n) - i\epsilon_{r,I}(m, n), \quad m = 0, \dots, M-1, n = 0, \dots, N-1, \end{aligned} \quad (2.18)$$

where

$$\kappa_m = 2\pi m/M \rightarrow \kappa_{m_0} \text{ as } M \rightarrow \infty, \quad \omega_n = 2\pi n/N \rightarrow \omega_{n_0} \text{ as } N \rightarrow \infty, \quad (2.19)$$

$$\epsilon_{r,R}(m, n) = \frac{1}{\sqrt{MN}} \sum_{x=0}^{M-1} \sum_{t=0}^{N-1} n_r(x, t) \cos(\kappa_m x + \omega_n t), \quad (2.20)$$

and

$$\epsilon_{r,I}(m, n) = \frac{1}{\sqrt{MN}} \sum_{x=0}^{M-1} \sum_{t=0}^{N-1} n_r(x, t) \sin(\kappa_m x + \omega_n t). \quad (2.21)$$

We extend the results of the previous section to two dimensions and consider unequal wavenumbers and unequal frequencies. As in section 2.1, $\text{cov}[\epsilon_{r,R}(m, n), \epsilon_{r',R}(m', n')] =$

$\text{cov}[\epsilon_r \mathcal{Q}(m, n), \epsilon_{r'} \mathcal{Q}(m', n')] = \text{cov}[\epsilon_r \mathcal{R}(m, n), \epsilon_{r'} \mathcal{Q}(m', n')] = 0$ if $r \neq r'$. If $r = r'$, we drop the subscript and have

$$\begin{aligned}
& E \{ \epsilon_{\mathcal{R}}(m, n) \epsilon_{\mathcal{R}}(m', n') \} \\
&= \frac{1}{(2\pi)^2 MN} \sum_{x=0}^{M-1} \sum_{t=0}^{N-1} \sum_{x'=0}^{M-1} \sum_{t'=0}^{N-1} \left\{ \int_{-\pi}^{\pi} \int_{-\pi}^{\pi} f(\kappa, \omega) e^{i[\kappa(x-x') + \omega(t-t')]} d\kappa d\omega \right. \\
&\quad \left. \cos(\kappa_m x + \omega_n t) \cos(\kappa_m x' + \omega_n t') \right\} \\
&= \frac{1}{4(2\pi)^2 MN} \int_{-\pi}^{\pi} \int_{-\pi}^{\pi} f(\kappa, \omega) \\
&\quad \{ [D_M(\kappa + \kappa_m) e^{i(\kappa + \kappa_m)(M-1)/2} D_N(\omega + \omega_n) e^{i(\omega + \omega_n)(N-1)/2} \\
&\quad + D_M(\kappa - \kappa_m) e^{i(\kappa - \kappa_m)(M-1)/2} D_N(\omega - \omega_n) e^{i(\omega - \omega_n)(N-1)/2}] \\
&\quad [D_M(\kappa + \kappa_{m'}) e^{-i(\kappa + \kappa_{m'})(M-1)/2} D_N(\omega + \omega_{n'}) e^{-i(\omega + \omega_{n'})(N-1)/2} \\
&\quad + D_M(\kappa - \kappa_{m'}) e^{-i(\kappa - \kappa_{m'})(M-1)/2} D_N(\omega - \omega_{n'}) e^{-i(\omega - \omega_{n'})(N-1)/2}] \} d\kappa d\omega \\
&= \frac{\cos[(\kappa_m - \kappa_{m'})(M-1)/2 + (\omega_n - \omega_{n'})(N-1)/2]}{2(2\pi)^2 MN} \\
&\quad \cdot \int_{-\pi}^{\pi} \int_{-\pi}^{\pi} D_M(\kappa - \kappa_m) D_M(\kappa - \kappa_{m'}) D_N(\omega - \omega_n) D_N(\omega - \omega_{n'}) f(\kappa, \omega) d\kappa d\omega \\
&\quad + \frac{\cos[(\kappa_m + \kappa_{m'})(M-1)/2 + (\omega_n + \omega_{n'})(N-1)/2]}{2(2\pi)^2 MN} \\
&\quad \cdot \int_{-\pi}^{\pi} \int_{-\pi}^{\pi} D_M(\kappa + \kappa_m) D_M(\kappa - \kappa_{m'}) D_N(\omega + \omega_n) D_N(\omega - \omega_{n'}) f(\kappa, \omega) d\kappa d\omega, \tag{2.22}
\end{aligned}$$

where $D_M(x) = \sin(Mx/2)/\sin(x/2)$ is the Dirichlet kernel. Here we have used the fact that for real $n(x, t)$, $f(-\kappa, -\omega) = f(\kappa, \omega)$.

Similarly,

$$\begin{aligned}
 & E \{ \epsilon_{\mathcal{A}}(m, n) \epsilon_{\mathcal{A}}(m', n') \} \\
 &= \frac{1}{(2\pi)^2 MN} \sum_{x=0}^{M-1} \sum_{t=0}^{N-1} \sum_{x'=0}^{M-1} \sum_{t'=0}^{N-1} \left\{ \int_{-\pi}^{\pi} \int_{-\pi}^{\pi} f(\kappa, \omega) e^{i[\kappa(x-x') + \omega(t-t')]} d\kappa d\omega \right. \\
 &\quad \left. \sin(\kappa_m x + \omega_n t) \sin(\kappa_m' x' + \omega_n' t') \right\} \\
 &= \frac{\cos[(\kappa_m - \kappa_m')(M-1)/2 + (\omega_n - \omega_n')(N-1)/2]}{2(2\pi)^2 MN} \\
 &\quad \cdot \int_{-\pi}^{\pi} \int_{-\pi}^{\pi} D_M(\kappa - \kappa_m) D_M(\kappa - \kappa_m') D_N(\omega - \omega_n) D_N(\omega - \omega_n') f(\kappa, \omega) d\kappa d\omega \\
 &\quad - \frac{\cos[(\kappa_m + \kappa_m')(M-1)/2 + (\omega_n + \omega_n')(N-1)/2]}{2(2\pi)^2 MN} \\
 &\quad \cdot \int_{-\pi}^{\pi} \int_{-\pi}^{\pi} D_M(\kappa + \kappa_m) D_M(\kappa - \kappa_m') D_N(\omega + \omega_n) D_N(\omega - \omega_n') f(\kappa, \omega) d\kappa d\omega, \tag{2.23}
 \end{aligned}$$

and

$$\begin{aligned}
 & E \{ \epsilon_{\mathcal{R}}(m, n) \epsilon_{\mathcal{A}}(m', n') \} \\
 &= \frac{1}{(2\pi)^2 MN} \sum_{x=0}^{M-1} \sum_{t=0}^{N-1} \sum_{x'=0}^{M-1} \sum_{t'=0}^{N-1} \left\{ \int_{-\pi}^{\pi} \int_{-\pi}^{\pi} f(\kappa, \omega) e^{i[\kappa(x-x') + \omega(t-t')]} d\kappa d\omega \right. \\
 &\quad \left. \cos(\kappa_m x + \omega_n t) \sin(\kappa_m' x' + \omega_n' t') \right\} \\
 &= \frac{\sin[(\kappa_m' - \kappa_m)(M-1)/2 + (\omega_n' - \omega_n)(N-1)/2]}{2(2\pi)^2 MN}
 \end{aligned}$$

$$\begin{aligned}
& \cdot \int_{-\pi}^{\pi} \int_{-\pi}^{\pi} D_M(\kappa - \kappa_m) D_M(\kappa - \kappa_{m'}) D_N(\omega - \omega_n) D_N(\omega - \omega_{n'}) f(\kappa, \omega) d\kappa d\omega \\
& + \frac{\sin[(\kappa_m + \kappa_{m'})(M-1)/2 + (\omega_n + \omega_{n'})(N-1)/2]}{2(2\pi)^2 MN} \\
& \cdot \int_{-\pi}^{\pi} \int_{-\pi}^{\pi} D_M(\kappa + \kappa_m) D_M(\kappa - \kappa_{m'}) D_N(\omega + \omega_n) D_N(\omega - \omega_{n'}) f(\kappa, \omega) d\kappa d\omega .
\end{aligned} \tag{2.24}$$

For a single wavenumber-frequency pair, by putting $m = m'$ and $n = n'$ in (2.22)-(2.24) we have

$$E\{\epsilon_{\mathcal{R}}^2(m, n)\} = A + \cos[\kappa_m(M-1) + \omega_n(N-1)] \cdot B, \tag{2.25}$$

$$E\{\epsilon_{\mathcal{I}}^2(m, n)\} = A - \cos[\kappa_m(M-1) + \omega_n(N-1)] \cdot B, \tag{2.26}$$

and

$$E\{\epsilon_{\mathcal{R}}(m, n)\epsilon_{\mathcal{I}}(m, n)\} = \sin[\kappa_m(M-1) + \omega_n(N-1)] \cdot B, \tag{2.27}$$

where

$$A = \frac{1}{2(2\pi)^2 MN} \int_{-\pi}^{\pi} \int_{-\pi}^{\pi} F_M(\kappa - \kappa_m) F_N(\omega - \omega_n) f(\kappa, \omega) d\kappa d\omega, \tag{2.28}$$

$$B = \frac{1}{2(2\pi)^2 MN} \int_{-\pi}^{\pi} \int_{-\pi}^{\pi} D_M(\kappa + \kappa_m) D_M(\kappa - \kappa_m) D_N(\omega + \omega_n) D_N(\omega - \omega_n) f(\kappa, \omega) d\kappa d\omega, \tag{2.29}$$

and $F_M(x) = D_M^2(x)$ is the Fejér kernel. Equation (2.28) approximates $f(\kappa_m, \omega_n)/2$, with bias given by $b(\kappa_m, \omega_n) = A - f(\kappa_m, \omega_n)/2$. Since

$$\begin{aligned}
& \frac{1}{(2\pi)^2 MN} \int_{-\pi}^{\pi} \int_{-\pi}^{\pi} F_M(\kappa - \kappa_m) F_N(\omega - \omega_n) d\kappa d\omega \\
& = \frac{1}{2\pi M} \int_{-\pi}^{\pi} F_M(\kappa - \kappa_m) d\kappa \cdot \frac{1}{2\pi N} \int_{-\pi}^{\pi} F_N(\omega - \omega_n) d\omega = 1,
\end{aligned}$$

by (2.11) we may write

$$b(\kappa_m, \omega_n) = \frac{1}{2(2\pi)^2 MN} \int_{-\pi}^{\pi} \int_{-\pi}^{\pi} F_M(\kappa - \kappa_m) F_N(\omega - \omega_n) [f(\kappa, \omega) - f(\kappa_m, \omega_n)] d\kappa d\omega .$$

If $|\kappa_m| < \pi$, $|\omega_n| < \pi$ and if $f(\kappa, \omega)$ is continuous and has continuous first partial derivatives for $\kappa \in [-\pi, \pi]$ and $\omega \in [-\pi, \pi]$, we have by the mean value theorem for a function of two variables

$$b(\kappa_m, \omega_n) = \frac{1}{2(2\pi)^2 MN} \int_{-\pi}^{\pi} \int_{-\pi}^{\pi} F_M(\kappa - \kappa_m) F_N(\omega - \omega_n) [(\kappa - \kappa_m) f_{\kappa}(\xi, \eta) + (\omega - \omega_n) f_{\omega}(\xi, \eta)] d\kappa d\omega , \quad (2.30)$$

where f_{κ} and f_{ω} denote the partial derivatives of f with respect to κ and ω , respectively, and $|\xi| < \pi$, $|\eta| < \pi$. Using (2.11), (2.30) becomes

$$\begin{aligned} b(\kappa_m, \omega_n) &= \frac{f_{\kappa}(\xi, \eta)}{4\pi M} \int_{-\pi}^{\pi} F_M(\kappa - \kappa_m)(\kappa - \kappa_m) d\kappa + \frac{f_{\omega}(\xi, \eta)}{4\pi N} \int_{-\pi}^{\pi} F_N(\omega - \omega_n)(\omega - \omega_n) d\omega \\ &= 0 \left(\frac{1}{M} \right) + 0 \left(\frac{1}{N} \right), \end{aligned} \quad (2.31)$$

as in the proof of Theorem 2.1.

By the second mean value theorem for integrals, (2.29) may be written for $\kappa_m \neq 0, \pi$, $\omega_n \neq 0, \pi$ (with $\inf f(\kappa, \omega) \leq K \leq \sup f(\kappa, \omega)$)

$$\begin{aligned} B &= \frac{K}{(2\pi)^2 MN} \int_{-\pi}^{\pi} D_M(\kappa + \kappa_m) D_M(\kappa - \kappa_m) d\kappa \int_{-\pi}^{\pi} D_N(\omega + \omega_n) D_N(\omega - \omega_n) d\omega \\ &= 0 \left(\frac{1}{M} \right) \cdot 0 \left(\frac{1}{N} \right), \end{aligned} \quad (2.32)$$

by Lemma (8.3.4) of Anderson [2], p. 471. This approach, applied to (2.22)-(2.24), shows that for unequal wavenumbers and frequencies,

$$\begin{aligned} E\{\epsilon_{\mathcal{R}}(m,n)\epsilon_{\mathcal{R}}(m',n')\} &\approx E\{\epsilon_{\mathcal{I}}(m,n)\epsilon_{\mathcal{I}}(m',n')\} \approx E\{\epsilon_{\mathcal{R}}(m,n)\epsilon_{\mathcal{I}}(m',n')\} \\ &= 0 \left(\frac{1}{M}\right) \cdot 0 \left(\frac{1}{N}\right), \quad m \neq m', n \neq n'. \end{aligned}$$

Finally, if $m = m'$ and $n \neq n'$ we have

$$\frac{K}{(2\pi)^2 MN} \int_{-\pi}^{\pi} F_M(\kappa - \kappa_m) d\kappa \int_{-\pi}^{\pi} D_N(\omega - \omega_n) D_N(\omega - \omega_{n'}) d\omega = 0 \left(\frac{1}{N}\right),$$

so that

$$E\{\epsilon_{\mathcal{R}}(m,n)\epsilon_{\mathcal{R}}(m,n')\} \approx E\{\epsilon_{\mathcal{I}}(m,n)\epsilon_{\mathcal{I}}(m,n')\} = 0 \left(\frac{1}{N}\right),$$

while

$$E\{\epsilon_{\mathcal{R}}(m,n)\epsilon_{\mathcal{I}}(m,n')\} = 0 \left(\frac{1}{M}\right) \cdot 0 \left(\frac{1}{N}\right), \quad n \neq n'.$$

Summarizing the main result of this section, by (2.25)-(2.27), (2.31) and (2.32), we have

$$E\{\epsilon_{\mathcal{R}}^2(m,n)\} \approx E\{\epsilon_{\mathcal{I}}^2(m,n)\} = f(\kappa_m, \omega_n)/2 + 0 \left(\frac{1}{M}\right) + 0 \left(\frac{1}{N}\right),$$

and

$$E\{\epsilon_{\mathcal{R}}(m,n)\epsilon_{\mathcal{I}}(m',n')\} = 0 \left(\frac{1}{M}\right) \cdot 0 \left(\frac{1}{N}\right).$$

Thus if $n_r(x,t)$ is a Gaussian process, $\epsilon_{\mathcal{R}}(m,n)$, $\epsilon_{\mathcal{R}}(m',n')$, $\epsilon_{\mathcal{I}}(m,n)$, $\epsilon_{\mathcal{I}}(m',n')$, $m \neq m'$, $n \neq n'$ are asymptotically normally and independently distributed.

Numerical integration of (2.28) is illustrated in Fig. 2.6, p. 35. Here $f(\kappa, \omega) = \cos(\kappa - \omega)$, $\kappa_m = .6\pi$, $\omega_n = 0, .35\pi, .6\pi$, and $.95\pi$, $M = 1000$ and $N = 100(100)1000$. The integral was computed by the trapezoidal method using 2000 values of the integrand, $f(\kappa_m, \omega_n)$ was subtracted and the result divided by $1/M + 1/N$ and by $1/N$. The results show $0(1/M) + 0(1/N)$ dependence, as indicated by (2.31). By (2.32), (2.29) is the product of two terms like the ones illustrated in Figs. 2.4 and 2.5.

2.3 Lipschitz Conditions and Order of Convergence

By (2.13), the bias in the one-dimensional periodogram is

$$b(\omega_n) = \frac{1}{2\pi N} \int_{-\pi}^{\pi} \left\{ \frac{\sin[(\omega - \omega_n)N/2]}{\sin[(\omega - \omega_n)/2]} \right\}^2 [f(\omega) - f(\omega_n)] d\omega .$$

For $|\omega_n| < \pi$, if f is continuous on $[-\pi, \pi]$ and differentiable on $(-\pi, \pi)$, we have shown in Theorem 2.1 that $b(\omega_n) = O(1/N)$. Hannan [15], p. 286 states that if $f \in \text{Lip } 1$ near ω_n , $b(\omega_n) = O(\ln N/N)$, and that this condition holds in particular if f is differentiable at ω_n . His definition of a Lipschitz condition (p.513) follows that of Zygmund [49], p.42 who defines the modulus of continuity as

$$\omega(\delta, f) = \sup |f(x_2) - f(x_1)|, \quad \text{for } x_1, x_2 \in [a, b], |x_1 - x_2| \leq \delta . \quad (2.33)$$

If, for some $\alpha > 0$, we have $\omega(\delta, f) \leq C\delta^\alpha$, with C independent of δ , f is said to satisfy a Lipschitz condition of order α in (a, b) , written $f \in \text{Lip } \alpha$.

Zygmund shows ((3.15), p.91) that if $f \in \text{Lip } \alpha$, $b(\omega_n) = O(1/N^\alpha)$ or $O(\ln N/N)$ according as $0 < \alpha < 1$ or $\alpha = 1$. The further restrictions that f be continuous and differentiable were used in Theorem 2.1 to invoke the mean value theorem to show $b(\omega_n) = O(1/N)$.

These restrictions imply $f \in \text{Lip } 1$, but the converse is not necessarily true. Another common definition of a Lipschitz condition (with constant K) is that

$$|f(x_2) - f(x_1)| \leq K|x_2 - x_1| . \quad (2.34)$$

This condition implies but is not implied by Zygmund's condition. The inequality (2.34) is not sufficient to show $O(1/N)$ convergence as in section 2.1 but (2.34) in addition to the assumption that f is monotonic would be sufficient. It can be shown (Royden [31], p. 108, problem 16) that (2.34) implies that f is absolutely continuous and hence differentiable a.e..

Olshen [26] uses Zygmund's proof to show that if $f \in \text{Lip } \alpha$, a remainder term is $O(1/N)$ or $O(\ln N/N)$ according as $0 < \alpha < 1$ or $\alpha = 1$. Pagano [27], generalizing Olshen's work to two dimensions but using a Lipschitz condition similar to a two-dimensional extension of (2.34), claims $O(M^{-\alpha} + N^{-\beta})$ convergence, requiring only that α and β be positive constants. If $\alpha = \beta = 1$, this result agrees with that of section 2.2, where, however, the two-dimensional analog of the restrictions of Theorem 2.1 were imposed.

In the one-dimensional case, Rosenblatt [30], p. 171 seems to be too restrictive in requiring that f be continuously differentiable to obtain $O(\ln N/N)$ convergence. Grenander and

Rosenblatt [13], p. 130, impose a restriction similar to (2.34), and thus could cite Zygmund rather than Fejér [9] (see Appendix 2A) for the $O(\ln N/N)$ result. Shumway [37] requires that f be absolutely continuous and hence differentiable a.e.

2.4 The Asymptotic Joint Distribution of Two-Dimensional Periodograms

In this section we revert in part to the notation of Chapter 1, in order to avoid confusion in subscripts. Let $\{y(x, t), x \in X, t \in T\}$ represent a set of observations of a two-dimensional zero mean wide-sense stationary stochastic process, where $X = \{0, 1, \dots, M-1\}$ and $T = \{0, 1, \dots, N-1\}$. On the lattice points (κ_m, ω_n) , where κ_m and ω_n are defined by (2.19), the periodogram of $y(x, t)$ is given by (1.9) and (1.6) as

$$I_{M, N, y}(\kappa_m, \omega_n) = |Y(m, n)|^2 = \frac{1}{MN} \left| \sum_{x=0}^{M-1} \sum_{t=0}^{N-1} y(x, t) e^{-i(\kappa_m x + \omega_n t)} \right|^2 \quad (2.35)$$

It has been shown in section 2.2 that

$$E\{I_{M, N, y}(\kappa_m, \omega_n)\} = f_y(\kappa_m, \omega_n) + O\left(\frac{1}{M}\right) + O\left(\frac{1}{N}\right),$$

if $f_y(\kappa, \omega)$, the spectral density of $y(x, t)$, is continuous with continuous first derivatives for $\kappa \in [-\pi, \pi]$ and $\omega \in [-\pi, \pi]$.

The process $y(x, t)$ can be represented as a moving average (1.10)

$$y(x, t) = \sum_{j=-\infty}^{\infty} \sum_{k=-\infty}^{\infty} \gamma(j, k) u(x-j, t-k), \quad (2.36)$$

where

$$\sum_{j=-\infty}^{\infty} \sum_{k=-\infty}^{\infty} |\gamma(j, k)|^2 < \infty. \quad (2.37)$$

(See Doob [8], p. 498, Anderson [2], p. 400). The residuals $u(x, t)$ are orthonormal, that is

$$\begin{aligned} E\{u(x, t)\} &= 0 \\ \text{var}\{u(x, t)\} &= 1 \\ \text{cov}\{u(x, t), u(x', t')\} &= 0, \quad x \neq x' \text{ or } t \neq t'. \end{aligned} \quad (2.38)$$

Hence the covariance function of $u(x, t)$ is

$$R_u(g, h) = E\{u(x, t)u(x + g, t + h)\} = \delta_{g,0}\delta_{h,0}, \quad (2.39)$$

where $\delta_{i,0}$ is one if $i = 0$ and is zero otherwise, and the spectral density is

$$f_u(\kappa, \omega) = \sum_{g=-\infty}^{\infty} \sum_{h=-\infty}^{\infty} R_u(g, h)e^{-i(\kappa g + \omega h)} \equiv 1,$$

so that $\{u(x, t)\}$ represents a "white noise" process. Using (2.36), (2.38) and (2.39), $E\{y(x, t)\} = 0$, and the covariance function of $y(x, t)$ is

$$\begin{aligned} R_y(g, h) &= E\{y(x, t)y(x + g, t + h)\} \\ &= \sum_j \sum_{j'} \sum_k \sum_{k'} \gamma(j, k)\gamma(j', k')E\{u(x - j, t - k)u(x - j' + g, t - k' + h)\} \\ &= \sum_j \sum_k \gamma(j, k)\gamma(j - g, k - h), \end{aligned}$$

independent of x and t , verifying the wide-sense stationarity of $\{y(x, t)\}$. The spectral density of the y process is

$$\begin{aligned} f_y(\kappa, \omega) &= \sum_{g=-\infty}^{\infty} \sum_{h=-\infty}^{\infty} R_y(g, h)e^{-i(\kappa g + \omega h)} \\ &= \sum_g \sum_h \sum_j \sum_k \gamma(j, k)\gamma(j - g, k - h)e^{-i(\kappa g + \omega h)} \\ &= \sum_{j'} \sum_{k'} \sum_j \sum_k \gamma(j, k)e^{-i(\kappa j + \omega k)} \gamma(j', k')e^{i(\kappa j' + \omega k')} \\ &= |\Gamma(\kappa, \omega)|^2, \end{aligned} \quad (2.40)$$

where

$$\Gamma(\kappa, \omega) = \sum_{j=-\infty}^{\infty} \sum_{k=-\infty}^{\infty} \gamma(j, k) e^{-i(\kappa j + \omega k)}.$$

Let the DFT (1.6) of $y(x, t)$ be represented by $Y(m, n)$. For fixed M and N , the dependence of m_M and n_N on M and N , respectively (see (2.19)) may be suppressed. Since for real $y(x, t)$,

$$\begin{aligned} Y(M-m, N-n) &= \frac{1}{\sqrt{MN}} \sum_{x=0}^{M-1} \sum_{t=0}^{N-1} y(x, t) e^{-2\pi i [(M-m)x/M + (N-n)t/N]} \\ &= \frac{1}{\sqrt{MN}} \sum_{x=0}^{M-1} \sum_{t=0}^{N-1} y(x, t) e^{2\pi i (mx/M + nt/N)} \end{aligned}$$

$= Y^*(m, n)$, the complex conjugate of $Y(m, n)$, these terms are redundant. Consider the set of lattice points

$$Q = \left\{ (m, n) : m = 0, \dots, M-1, n = 1, \dots, \frac{N}{2} - 1 \right\} + \left\{ (m, n) : m = 0, \dots, \frac{M}{2}, n = 0, \frac{N}{2} \right\} \quad (2.41)$$

where M and N are assumed to be even for convenience. Then the transformed set of observations $\{Y(m, n) : (m, n) \in Q\}$ are a set of sufficient statistics. Within Q , define the set of four points

$$D = \left\{ (m, n) : (m, n) = (jM/2, kN/2), j, k = 0, 1 \right\}. \quad (2.42)$$

$Y(m, n)$ is in general complex for $(m, n) \in Q$, but is purely real for $(m, n) \in D$. This distinction will govern the degrees of freedom of the chi-square variates to be considered below.

Let the DFT of $u(x, t)$ be represented by

$$U(m, n) = \frac{1}{\sqrt{MN}} \sum_{x=0}^{M-1} \sum_{t=0}^{N-1} u(x, t) e^{-i(\kappa m x + \omega n t)} = U_{\mathcal{R}}(m, n) - iU_{\mathcal{I}}(m, n).$$

Pagano [27] shows that if $f(\kappa, \omega)$ is continuous, if (2.36)–(2.38) are satisfied, and if the random variables $u(\cdot, \cdot)$ are mutually independent and satisfy the “central limit condition”

$$U(0,0) \xrightarrow{L} N(0,1),$$

then the random variables $I_{M,N,y}(\kappa_m, \omega_n)$ are asymptotically independent and (in our notation)

$$I_{M,N,y}(\kappa_m, \omega_n) \xrightarrow{L} \begin{cases} \frac{1}{2} f(\kappa_m, \omega_n) \chi_2^2, & (m,n) \in Q-D \\ f(\kappa_m, \omega_n) \chi_1^2, & (m,n) \in D, \end{cases} \quad (2.43)$$

where χ_v^2 denotes a chi-square random variable with v degrees of freedom. We conclude from (2.43) and Theorem 2 of Chernoff [5], section 2 that the ratio of independent sums of periodograms has a distribution asymptotically proportional to the F distribution. This conclusion, and hence the conclusion that the type I error of tests based on such ratios converges to the nominal type I error of an F test, also follows from Theorem 2.2 below, which is an extension of the work of Walker [44], Olshen [26], and Pagano [27]. If asymptotic normality can be assumed a priori, then the result follows from Theorem 8.10.2 of Anderson [1], p. 224, which is an application of Chernoff's theorem.

Theorem 2.2. Let $f_y(\kappa_j, \omega_k) \neq 0, j = 1, \dots, J, k = 1, \dots, K$. Then as $M \rightarrow \infty$ and $N \rightarrow \infty$, the joint distribution of $I_{M,N,y}(\kappa_j, \omega_k), j = 1, \dots, J, k = 1, \dots, K$ tends to that of JK mutually independent random variables with

$$I_{M,N,y}(\kappa_j, \omega_k) \xrightarrow{L} \begin{cases} \frac{1}{2} f_y(\kappa_j, \omega_k) \chi_2^2, & (j,k) \in Q-D \\ f_y(\kappa_j, \omega_k) \chi_1^2, & (j,k) \in D. \end{cases}$$

Proof. Let

$$S_{MN} = \sum_{x=0}^{M-1} \sum_{t=0}^{N-1} c(x,t) u(x,t),$$

where

$$c(x,t) = \sum_{j=1}^J \sum_{k=1}^K [a(j,k) \cos(\kappa_j x + \omega_k t) + b(j,k) \sin(\kappa_j x + \omega_k t)],$$

with $a(j, k)$ and $b(j, k)$ arbitrary. Then

$$S_{MN} = \sqrt{MN} \sum_{j=1}^J \sum_{k=1}^K [a(j, k)U_{\mathcal{R}}(j, k) + b(j, k)U_{\mathcal{Q}}(j, k)] . \quad (2.44)$$

Let

$$\begin{aligned} s_{MN}^2 &= E\{S_{MN}^2\} = \sum_{x=0}^{M-1} \sum_{t=0}^{N-1} c^2(x, t) \\ &= \frac{MN}{2} \sum_{\substack{j=1 \\ (j,k) \in Q-D}}^J \sum_{k=1}^K [a^2(j, k) + b^2(j, k)] + MN \sum_{\substack{j=1 \\ (j,k) \in D}}^J \sum_{k=1}^K a^2(j, k) . \end{aligned} \quad (2.45)$$

Let $\eta(x, t) = c(x, t)u(x, t)$, and let $G_{x,t}(\eta)$ be the distribution function of $\eta(x, t)$. For arbitrary $\delta > 0$, let

$$\begin{aligned} g_{MN}(\delta) &= \frac{1}{s_{MN}^2} \sum_{x=0}^{M-1} \sum_{t=0}^{N-1} \int_{|\eta| \geq \delta s_{MN}} \eta^2 dG_{x,t}(\eta) \\ &= \frac{1}{s_{MN}^2} \sum_{x=0}^{M-1} \sum_{t=0}^{N-1} c^2(x, t) \int_{|u| \geq \frac{\delta s_{MN}}{|c(x,t)|}} u^2 dF_{x,t}(u) , \end{aligned}$$

where $F_{x,t}(u)$ is the distribution function of $u(x, t)$. Since

$$|c(x, t)| \leq \sum_{j=1}^J \sum_{k=1}^K [|a(j, k)| + |b(j, k)|] , \quad \text{and } s_{MN}^2 \sim MN, g_{MN}(\delta) \rightarrow 0 \text{ as } M, N \rightarrow \infty .$$

Hence by the Lindeberg-Feller theorem (Loève [25], p. 280), $S_{MN}/s_{MN} \xrightarrow{\mathcal{L}} N(0, 1)$, so that

$$S_{MN}/\sqrt{MN} \xrightarrow{\mathcal{L}} N \left(0, \frac{1}{2} \sum_{\substack{j=1 \\ (j,k) \in Q-D}}^J \sum_{k=1}^K [a^2(j, k) + b^2(j, k)] + \sum_{\substack{j=1 \\ (j,k) \in D}}^J \sum_{k=1}^K a^2(j, k) \right) \quad (2.46)$$

using (2.45). Let $\phi_{MN}(\theta) = E\{e^{i\theta S_{MN}/\sqrt{MN}}\}$ be the characteristic function of S_{MN}/\sqrt{MN} . Then by (2.46) and the Lévy-Cramér continuity theorem (Loève [25], p. 191), as $M, N \rightarrow \infty$

$$\phi_{MN}(\theta) \rightarrow \phi(\theta)$$

for all real θ , where $\phi(\theta)$ is the characteristic function of a random variable distributed as the right-hand side of (2.46). That is, using (2.44),

$$\begin{aligned} \lim_{\substack{M \rightarrow \infty \\ N \rightarrow \infty}} E\{e^{i\theta S_{MN}/\sqrt{MN}}\} &= \lim_{\substack{M \rightarrow \infty \\ N \rightarrow \infty}} E\left\{e^{i\theta} \sum_{j=1}^J \sum_{k=1}^K [a(j,k) U_{\mathcal{R}}(j,k) + b(j,k) U_{\mathcal{I}}(j,k)]\right\} \\ &= \exp\left\{-\frac{1}{2} \left\{ \frac{\theta^2}{2} \sum_{\substack{j=1 \\ (j,k) \in Q-D}}^J \sum_{k=1}^K [a^2(j,k) + b^2(j,k)] + \theta^2 \sum_{\substack{j=1 \\ (j,k) \in D}}^J \sum_{k=1}^K a^2(j,k) \right\}\right\}. \end{aligned}$$

The limiting joint distribution of $U_{\mathcal{R}}(j,k), U_{\mathcal{I}}(j,k), j = 1, \dots, J, k = 1, \dots, K$ is thus that of $2JK$ mutually independent random variables, each distributed as $N(0, 1/2)$ if $(j,k) \in Q - D$ or $N(0, 1)$ if $(j,k) \in D$.

The limiting joint distribution of $I_{M,N,u}(\kappa_j, \omega_k) = |U(m,n)|^2, j = 1, \dots, J, k = 1, \dots, K$ is therefore that of JK mutually independent random variables, each distributed as $\frac{1}{2}\chi_2^2$ or χ_1^2 according as $(j,k) \in Q - D$ or $(j,k) \in D$. The conclusion then follows from (2.40) and the fact that

$$I_{M,N,y}(\kappa_j, \omega_k) \xrightarrow{P} |\Gamma(\kappa_j, \omega_k)|^2 I_{M,N,u}(\kappa_j, \omega_k),$$

as is shown by Pagano [27]. Q.E.D.

Corollary. If $\Gamma(\dots)$ is continuous, then the limiting joint distribution of $Y_{\mathcal{R}}(j,k), Y_{\mathcal{I}}(j,k), j = 1, \dots, J, k = 1, \dots, K$ is that of $2JK$ mutually independent random variables each distributed as $N(0, f_y(\kappa_j, \omega_k)/2)$ or $N(0, f_y(\kappa_j, \omega_k))$ according as $(j,k) \in Q - D$ or $(j,k) \in D$.

The proof follows from the above, from (2.40), and the fact that if $\Gamma(\dots)$ is continuous, $Y(j,k)$ converges in mean square to $\Gamma(\kappa_j, \omega_k) U(j,k)$. (See Pagano [27].)

This theorem and corollary are the justification for the approximate test statistics used in the following chapters.

APPENDIX 2A
ASYMPTOTIC BEHAVIOR OF THE INTEGRAL OF THE
MODULUS OF THE DIRICHLET KERNEL

This appendix follows Fejér [9].

Lemma. Let $f(x)$ be an arbitrary function, finite and continuous on (a, b) . Then

$$\lim_{n \rightarrow \infty} \int_a^b f(x) |\sin nx| dx = \frac{2}{\pi} \int_a^b f(x) dx .$$

Proof.

$$\text{Let } (j-1) \frac{\pi}{n} < a \leq j \frac{\pi}{n} < (j+1) \frac{\pi}{n} < \dots < k \frac{\pi}{n} \leq b < (k+1) \frac{\pi}{n} .$$

$$\text{Then } \int_a^b f(x) |\sin nx| dx = \int_{j\pi/n}^{(j+1)\pi/n} f(x) |\sin nx| dx + \dots + \int_{(k-1)\pi/n}^{k\pi/n} f(x) |\sin nx| dx + o(1) .$$

$$\begin{aligned} \text{Now, } \int_{m\pi/n}^{(m+1)\pi/n} |\sin nx| dx &= \frac{1}{n} \int_{m\pi}^{(m+1)\pi} |\sin x| dx = \frac{(-1)^m}{n} \int_{m\pi}^{(m+1)\pi} \sin x dx \\ &= -\frac{(-1)^m}{n} (-2 \cos m\pi) = \frac{2}{n}, \quad \forall m . \end{aligned}$$

Hence, by the second mean value theorem for integrals, if $f(x)$ is integrable on (a, b) ,

$$\int_a^b f(x) |\sin nx| dx = \frac{2}{n} (f_1 + f_2 + \dots + f_{k-j}) + o(1) ,$$

where $m_i \leq f_i \leq M_i$, $i = 1, \dots, k-j$, and m_i and M_i are respectively the infimum and supremum of $f(x)$ on the i th interval.

Since

$$\begin{aligned} \int_a^b f(x) dx &= \int_a^{j\pi/n} f(x) dx + \int_{j\pi/n}^{(j+1)\pi/n} f(x) dx + \dots + \int_{(k-1)\pi/n}^{k\pi/n} f(x) dx + \int_{k\pi/n}^b f(x) dx \\ &= \frac{\pi}{n} (f_1 + f_2 + \dots + f_{k-j}) + o(1), \end{aligned}$$

by the first mean value theorem for integrals, it follows that

$$\begin{aligned} \int_a^b f(x) |\sin nx| dx &= \frac{2}{\pi} \cdot \frac{\pi}{n} (f_1 + \dots + f_{k-j}) + o(1) \\ &= \frac{2}{\pi} \int_a^b f(x) dx + o(1). \quad \text{Q.E.D.} \end{aligned}$$

We now apply this lemma to evaluate the "Lebesgue constants" (Fejér [9], Zygmund [49], p. 67), L_n .

Let

$$L_n = \frac{2}{\pi} \int_0^{\pi/2} \frac{|\sin(2n+1)t|}{\sin t} dt = \lambda_n + \mu_n, \quad (2A.1)$$

where

$$\lambda_n = \frac{2}{\pi} \int_0^{\pi/2} \frac{|\sin(2n+1)t|}{t} dt$$

and

$$\mu_n = \frac{2}{\pi} \int_0^{\pi/2} \left(\frac{1}{\sin t} - \frac{1}{t} \right) |\sin(2n+1)t| dt.$$

By the lemma,

$$\lim_{n \rightarrow \infty} \mu_n = \frac{4}{\pi^2} \int_0^{\pi/2} \left(\frac{1}{\sin t} - \frac{1}{t} \right) dt = o(1). \quad (2A.2)$$

We can write

$$\lambda_n = \nu_n + \zeta_n, \quad (2A.3)$$

where

$$\nu_n = \frac{2}{\pi} \int_0^{(n+1)\pi/(2n+1)} \frac{|\sin(2n+1)t|}{t} dt$$

and

$$\zeta_n = \frac{2}{\pi} \int_{(n+1)\pi/(2n+1)}^{\pi/2} \frac{|\sin(2n+1)t|}{t} dt$$

$$= \frac{2}{\pi} \int_{(n+1)\pi}^{(2n+1)\pi/2} \frac{|\sin t|}{t} dt$$

$$\leq \frac{2}{\pi} \ln \frac{n + \frac{1}{2}}{n+1} = o(1). \quad (2A.4)$$

Now

$$\nu_n = \frac{2}{\pi} \int_0^{(n+1)\pi} \frac{|\sin t|}{t} dt$$

$$= \frac{2}{\pi} \left\{ \int_0^\pi + \int_\pi^{2\pi} + \dots + \int_{n\pi}^{(n+1)\pi} \right\} \frac{|\sin t|}{t} dt$$

$$= \frac{2}{\pi} \int_0^\pi \left(\frac{1}{t} + \frac{1}{t+\pi} + \dots + \frac{1}{t+n\pi} \right) \sin t dt$$

$$= \frac{2}{\pi} \int_0^1 \left(\frac{1}{t} + \frac{1}{t+1} + \dots + \frac{1}{t+n} \right) \sin \pi t dt.$$

The digamma function may be expressed as (Whittaker and Watson [46], p. 241)

$$\frac{\Gamma'(x)}{\Gamma(x)} = -C - \frac{1}{x} + \sum_{n=1}^{\infty} \left(\frac{1}{n} - \frac{1}{x+n} \right),$$

where C is the Euler-Mascheroni constant.

Thus

$$\begin{aligned} \frac{1}{x} + \frac{1}{x+1} + \dots + \frac{1}{x+n} &= -\frac{\Gamma'(x)}{\Gamma(x)} - C + \sum_{k=1}^n \frac{1}{k} + \sum_{k=n+1}^{\infty} \left(\frac{1}{k} - \frac{1}{x+k} \right) \\ &= -\frac{\Gamma'(x)}{\Gamma(x)} + \ln n + o(1), \end{aligned}$$

using (0.131) of Gradshteyn and Ryzhik [12].

Hence

$$\begin{aligned} \nu_n &= \frac{2}{\pi} \int_0^1 \left(\ln n - \frac{\Gamma'(t)}{\Gamma(t)} \right) \sin \pi t \, dt + o(1) \\ &= \frac{4}{\pi^2} \ln n + o(1). \end{aligned} \tag{2A.5}$$

By (2A.1)-(2A.5), we have

$$L_n = \frac{4}{\pi^2} \ln n + o(1),$$

so that

$$\frac{L_n}{n} = \frac{1}{2\pi n} \int_{-\pi}^{\pi} \left| \frac{\sin \left[\left(n + \frac{1}{2} \right) t \right]}{\sin (t/2)} \right| dt = o(\ln n/n).$$

Finally, letting $N = 2n + 1$ we have

$$\frac{1}{2\pi N} \int_{-\pi}^{\pi} |D_N(\omega)| \, d\omega = o(\ln N/N),$$

where $D_N(\omega) = \sin(N\omega/2)/\sin(\omega/2)$ is the Dirichlet kernel.

Appendix 2B

NUMERICAL CALCULATIONS

2000 VALUES		F(Z)=COS(Z)						
N	I-F(Z)		I-F(Z)		I-F(Z)		I-F(Z)	
	----- 1/N		----- LN(N)/N		----- 1/N		----- LN(N)/N	
	z= 0. PI		0. PI		.35 PI		.35 PI	
100	-.999916		-.217129		-.453952		-.098574	
200	-.999832		-.188707		-.453915		-.085672	
300	-.999747		-.175278		-.453876		-.079574	
400	-.999663		-.166848		-.453838		-.075747	
500	-.999578		-.160843		-.453799		-.073021	
600	-.999494		-.156246		-.453761		-.070934	
700	-.999409		-.152556		-.453722		-.069259	
800	-.999325		-.149496		-.453685		-.067870	
900	-.999240		-.146895		-.453646		-.066689	
1000	-.999156		-.144643		-.453608		-.065666	
	z= .60 PI		.60 PI		.95 PI		.95 PI	
100	.308990		.067096		.987742		.214485	
200	.308964		.058314		.987524		.186384	
300	.308938		.054164		.987571		.173143	
400	.308912		.051559		.987364		.164795	
500	.308885		.049703		.987394		.158883	
600	.308860		.048282		.987210		.154326	
700	.308834		.047142		.987212		.150695	
800	.308808		.046197		.987062		.147662	
900	.308782		.045393		.987022		.145099	
1000	.308756		.044697		.986923		.142872	

Fig. 2.1—Illustration of $O(1/N)$ Convergence of the Bias due to the Fejér Kernel, $f(Z) = \cos(Z)$

2000 VALUES		F(Z)=Z SIN(Z)							
N	$\frac{I-F(Z)}{1/N}$		$\frac{I-F(Z)}{\ln(N)/N}$		$\frac{I-F(Z)}{1/N}$		$\frac{I-F(Z)}{\ln(N)/N}$		
	0.	PI	0.	PI	.35	PI	.35	PI	
100	1.386346		.301041		-.061378		-.013328		
200	1.386308		.261651		-.061209		-.011552		
300	1.386301		.243049		-.061152		-.010721		
400	1.386299		.231379		-.061056		-.010190		
500	1.386298		.223071		-.060982		-.009813		
600	1.386297		.216713		-.060893		-.009519		
700	1.386297		.211613		-.060815		-.009283		
800	1.386296		.207386		-.060728		-.009085		
900	1.386296		.203795		-.060649		-.008916		
1000	1.386296		.200687		-.060563		-.008767		
z=									
	.60	PI	.60	PI	.95	PI	.95	PI	
100	-1.408690		-.305893		1.663046		.361126		
200	-1.408647		-.265867		1.672814		.315725		
300	-1.408516		-.246944		1.669825		.292757		
400	-1.408371		-.235063		1.671407		.278965		
500	-1.408223		-.226599		1.670469		.268797		
600	-1.408073		-.220117		1.671214		.261253		
700	-1.407923		-.214915		1.670695		.255026		
800	-1.407772		-.210599		1.671209		.250008		
900	-1.407621		-.206930		1.670821		.245622		
1000	-1.407469		-.203752		1.671267		.241941		

Fig. 2.2—Illustration of $O(1/N)$ Convergence of the Bias due to the Fejér Kernel, $f(Z) = Z \sin Z$

2000 VALUES		INTEGRAL[ABS(DIRICHLET KERNEL)]	
N	$\frac{I(ABS)}{1/N}$	$I(ABS)$	$\frac{I(ABS)}{LN(N)/N}$
100	2.857030	.620396	
200	3.142686	.593148	
300	3.300262	.578609	
400	3.446217	.575188	
500	3.555307	.572089	
600	3.581973	.559952	
700	3.647627	.556798	
800	3.622720	.541949	
900	3.746962	.550830	
1000	4.017716	.581624	

Fig. 2.3—Numerical Integration of the Absolute Value of the Dirichlet Kernel

2000 VALUES		F(X)=COS(X)			
N	INT. ----- 1/N	INT. ----- LN(N)/N	INT. ----- 1/N	INT. ----- LN(N)/N	
z=	.10 PI	.10 PI	.35 PI	.35 PI	
100	-1.000083	-.217165	1.000047	.217157	
200	-1.000164	-.188770	-1.000095	-.188757	
300	-1.000246	-.175365	1.000142	.175347	
400	-1.000327	-.166959	-1.000190	-.166936	
500	-1.000409	-.160977	1.000236	.160949	
600	-1.000491	-.156402	-1.000284	-.156369	
700	-1.000572	-.152734	1.000331	.152697	
800	-1.000654	-.149695	-1.000379	-.149654	
900	-1.000736	-.147115	1.000426	.147070	
1000	-1.000817	-.144883	-1.000473	-.144833	
z=	.60 PI	.60 PI	.85 PI	.85 PI	
100	-.999949	-.217136	.999543	.217048	
200	-.999897	-.188720	-.999115	-.188572	
300	-.999845	-.175295	.998658	.175087	
400	-.999794	-.166870	-.998229	-.166608	
500	-.999742	-.160870	.997773	.160553	
600	-.999690	-.156276	-.997341	-.155909	
700	-.999638	-.152591	.996889	.152172	
800	-.999585	-.149535	-.996453	-.149067	
900	-.999533	-.146938	.996005	.146420	
1000	-.999481	-.144690	-.995564	-.144123	

Fig. 2.4—Numerical Integration of Eq. (2.14) with $f(\omega) = \cos\omega$

2000 VALUES		F(X)=X SIN(X)			
N		INT.	INT.	INT.	INT.
		----- 1/N	----- LN(N)/N	----- 1/N	----- LN(N)/N
	Z=	.10 PI	.10 PI	.35 PI	.35 PI
100		1.361562	.295660	-1.067288	-.231759
200		1.361516	.256971	1.067273	.201436
300		1.361500	.238701	-1.067145	-.187094
400		1.361489	.227238	1.067056	.178096
500		1.361480	.219077	-1.066946	-.171684
600		1.361471	.212832	1.066850	.166775
700		1.361462	.207823	-1.066743	-.162835
800		1.361454	.203670	1.066645	.159567
900		1.361445	.200142	-1.066539	-.156789
1000		1.361437	.197088	1.066440	.154383
	Z=	.60 PI	.60 PI	.85 PI	.85 PI
100		.323354	.070215	1.524844	.331116
200		.322946	.060952	-1.524287	-.287693
300		.322625	.056563	1.525236	.267408
400		.322318	.053796	-1.525663	-.254639
500		.322015	.051816	1.526375	.245611
600		.321713	.050292	-1.526897	-.238692
700		.321412	.049062	1.527562	.233177
800		.321111	.048037	-1.528110	-.228601
900		.320811	.047161	1.528760	.224739
1000		.320510	.046399	-1.529316	-.221391

Fig. 2.5—Numerical Integration of Eq. (2.14) with $f(\omega) = \omega \sin \omega$

2000 VALUES $F(K,W) = \cos(K-W)$, $KM = 1.884954$

N	$I-F(K,W)$ ----- $1/M+1/N$		$I-F(K,W)$ ----- $1/N$		$I-F(K,W)$ ----- $1/M+1/N$		$I-F(K,W)$ ----- $1/N$	
	WN=	0. PI	0. PI		.35 PI		.35 PI	
M=1000								
100		.308688	.339557		-.706357		-.776993	
200		.308672	.370406		-.706320		-.847584	
300		.308658	.401256		-.706289		-.918176	
400		.308646	.432105		-.706262		-.988767	
500		.308636	.462955		-.706239		-1.059358	
600		.308628	.493804		-.706218		-1.129949	
700		.308620	.524654		-.706201		-1.200541	
800		.308613	.555503		-.706185		-1.271132	
900		.308607	.586353		-.706170		-1.341724	
1000		.308601	.617202		-.706157		-1.412315	
	WN=	.60 PI	.60 PI		.95 PI		.95 PI	
M=1000								
100		-.998939	-1.098833		-.453548		-.498903	
200		-.998887	-1.198664		-.453487		-.544184	
300		-.998843	-1.298496		-.453498		-.589547	
400		-.998805	-1.398327		-.453451		-.634832	
500		-.998772	-1.498158		-.453459		-.680189	
600		-.998743	-1.597989		-.453425		-.725481	
700		-.998718	-1.697821		-.453429		-.770830	
800		-.998696	-1.797652		-.453407		-.816132	
900		-.998675	-1.897483		-.453404		-.861468	
1000		-.998657	-1.997315		-.453393		-.906786	

Fig. 2.6—Illustration of $O(1/M) + O(1/N)$ Convergence of the Bias due to the Fejér Kernel in two dimensions

3. APPROXIMATE LIKELIHOOD RATIO TESTS FOR TWO-DIMENSIONAL SIGNALS

3.1 Signals Common to R Stationary Noise Processes

Let $\{y_r(x, t), x \in X, t \in T, r = 1, \dots, R\}$ once more represent a collection of observations, where $X = \{0, 1, \dots, M - 1\}$, and $T = \{0, 1, \dots, N - 1\}$. Let

$$y_r(x, t) = s(x, t) + n_r(x, t), \quad (3.1)$$

where $s(x, t)$ is a fixed signal common to all R replications, and $n_r(x, t)$ is a realization of a two-dimensional zero mean wide-sense stationary noise process. It has been shown in Chapter 2 that the variance of $\epsilon_r(m, n)$, the DFT of $n_r(x, t)$, is $f(\kappa_m, \omega_n) + O(M^{-1}) + O(N^{-1})$, and that the correlation between its real and imaginary parts is $O(M^{-1}) \cdot O(N^{-1})$, where $f(\kappa_m, \omega_n)$ is a continuously differentiable spectral density. κ_m and ω_n are defined in (2.19). We assume that $n_r(x, t)$ can be represented as a moving average as in (2.36), with $\Gamma(\kappa, \omega)$ continuous, so that by the corollary to Theorem 2.2, $\epsilon_r(m, n)$ is asymptotically normally distributed.

Let $S(m, n)$ represent the DFT of $s(x, t)$. Then

$$Y_r(m, n) = S(m, n) + \epsilon_r(m, n), (m, n) \in Q, \quad (3.2)$$

where Q is defined by (2.41). With D given by (2.42), and assuming the asymptotic distribution, the development given by Shumway [37] may be extended to two dimensions. The approximate joint likelihood of the RMN real observations

$$\{Y_{Rr}(m, n), Y_{I_r}(m, n) : (m, n) \in Q - D, r = 1, \dots, R\}$$

and

$$\{Y_{Rr}(m, n) : (m, n) \in D, r = 1, \dots, R\}$$

may be written as $L = L_{Q-D} \cdot L_D$, where

$$L_{Q-D} = \prod_m \prod_{\substack{n \\ (m,n) \in Q-D}} [\pi f(\kappa_m, \omega_n)]^{-R} \exp \left\{ -\frac{1}{f(\kappa_m, \omega_n)} \sum_{r=1}^R |Y_r(m,n) - S(m,n)|^2 \right\} \quad (3.3)$$

and

$$L_D = \prod_{j=0}^1 \prod_{k=0}^1 [2\pi f(jM/2, kN/2)]^{-R/2} \cdot \exp \left\{ -\frac{1}{2f(jM/2, kN/2)} \sum_{r=1}^R [Y_{Rr}(jM/2, kN/2) - S_{Rr}(jM/2, kN/2)]^2 \right\}. \quad (3.4)$$

Letting $\partial \log L / \partial S_{Rr}(m, n) = 0$ and $\partial \log L / \partial S_{Qr}(m, n) = 0$, we obtain

$$\hat{S}_{Rr}(m, n) = \frac{1}{R} \sum_{r=1}^R Y_{Rr}(m, n) = \bar{Y}_{Rr}(m, n),$$

and

$$\hat{S}_{Qr}(m, n) = \frac{1}{R} \sum_{r=1}^R Y_{Qr}(m, n) = \bar{Y}_{Qr}(m, n),$$

so that

$$\hat{S}(m, n) = \hat{S}_{Rr}(m, n) - i\hat{S}_{Qr}(m, n) = \bar{Y}(m, n). \quad (3.5)$$

Similarly letting $\partial \log L / \partial f(\kappa_m, \omega_n) = 0$, we obtain

$$\hat{f}(\kappa_m, \omega_n) = \frac{1}{R} \sum_{r=1}^R |Y_r(m, n) - \bar{Y}(m, n)|^2, \quad (m, n) \in Q - D,$$

and

$$\hat{f}(\kappa_m, \omega_n) = \frac{1}{R} \sum_{r=1}^R [Y_{rR}(m, n) - \bar{Y}_R(m, n)]^2, \quad (m, n) \in D. \quad (3.6)$$

Assuming the asymptotic distribution, for $(m, n) \in Q - D$,

$$\frac{\sqrt{R}[\bar{Y}_R(m, n) - S_R(m, n)]}{\left[\frac{f(\kappa_m, \omega_n)}{2}\right]^{1/2}}$$

and

$$\frac{\sqrt{R}[\bar{Y}_Q(m, n) - S_Q(m, n)]}{\left[\frac{f(\kappa_m, \omega_n)}{2}\right]^{1/2}}$$

are independent, each distributed as $N(0,1)$, and are independent of $R \hat{f}(\kappa_m, \omega_n)/[f(\kappa_m, \omega_n)/2]$ which is distributed as $\chi^2(2(R-1))$, while $\sqrt{R} [\bar{Y}_R(m, n) - S_R(m, n)]/[f(\kappa_m, \omega_n)]^{1/2}$ and $R \hat{f}(\kappa_m, \omega_n)/f(\kappa_m, \omega_n)$ are similarly distributed when $(m, n) \in D$. (cf. Wilks [47], p. 208.)

Thus, under the null hypothesis,

$$\mathcal{F}(m, n) = \frac{R|\bar{Y}(m, n)|^2}{\sum_{r=1}^R \frac{|Y_r(m, n) - \bar{Y}(m, n)|^2}{R-1}} \quad (3.7)$$

has asymptotically the F distribution with 2 and $2(R-1)$ degrees of freedom when $(m, n) \in Q - D$, and 1 and $R-1$ degrees of freedom when $(m, n) \in D$. Under the alternate hypothesis, $\mathcal{F}(m, n)$ has asymptotically the non-central F distribution with the same degrees of freedom and non-centrality parameter

$$\delta^2(m, n) = \begin{cases} R|S(m, n)|^2/[f(\kappa_m, \omega_n)/2], & (m, n) \in Q - D \\ R[S_R(m, n)]^2/f(\kappa_m, \omega_n), & (m, n) \in D. \end{cases} \quad (3.8)$$

An analysis of power table, analogous to an analysis of variance table may be written for each wavenumber-frequency combination as shown below.

TABLE 3.1
ANALYSIS OF POWER AT WAVENUMBER κ_m
AND FREQUENCY ω_n

Source	Power	Degrees of† Freedom
Due to Signal	$R \bar{Y}(m,n) ^2$	d
Due to Noise	$\sum_{r=1}^R Y_r(m,n) - \bar{Y}(m,n) ^2$	$d(R-1)$
Total	$\sum_{r=1}^R Y_r(m,n) ^2$	dR

† $d = 2$ if $(m, n) \in Q - D$, $d = 1$ if $(m, n) \in D$.

3.2 Plane Wave Signals

Let $s(x, t)$ be a superposition of J two-dimensional plane wave signals of the form

$$s(x, t) = \sum_{j=1}^J A_j \cos(\kappa_j x + \omega_j t - \phi_j) \quad (3.9)$$

where $\kappa_j = 2\pi k_j/M$, $k_j \in \{0, 1, \dots, M/2\}$ represents wavenumber, $\omega_j = 2\pi f_j/N$, $f_j \in \{0, 1, \dots, N/2\}$ represents frequency, and $\phi_j \in [0, 2\pi]$ is an unknown phase. Parameter estimation for n -dimensional plane waves has recently been discussed by Hinich and Shaman [17]. The signal (3.9) may be considered either as a deterministic signal with unknown parameters, or as a random signal conditioned on the random variables A_j and ϕ_j . The stochastic signal model arises naturally in many physical contexts as, for example, when the j th component at each spatial point x represents the superposition of many plane waves of the same frequency with uniformly distributed phases. Baron Rayleigh [29] showed in 1880 that the resultant amplitude A_j has the distribution which now bears his name:

$$dF_A(A_j) = \frac{1}{\sigma_j^2} A_j e^{-A_j^2/2\sigma_j^2} dA_j, \quad A_j > 0,$$

where

$$\sigma_j^2 = \frac{1}{2} \sum_k n_{jk} A_{jk}^2$$

and n_{jk} is the number of subcomponents with amplitude A_{jk} . The amplitudes A_j and phases ϕ_j are independent, and are independent of $A_{j'}$ and $\phi_{j'}$ for $j' \neq j$.

If we let $a_j = A_j \cos \phi_j$ and $b_j = A_j \sin \phi_j$, then

$$s(x, t) = \sum_{j=1}^J [a_j \cos(\kappa_j x + \omega_j t) + b_j \sin(\kappa_j x + \omega_j t)] ,$$

where a_j and b_j are distributed independently as $N(0, \sigma_j^2)$. This signal process is wide-sense stationary with correlation function

$$\begin{aligned} R_s(\chi, \tau) &= E[s(x + \chi, t + \tau)s(x, t)] \\ &= \sum_{j=1}^J \sigma_j^2 \cos(\kappa_j \chi + \omega_j \tau) . \end{aligned} \quad (3.10)$$

Eq. (3.1) represents a set of observations at discrete spatial and temporal points of a continuous space-time phenomenon. For a finite set of (x, t) pairs to properly represent a continuous function, it is necessary that the latter vanish for values of its arguments outside of finite intervals. Thus (3.1) represents a sampled version of a truncated continuous space-time function. Then

$$\begin{aligned} \int_{-\infty}^{\infty} \int_{-\infty}^{\infty} |R_s(\chi, \tau)| d\chi d\tau &= \int_{-X}^X \int_{-T}^T |R_s(\chi, \tau)| d\chi d\tau \\ &\leq 4 X T \sum_{j=1}^J \sigma_j^2 < \infty , \end{aligned}$$

so that $R_s(\chi, \tau)$ is absolutely integrable. The signal spectral density function (1.5),

$$F_s''(\kappa, \omega) = \int_{-\infty}^{\infty} \int_{-\infty}^{\infty} e^{-i(\kappa\chi + \omega\tau)} R_s(\chi, \tau) d\chi d\tau ,$$

exists and is bounded and continuous, by an extension of the Corollary on p. 188 of Loève [25]. In connection with the discrete representation, it is useful to consider the idealized situation in which (3.10) is valid for all χ and τ . In this case a signal spectral density function does not exist in the ordinary sense, but by (1.4)

$$R_s(\chi, \tau) = \int_{-\pi}^{\pi} \int_{-\pi}^{\pi} \frac{e^{i(\kappa\chi + \omega\tau)} dF_s(\kappa, \omega)}{(2\pi)^2},$$

where the spectral distribution function

$$F_s(\kappa, \omega) = 2\pi^2 \sum_{\substack{j=-J \\ j \neq 0}}^I \sigma^2 |j|, \kappa_I \leq |\kappa| < \kappa_{I+1}, \omega_I \leq |\omega| < \omega_{I+1}$$

is a two-dimensional step function, a generalization of that considered by Anderson [2], p. 385.

Substituting (3.9) in (3.1) and transforming, we have

$$\begin{aligned} Y_r(m, n) &= \frac{1}{\sqrt{MN}} \sum_{x=0}^{M-1} \sum_{t=0}^{N-1} y_r(x, t) e^{-2\pi i(mx/M + nt/N)} \\ &= \frac{1}{2\sqrt{MN}} \sum_{j=1}^J A_j \left[e^{-i\phi_j} \sum_{x=0}^{M-1} \sum_{t=0}^{N-1} e^{2\pi i(k_j - m)x/M} e^{2\pi i(f_j - n)t/N} \right. \\ &\quad \left. + e^{i\phi_j} \sum_{x=0}^{M-1} \sum_{t=0}^{N-1} e^{-2\pi i(k_j + m)x/M} e^{-2\pi i(f_j + n)t/N} \right] + \epsilon_r(m, n) \\ &= \frac{\sqrt{MN}}{2} \sum_{j=1}^J A_j [e^{-i\phi_j} \delta_{k_j m} \delta_{f_j n} + e^{i\phi_j} \delta_{k_j, M-m} \delta_{f_j, N-n}] + \epsilon_r(m, n), \end{aligned}$$

$$m = 0, \dots, M-1; n = 0, \dots, N-1; r = 1, \dots, R, \tag{3.11}$$

where the Kronecker deltas are to be considered mod M or mod N . As before, the $Y_r(m,n)$ are independent for $(m,n) \in Q$. For each (m,n) , $S(m,n) = 0$ under the null hypothesis. Under the alternate hypothesis $m = k_j$ and $n = f_j$ for one and only one j , so the notation may be simplified with (3.11) replaced by

$$Y_r(m,n) = B(m,n) + \epsilon_r(m,n) \quad \text{when } (m,n) \in Q - D, \quad (3.12)$$

where $B(m,n) = (1/2) \sqrt{MN} A_j e^{-i\phi_j}$ for some $j \in \{1, \dots, J\}$.

The points $(m,n) \in D$ are of no practical consequence, since they can be examined by an analysis at a different sampling rate. For testing, we consider the data array to be relabeled to yield the $2M'N'R$ real variables $Y_{Rr}(m,n)$, $Y_{I_r}(m,n)$, $m = 1, \dots, M' < M$, $n = 1, \dots, N' < N/2$, $r = 1, \dots, R$, but will drop the primes on M and N .

The difficulty in detecting a signal depends on its strength relative to that of the noise, parameterized by the signal to noise ratio. For a deterministic (or conditional) sinusoidal signal component of amplitude A , the signal to noise ratio is independent of wavenumber and frequency and is defined as

$$\begin{aligned} S/N &= \frac{A^2/2}{\frac{1}{(2\pi)^2} \int_{-\pi}^{\pi} \int_{-\pi}^{\pi} f(\kappa, \omega) d\kappa d\omega} \\ &= \frac{A^2/2}{R(0,0)} = \frac{A^2/2}{\text{var}[n(x,t)]} \\ &\approx \frac{\frac{1}{MN} \sum_{m=0}^{M-1} \sum_{n=0}^{N-1} |S(m,n)|^2}{\frac{1}{MN} \sum_{m=0}^{M-1} \sum_{n=0}^{N-1} f(\kappa_m, \omega_n)}, \end{aligned} \quad (3.13)$$

where

$$R(\chi, \tau) = E[n(x + \chi, t + \tau)n(x, t)] = \int_{-\pi}^{\pi} \int_{-\pi}^{\pi} e^{i(\kappa\chi + \omega\tau)} f(\kappa, \omega) d\kappa d\omega / (2\pi)^2$$

is the correlation function of the noise. The non-centrality parameter (3.8) for a particular (m, n) cell is MNR times (S/N) times the ratio of the average spectral density to that of the particular cell. The factor MNR may be termed a "processing gain."

For stochastic sinusoidal signal components with uniformly distributed phase and amplitude A_j having a Rayleigh distribution with parameter σ_j , the signal to noise ratio may be defined equivalently as

$$\begin{aligned}
 S/N &= \frac{E(A_j^2/2)}{\frac{1}{(2\pi)^2} \int_{-\pi}^{\pi} \int_{-\pi}^{\pi} f(\kappa, \omega) d\kappa d\omega} = \frac{\sigma_j^2}{R(0,0)} = \frac{R_{s_j}(0,0)}{R(0,0)} = \frac{\text{var}[s_j(x,t)]}{\text{var}[n(x,t)]} \\
 &\approx \frac{\frac{1}{MN} \sum_{m=0}^{M-1} \sum_{n=0}^{N-1} \text{var}[S(m,n)]}{\frac{1}{MN} \sum_{m=0}^{M-1} \sum_{n=0}^{N-1} \text{var}[\epsilon(m,n)]} = \frac{\frac{1}{MN} \sum_{m=0}^{M-1} \sum_{n=0}^{N-1} p(m,n)}{\frac{1}{MN} \sum_{m=0}^{M-1} \sum_{n=0}^{N-1} f(\kappa_m, \omega_n)}, \quad (3.14)
 \end{aligned}$$

where $R_{s_j}(\chi, \tau)$ is the j th component of (3.10), and $p(m, n) = (MN/2)\sigma_j^2 \delta_{k_{jm}} \delta_{f_{jn}}$ is the variance of $S(m, n)$. In the last two forms of (3.14), we have $\text{var}[S(M-m, N-n)] = \text{var}[S(m, n)]$ and $\text{var}[\epsilon(M-m, N-n)] = \text{var}[\epsilon(m, n)]$.

With the stochastic signal model or the deterministic or conditional signal models, the DFT transforms a multivariate problem in the space-time domain into an asymptotically univariate problem in the wavenumber-frequency domain. The total effect of signal energy and noise energy and hence the discrimination information (Kullback [22], p. 9, Kullback [23], p. 92.4) from R replications is distributed over the entire $M \times N$ array in the space-time domain. In the wavenumber-frequency domain however, the effect of signal energy but not the effect of noise energy is concentrated, so that the information for discrimination in favor of H_1 against H_0 is also concentrated. Thus the DFT not only yields noise variables which are asymptotically uncorrelated, but also concentrates the discrimination information for these models. The asymptotic independence of the $\epsilon(m, n)$ shown in Chapter 2 and the inherent independence of the $S(m, n)$ from signal components with differing values of $j = 1, \dots, J$, allow the consideration of MN independent hypothesis testing problems in the wavenumber-frequency domain. With these models, the problems of interest are detection of the independent signal components and not the estimation of the waveform (3.9). Thus there is no need for the inverse transform to the space-time domain. After detection, estimates of the component waveforms are available without the inverse transform.

3.3 Simulated Tests in the Common Signal Case

A computer simulation of the approximate likelihood ratio test developed in section 3.1, using the plane wave signals of section 3.2 has been made. Simulation was performed in the wavenumber-frequency domain, starting with (3.12). There were several reasons for this starting point rather than (3.1), the primary one being cost. Available computer time can be spent either on the two-dimensional transformations or in obtaining more replications in the interesting regions of extremely low probabilities. If a suitable correlation structure in the space-time domain were postulated, it could be simulated using (2.36) or by the two-dimensional inverse transform of the corresponding spectral density. The latter would be followed by a re-transformation for the analysis. In some applications it is desirable to analyze data that has already been transformed for other purposes. Since the analysis of power at each wavenumber-frequency cell provides the desired information, no transformation is required in this simulation. Finally, since an array of convenient size to simulate is but a small scale model of realistic arrays of interest, reality is closer to the asymptotic approximations than to a space-time simulation of this small scale model. I therefore chose to assume that we have reached "asymptopia" in the wavenumber-frequency space, and test the procedure from this point. Since the theory is exact, simulation serves as a check on the computations and a reference for the approximate procedures to be considered later.

Some signal detection applications require a test level smaller than that of the usual F tables. (Type I errors less than 10^{-4} are not uncommon.) Furthermore, Pearson-Hartley and Fox charts for the power of the test exist only for test levels higher than those of interest. Thus the tables had to be extended.

A computer program for the central and non-central F distribution was written, using brute-force numerical integration of Eq. (10) of Anderson [1], p. 114. Up to 100 terms of the sum were used for each non-central density point, 1000 terms were used in the trapezoidal method of numerical integration for the central F , but 10 terms seemed to suffice for the non-central integration. Within the range of the available tables and charts, spot checks showed agreement with my calculations.

An independent test was simulated at each of the 256 combinations of $M = 8$ wavenumber points and $N = 32$ frequency points. A pseudo-random sequence algorithm written by F.M. Young (private communication) was used to simulate uniformly distributed random variables. This algorithm combines subsequences to yield a pseudo-random sequence length on a small (Honeywell 1648 with 16 bit words) computer much longer than the standard algorithms found on larger machines. A very long pseudo-random sequence length was found to be necessary in order to reliably simulate the extreme tails of the F distribution. $N(0,1)$ random variables were obtained via the Box-Muller [4] transformation. Independent and

uniformly distributed random variables to represent the phase ϕ for each of the assumed signal components were simulated by a separate copy of the pseudo-random algorithm. This permits testing different "signals" with the same "noise" and vice-versa, if desired.

Fig. 3.1 is a typical computer printout of the results of one run of this simulation. The format was designed to display the results of all 256 tests, rather than 256 separate results in the form of Table 3.1. Eight replications of the 8×32 data array were generated in accordance with (3.12), assuming a white Gaussian noise process with $f(\kappa_m, \omega_n) \equiv 1$. The numbers labeled "INIT." are the initialization parameters of the pseudo-random generators and are printed to allow re-generation of either the "signal" sequence or the "noise" sequence. They are either specified in advance, or are related to prior computation time and time of day. For 23 of the 256 cells, identified by "*", the null hypothesis was in fact false. Signal components with a signal to noise ratio (3.13) of 0.01566, or -18.05 dB were added to the noise in these cells. The resulting non-centrality parameter is 64. $\mathcal{F}(m,n)$, given by (3.7), has 2 and 14 degrees of freedom, and was computed for each (m,n) combination. A transpose of the matrix ($\mathcal{F}'(m,n)$) is shown in the figure. The ">" symbol identifies those \mathcal{F} which fall in the rejection region of a test of size $\alpha = 10^{-6}$. Thus an entry of a number not followed by either symbol identifies correct rejection. The "*" symbol alone indicates a type II error (miss) and "*>" indicates detection, both at the 10^{-6} level. A type I error (false alarm) would be identified by ">" without the asterisk, but none have occurred in this run.

Theoretical probabilities and observed relative frequencies are tabulated at the bottom of the figure. "ALPHA" represents the level of the test, with $.4 \geq \alpha \geq 10^{-6}$. "FR.FA" indicates the relative frequency of type I errors at each of the above test levels. "PR(D)" and "FR(D)" represent the probabilities and relative frequencies of detection, respectively, at each of the above test levels.

Fig. 3.2 is a portion of the printout of 100 similar runs in succession, with a slight change in format. Since the object is to tabulate the results of a large sample, the run number, coordinates and \mathcal{F} value are printed for only those (m,n) for which $\mathcal{F}(m,n)$ indicates rejection at $\alpha = 10^{-5}$, with the symbol ">" indicating rejection at $\alpha = 10^{-6}$ as well. $H_1(m,n)$ is indicated by $*m,n$. All the entries shown in the figure indicate correct detection, most at the level $\alpha = 10^{-6}$.

Theoretical probabilities and observed relative frequencies are again tabulated at the bottom of the figure, with the same notation as in Fig. 3.1. There are now 23300 samples for which H_0 is true, and 2300 samples for which H_1 is true. The results show good agreement with the theory.

Some results of simulation with non-white noise are shown in Figs. 3.3 and 3.4. The noise spectral density was

SIGNALS COMMON TO 8 REALIZATIONS OF NORMALLY DISTRIBUTED NOISE
SPECTRAL DENSITY=1.0

SIMULATED ARRAY= 8 X 64 WITH 8 REPS/RUN (8 X 32 COMPLEX VARIATES)
INIT. N: 3388 1062 3389 1062 P: 3391 1062 3392 1062

23 SIGNAL COMPONENTS: S/N=0.01566 (-18.05 DB)

N\M	F(M,N)							
	1	2	3	4	5	6	7	8
1	0.72	2.37	0.02	0.47	0.32	1.20	3.18	0.03
2	4.94	0.93	3.81	50.97*>	0.05	0.86	1.41	0.16
3	0.21	0.41	1.04	0.26	2.34	0.30	0.87	0.14
4	0.20	0.62	3.14	4.17	0.46	0.15	0.58	0.38
5	0.62	0.33	1.08	1.57	43.12*	1.51	1.61	0.82
6	2.16	2.73	2.63	0.20	0.20	0.71	0.20	0.02
7	0.21	1.03	0.85	0.11	65.13*>	0.54	0.00	0.10
8	0.58	0.19	0.64	0.51	2.67	1.84	0.22	0.15
9	1.86	1.36	37.14*	1.77	0.46	25.11*	0.50	0.03
10	0.95	0.19	1.96	0.13	0.53	1.64	2.81	2.66
11	0.10	1.19	1.84	0.26	5.06	0.56	0.69	0.12
12	1.16	1.84	17.42*	0.19	2.20	0.06	1.54	2.09
13	0.90	2.23	0.41	0.97	53.33*>	0.09	0.44	0.45
14	1.02	2.66	1.08	0.89	0.38	30.67*	0.44	0.20
15	0.29	1.83	1.65	0.38	0.77	1.19	5.21	2.63
16	0.57	0.02	29.72*	1.87	1.02	2.58	6.95	0.39
17	0.93	0.41	0.44	1.55	0.30	2.75	0.62	0.14
18	0.94	0.26	0.02	0.05	0.44	0.24	47.88*>	1.78
19	0.65	0.80	21.20*	0.26	0.43	0.21	0.64	0.60
20	0.59	0.80	1.26	2.44	5.60	33.24*	0.61	0.09
21	0.03	0.07	1.21	0.54	0.44	0.91	1.45	0.70
22	1.19	0.23	3.74	0.45	0.44	2.10	21.79*	0.38
23	0.42	23.51*	4.74	0.67	0.45	0.77	1.89	0.04
24	0.29	2.75	0.76	0.32	1.27	1.45	0.84	0.53
25	0.14	5.18	0.83	0.51	1.20	0.05	0.55	0.23
26	20.24*	0.98	1.92	49.76*>	2.48	27.82*	0.49	21.14*
27	2.95	0.36	0.97	0.49	0.41	0.21	0.53	10.06
28	3.85	1.01	1.08	0.85	0.33	0.19	0.57	2.35
29	2.23	2.61	0.07	0.36	20.27*	3.13	0.03	55.61*>
30	17.86*	0.85	0.82	0.96	0.48	0.68	0.06	0.17
31	0.20	0.34	0.80	0.21	0.20	0.40	0.16	1.34
32	0.07	0.04	0.07	13.90*	1.36	1.28	52.63*>	2.67

PROB. FALSE ALARM (TYPE I ERROR) 233 SAMPLES

ALPHA: .40 .30 .20 .10 .05 .01 .0010 .00010 .000010 .0000010
FR.FA: 0.35 0.27 0.21 0.09 0.05 0.01 0.0000 0.000000 0.000000 0.0000000

PROB. DETECTION (POWER OF TEST) 23 SAMPLES

PR(D): 1.00 1.00 1.00 1.00 1.00 1.00 0.99 0.90 0.63 0.30
FR(D): 1.00 1.00 1.00 1.00 1.00 1.00 1.00 0.87 0.52 0.30

Fig. 3.1—Simulation of Likelihood Ratio Test for Signals Common to
R Replications: Results of One Run, White Noise

NRL REPORT 7466

UNCLASSIFIED

SIGNALS COMMON TO 8 REALIZATIONS OF NORMALLY DISTRIBUTED NOISE
SPECTRAL DENSITY=1.0

SIMULATED ARRAY= 8 X 64 WITH 8 REPS/RUN (8 X 32 COMPLEX VARIATES)
INIT. N: 1751 11922 1752 11922 P: 1753 11922 1754 11922

23 SIGNAL COMPONENTS: S/N=0.01566 (-18.05 DB)

[(M,N,F): F(M,N)>F(.00001;2,14)]

RUN	M, N: F	M, N: F	M, N: F	M, N: F	M, N: F
1	*5, 5 35.09	*6, 9 31.79	*3,12 30.43	*3,16 40.52	*7,18 32.06
1	*3,19 29.58	*6,20 43.68>	*7,22 66.15>	*2,23 44.55>	*1,26 74.47>
1	*5,29 42.27	*1,30 51.23>	*4,32 33.48	*7,32 54.50>	
2	*4, 2 52.42>	*5, 5 33.67	*5, 7 47.90>	*3, 9 73.38>	*3,16 45.76>
2	*3,19 52.21>	*7,22 35.50	*2,23 42.64	*4,26 38.89	*6,26 35.91
2	*8,26 57.76>	*5,29 31.06	*8,29 96.08>	*1,30 54.58>	*7,32 48.39>
3	*5, 7 54.07>	*3,12 30.97	*6,14 73.32>	*7,18 93.65>	*3,19 42.95
3	*6,20 60.71>	*7,22 64.85>	*2,23 36.48	*4,26 115.46>	*6,26 46.27>
3	*4,32 40.05	*7,32 42.08			
4	*4, 2 31.32	*5, 5 66.02>	*5, 7 32.82	*3, 9 43.13	*5,13 54.45>
4	*6,14 47.60>	*3,16 29.67	*7,18 60.70>	*3,19 51.74>	*7,22 34.09
4	*2,23 50.25>	*1,26 93.27>	*4,26 52.28>	*5,29 65.64>	*8,29 33.78
4	*1,30 38.06	*4,32 35.15			
97	*5, 5 32.46	*5, 7 35.01	*6, 9 34.80	*3,12 32.33	*6,14 77.58>
97	*3,16 67.18>	*6,20 32.60	*2,23 63.09>	*1,26 32.01	*6,26 54.94>
97	*8,26 86.67>	*5,29 44.34>	*8,29 60.12>	*4,32 48.81>	
98	*5, 5 50.40>	*5, 7 47.09>	*3, 9 36.20	*6, 9 97.07>	*3,12 49.15>
98	*5,13 41.40	*6,14 54.56>	*7,22 56.54>	*4,26 53.74>	*6,26 80.88>
98	*8,26 53.03>	*8,29 77.67>	*1,30 62.89>	*4,32 33.17	
99	*4, 2 56.00>	*5, 5 51.36>	*3, 9 35.30	*6, 9 49.43>	*5,13 63.85>
99	*6,14 59.05>	*7,18 42.64	*3,19 81.54>	*6,20 38.96	*2,23 57.68>
99	*6,26 42.43	*8,26 56.47>	*4,32 38.78	*7,32 74.84>	
100	*4, 2 56.72>	*5, 5 63.66>	*5, 7 41.01	*6, 9 30.29	*3,19 96.80>
100	*7,22 76.70>	*2,23 41.92	*1,26 33.68	*6,26 38.07	*1,30 49.44>
100	*4,32 42.69				

PROB. FALSE ALARM (TYPE I ERROR) 23300 SAMPLES

ALPHA: .40 .30 .20 .10 .05 .01 .0010 .00010 .000010 .0000010
FR.FA: 0.40 0.30 0.20 0.10 0.05 0.01 0.0009 0.00004 0.000000 0.0000000

PROB. DETECTION (POWER OF TEST) 2300 SAMPLES

PR(D): 1.00 1.00 1.00 1.00 1.00 1.00 0.99 0.90 0.63 0.30
FR(D): 1.00 1.00 1.00 1.00 1.00 1.00 0.99 0.90 0.62 0.31

Fig. 3.2—Simulation of Likelihood Ratio Test for Signals Common to R Replications: Summary of 100 Runs, White Noise

SIGNALS COMMON TO 8 REALIZATIONS OF NORMALLY DISTRIBUTED NOISE
SPECTRAL DENSITY= $F(K,W)=1+.25*\text{COS}(K+\text{PI}/4)*\text{COS}(2W)$

SIMULATED ARRAY= 8 X 64 WITH 8 REPS/RUN (8 X 32 COMPLEX VARIATES)
INIT. N: 3388 1062 3389 1062 P: 3391 1062 3392 1062

6 SIGNAL COMPONENTS: S/N=0.01566 (-18.05 DB)

N\M	F(M,N)							
	1	2	3	4	5	6	7	8
1	0.72	2.37	0.02	0.47	0.32	1.20	3.18	0.03
2	4.94	0.93	3.81	1.89	0.05	0.86	1.41	0.16
3	0.21	0.41	1.04	0.26	2.34	0.30	0.87	0.14
4	0.20	0.62	3.14	4.17	0.46	0.15	0.58	0.38
5	0.62	0.33	1.08	1.57	48.95*>	1.51	1.61	0.82
6	2.16	2.73	2.63	0.20	0.20	0.71	0.20	0.02
7	0.21	1.03	0.85	0.11	3.32	0.54	0.00	0.10
8	0.58	0.19	0.64	0.51	2.67	1.84	0.22	0.15
9	1.86	1.36	3.73	1.77	0.46	2.37	0.50	0.03
10	0.95	0.19	1.96	0.13	0.53	1.64	2.81	2.66
11	0.10	1.19	1.84	0.26	5.06	0.56	0.69	0.12
12	1.16	1.84	4.18	0.19	2.20	29.24*	1.54	2.09
13	0.90	2.23	0.41	0.97	0.11	0.09	0.44	0.45
14	1.02	2.66	1.08	0.89	0.38	0.62	0.44	0.20
15	0.29	1.83	1.65	0.38	0.77	1.19	5.21	2.63
16	0.57	0.02	31.89#	1.87	1.02	2.58	6.95	0.39
17	0.93	0.41	0.44	1.55	0.30	2.75	0.62	0.14
18	0.94	0.26	0.02	0.05	0.44	0.24	1.09	1.78
19	0.65	0.80	0.11	0.26	0.43	0.21	0.64	0.60
20	0.59	0.80	1.26	2.44	5.60	0.56	0.61	0.09
21	0.03	0.07	1.21	0.54	0.44	0.91	1.45	0.70
22	1.19	0.23	3.74	0.45	0.44	2.10	0.39	0.38
23	0.42	1.96	4.74	0.67	0.45	0.77	1.89	0.04
24	0.29	2.75	37.19†	0.32	1.27	1.45	81.54#>	0.53
25	0.14	5.18	0.83	0.51	1.20	0.05	0.55	0.23
26	0.25	0.98	1.92	0.22	2.48	0.79	0.45	2.00
27	2.95	0.36	0.97	0.49	0.41	0.21	0.53	10.06
28	3.85	1.01	1.08	0.85	0.33	0.19	0.57	2.35
29	2.23	2.61	0.07	0.36	3.87	3.13	0.03	0.39
30	0.42	0.85	0.82	0.96	0.48	0.68	0.06	0.17
31	0.20	0.34	0.80	0.21	0.20	0.40	0.16	1.34
32	0.07	0.04	0.07	1.49	1.36	1.28	49.56†>	2.67

PROB. FALSE ALARM (TYPE I ERROR) 250 SAMPLES

ALPHA: .40 .30 .20 .10 .05 .01 .0010 .00010 .000010 .0000010
FR.FA: 0.37 0.29 0.22 0.10 0.06 0.01 0.0000 0.000000 0.000000 0.0000000

PROB. DETECTION (POWER OF TEST) 2 SAMPLES EACH

PR(D#): 1.00 1.00 1.00 1.00 1.00 1.00 1.00 0.98 0.85 0.54
FR(D#): 1.00 1.00 1.00 1.00 1.00 1.00 1.00 1.00 1.00 0.50
PR(D*): 1.00 1.00 1.00 1.00 1.00 1.00 0.99 0.90 0.63 0.30
FR(D*): 1.00 1.00 1.00 1.00 1.00 1.00 1.00 1.00 0.50 0.50
PR(D†): 1.00 1.00 1.00 1.00 1.00 1.00 0.96 0.78 0.44 0.17
FR(D†): 1.00 1.00 1.00 1.00 1.00 1.00 1.00 1.00 1.00 0.50

Fig. 3.3—Simulation of Likelihood Ratio Test for Signals Common to
R Replications: Results of One Run, Nonwhite Noise

SIGNALS COMMON TO 8 REALIZATIONS OF NORMALLY DISTRIBUTED NOISE
 SPECTRAL DENSITY= $F(K,W)=1+.25*\text{COS}(K+\text{PI}/4)*\text{COS}(2W)$

SIMULATED ARRAY= 8 X 64 WITH 8 REPS/RUN (8 X 32 COMPLEX VARIATES)
 INIT. N: 1751 11922 1752 11922 P: 1753 11922 1754 11922

6 SIGNAL COMPONENTS: S/N=0.01566 (-18.05 DB)

[(M,N,F): F(M,N)>F(.00001;2,14)]

RUN	M, N: F	M, N: F	M, N: F	M, N: F	M, N: F
1	*6,12 36.63	#3,16 51.69>	#7,24 30.41	†7,32 43.58>	
2	#3,16 70.62>	#7,24 55.12>	†7,32 41.07		
3	*6,12 55.72>	†3,24 40.59	#7,24 93.47>	†7,32 33.21	
4	*5, 5 41.22	*6,12 73.35>	#3,16 30.89	†3,24 29.67	#7,24 35.47
4	†7,32 34.33				
5	*5, 5 45.22>	*6,12 57.29>	#3,16 33.74	†7,32 29.54	
6	*5, 5 41.80	#3,16 48.26>	#7,24 44.83>	†7,32 66.96>	
7	†3,24 68.77>	#7,24 54.16>	†7,32 41.75		
8	*5, 5 34.77	#3,16 38.26	†3,24 51.91>		
9	*5, 5 36.55	#3,16 39.27	#7,24 82.68>		
10	*6,12 37.39	#3,16 59.51>	#7,24 54.36>		
11	*5, 5 39.59	*6,12 43.13	#7,24 39.59	†7,32 34.59	
12	*6,12 37.52	#3,16 34.63	†3,24 29.44	#7,24 30.27	†7,32 41.10
13	*5, 5 34.36	*6,12 38.51	#3,16 52.59>	†3,24 33.71	#7,24 62.03>
93	*5, 5 38.79	*6,12 33.22	#3,16 50.96>		
94	*6,12 39.87	#3,16 29.40	†3,24 36.98	#7,24 52.74>	
95	*5, 5 60.74>	#3,16 45.59>	†3,24 52.38>	#7,24 30.90	
96	*5, 5 84.96>	#3,16 41.09	#7,24 77.92>		
97	*5, 5 32.51	*6,12 38.68	#3,16 80.22>	†3,24 58.85>	#7,24 31.36
98	*5, 5 50.95>	#7,24 40.13			
99	*5, 5 60.02>	#7,24 46.82>	†7,32 105.29>		
100	*5, 5 67.47>	*6,12 34.17	#3,16 53.11>	†3,24 40.94	#7,24 29.79

PROB. FALSE ALARM (TYPE I ERROR) 25000 SAMPLES

ALPHA: .40 .30 .20 .10 .05 .01 .0010 .00010 .000010 .0000010
 FR.FA: 0.40 0.30 0.20 0.10 0.05 0.01 0.0009 0.00004 0.000000 0.0000000

PROB. DETECTION (POWER OF TEST) 200 SAMPLES EACH

PR(D#): 1.00 1.00 1.00 1.00 1.00 1.00 1.00 0.98 0.85 0.54
 FR(D#): 1.00 1.00 1.00 1.00 1.00 1.00 1.00 0.98 0.89 0.60
 PR(D*): 1.00 1.00 1.00 1.00 1.00 1.00 0.99 0.90 0.63 0.30
 FR(D*): 1.00 1.00 1.00 1.00 1.00 1.00 0.99 0.91 0.68 0.36
 PR(D†): 1.00 1.00 1.00 1.00 1.00 1.00 0.96 0.78 0.44 0.17
 FR(D†): 1.00 1.00 1.00 1.00 1.00 1.00 0.97 0.77 0.47 0.19

Fig. 3.4—Simulation of Likelihood Ratio Test for Signals Common to R Replications: Summary of 100 Runs, Nonwhite Noise

$$f(\kappa, \omega) = 1 + \cos(\kappa + \pi/4) \cos(2\omega)/4. \quad (3.15)$$

Six signal components with the same signal to noise ratio as before (-18.05 dB) were added, two each in regions of low ($f = 0.75$), medium ($f = 1.0$) and high ($f = 1.25$) noise spectral density. These are indicated by the symbols “#”, “*” and “↑”, respectively. The respective non-centrality parameters are 85.33, 64 and 51.2. Figure 3.3 is a computer printout of a single run, and Fig. 3.4 is a portion of the printout of 100 successive runs. The notation is that of Figs. 3.1 and 3.2, except that the probabilities and relative frequencies of detection are listed separately for signals in each of the three types of noise regions. The agreement is quite satisfactory.

3.4 Signals with Unknown Epochs

In many applications to periodic phenomena, the assumption of a fixed signal common to all replications is not valid if “replications” are to be obtained over successive spatial or temporal intervals. The epoch of an otherwise fixed signal may vary in successive realizations. For periodic signals, the relative phase between realizations or the epoch of each realization depends on the signal frequency. This is not a serious problem if a hypothesis test for a single specified frequency component is to be made. In general, however, the alternate hypothesis is composite and the problem becomes more difficult.

In view of Fourier's theorem and its various extensions, a fairly general model for two-dimensional periodic signals is a more realistic version of the model used in section 3.2. Consider a signal component represented by $s(x, t) = A \cos(\kappa x + \omega t)$ for continuous x and t , where

$$\kappa = 2\pi(k + \delta_k)/M, \quad |\delta_k| \leq \frac{1}{2}, \quad k = 0, \dots, M/2,$$

and

$$\omega = 2\pi(f + \delta_f)/N, \quad |\delta_f| \leq \frac{1}{2}, \quad f = 0, \dots, N/2. \quad (3.16)$$

Observations at discrete spatial and temporal points $x = 0, \dots, M - 1, t = 0, \dots, N - 1$ yields

$$y_1(x, t) = A \cos [2\pi(k + \delta_k)x/M + 2\pi(f + \delta_f)t/N - \phi] + n_1(x, t), \quad (3.17)$$

where ϕ is the phase relative to the origin of observations. Consider R realizations, obtained during successive time intervals.

Then

$$\begin{aligned}
 y_r(x, t) &= s_1(x, t + (r-1)N) + n_r(x, t) \\
 &= A \cos [2\pi(k + \delta_k)x/M + 2\pi(f + \delta_f)t/N + \alpha_r] + n_r(x, t) , \quad (3.18)
 \end{aligned}$$

where $\alpha_r = 2\pi\delta_f(r-1) - \phi$, $r = 1, \dots, R$.

If δ_k and δ_f are both zero, i.e., if the signal is a member of the basis set used in the DFT, then (3.18) reduces to a special case of the model considered in sections 3.1-3.3. In general, it cannot be assumed that the signals are members of the basis set, so that we no longer have a fixed signal common to all realizations, and no true replications are possible. In this section, we will attempt to make reasonable estimates of the unknown α_r . In the next chapter we will eliminate this unknown, thereby altering the problem.

Since wavenumber resolution and frequency resolution are limited to $\Delta k = 1/M$ and $\Delta f = 1/N$ respectively, we may write

$$y_r(x, t) = A \cos (2\pi kx/M + 2\pi ft/N + \alpha_r) + n_r(x, t) . \quad (3.19)$$

In obtaining (3.19) from (3.18), we are ignoring the effect of non-zero δ_k and δ_f on wavenumber and frequency, but not on phase. Non-zero δ_k and δ_f means that signal energy will be distributed over the entire wavenumber-frequency space, rather than being concentrated in a single cell. In general, if $S_r(m, n) \neq 0$, a signal effect may be expected in three adjacent cells when δ_k and δ_f are not zero. For the weak signals which are of primary interest, the signal effect beyond these four cells may safely be ignored. It is notationally convenient to maintain the fiction that the energy from each signal component is concentrated in a single (m, n) cell. Signal detectability on a cell by cell basis will of course require greater signal energy when that energy is spread over a cluster of four cells.

Generalizing to J signal components, the model becomes

$$\begin{aligned}
 y_r(x, t) &= \sum_{j=1}^J A_j \cos (2\pi k_j x/M + 2\pi f_j t/N + \alpha_{jr}) + n_r(x, t) , \\
 x &= 0, \dots, M-1, t = 0, \dots, N-1, r = 1, \dots, R . \quad (3.20)
 \end{aligned}$$

The DFT is as in (3.11), with $\alpha_r = 2\pi \delta_f(r-1) - \phi_j$ replacing $-\phi_j$. With the same simplifications as (3.12) when the null hypothesis is not valid it yields

$$Y_r(m, n) = B(m, n)e^{i\beta_r(m, n)} + \epsilon_r(m, n) \text{ when } (m, n) \in Q - D, \quad (3.21)$$

where $B(m, n) = (1/2)\sqrt{MN}A_j e^{-i\phi_j}$ and $\beta_r(m, n) = \alpha_r + \phi_j = 2\pi\delta_{jf}(r-1)$, for some $j \in \{1, \dots, J\}$. As in section 3.2, we consider the data array to be relabeled to yield the $2M'N'R$ real variables

$Y_{\mathcal{R}r}(m, n)$, $Y_{\mathcal{I}r}(m, n)$, $m = 1, \dots, M' < M$, $n = 1, \dots, N' < N/2$, $r = 1, \dots, R$, but drop the primes on M and N when testing hypotheses.

Letting $Y'_r(m, n) = Y_r(m, n)e^{-i\beta_r(m, n)}$, (3.21) becomes

$$Y'_r(m, n) = B(m, n) + \epsilon'_r(m, n) \quad (3.22)$$

where

$$\epsilon'_r(m, n) = \epsilon'_{\mathcal{R}r}(m, n) - i \epsilon'_{\mathcal{I}r}(m, n),$$

$$\epsilon'_{\mathcal{R}r}(m, n) = \epsilon_{\mathcal{R}r}(m, n) \cos \beta_r(m, n) - \epsilon_{\mathcal{I}r}(m, n) \sin \beta_r(m, n),$$

and

$$\epsilon'_{\mathcal{I}r}(m, n) = \epsilon_{\mathcal{R}r}(m, n) \sin \beta_r(m, n) + \epsilon_{\mathcal{I}r}(m, n) \cos \beta_r(m, n).$$

Then $\epsilon'_{\mathcal{R}r}(m, n)$ and $\epsilon'_{\mathcal{I}r}(m, n)$ are each distributed as $N(0, (1/2) f(\kappa_m, \omega_n))$, and

$$\text{cov} \left(\epsilon'_{\mathcal{R}r}(m, n), \epsilon'_{\mathcal{I}r}(m, n) \right) = 0 \left(\frac{1}{M} \right) \cdot 0 \left(\frac{1}{N} \right).$$

Equation (3.22) has the same form as (3.12) and (3.2), so that

$$\hat{B}(m, n) = \hat{B}_{\mathcal{R}}(m, n) + i\hat{B}_{\mathcal{I}}(m, n) = \bar{Y}'(m, n) = \frac{1}{R} \sum_{r=1}^R Y_r(m, n)e^{-i\beta_r(m, n)}, \quad (3.23)$$

by (3.5). If one is willing to accept a less powerful test and pay the price of increased com-

putation, a modification of the development of section 3.1 can be applied even though $\beta_r(m, n)$ is unknown. Consider replacing (3.23) as an estimator of $B(m, n)$ by

$$\hat{B}(m, n) = \frac{1}{R} \sum Y_r(m, n) e^{-i\gamma_r(m, n)}, \quad (3.24)$$

with $\gamma_r(m, n)$ to be chosen. Then

$$\hat{B}_R(m, n) = \frac{1}{R} \sum_{r=1}^R [Y_{Rr}(m, n) \cos \gamma_r(m, n) - Y_{\Im r}(m, n) \sin \gamma_r(m, n)] \quad (3.25)$$

is normal with mean

$$\begin{aligned} E\{\hat{B}_R\} &= \frac{1}{R} \sum_{r=1}^R [(B_R \cos \beta_r - B_{\Im} \sin \beta_r) \cos \gamma_r + (B_R \sin \beta_r + B_{\Im} \cos \beta_r) \sin \gamma_r] \\ &= \frac{1}{R} \sum_{r=1}^R [B_R \cos(\gamma_r - \beta_r) + B_{\Im} \sin(\gamma_r - \beta_r)] \end{aligned}$$

and variance $f(\kappa_m, \omega_n)/2R$, and

$$\hat{B}_{\Im}(m, n) = -\frac{1}{R} \sum_{r=1}^R [Y_{Rr}(m, n) \sin \gamma_r(m, n) + Y_{\Im r}(m, n) \cos \gamma_r(m, n)] \quad (3.26)$$

is

$$N\left(-\frac{1}{R} \sum_{r=1}^R [B_R \sin(\gamma_r - \beta_r) - B_{\Im} \cos(\gamma_r - \beta_r)], f/2R\right).$$

Signal power at the point (m, n) is given by $R |B(m, n)|^2$ and estimated by $R |\hat{B}(m, n)|^2$, where $R |\hat{B}(m, n)|^2 / [f(\kappa_m, \omega_n)/2]$ has the non-central chi-square distribution with 2 degrees of freedom and non-centrality parameter

$$\begin{aligned} \delta_{\text{eff}}^2(m, n) &= RE^2 \{\hat{B}_R(m, n)\} / [f(\kappa_m, \omega_n)/2] + RE^2 \{\hat{B}_{\Im}(m, n)\} / [f(\kappa_m, \omega_n)/2] \\ &= R |B|^2 \left\{ \left[\frac{1}{R} \sum_{r=1}^R \cos(\gamma_r - \beta_r) \right]^2 + \left[\frac{1}{R} \sum_{r=1}^R \sin(\gamma_r - \beta_r) \right]^2 \right\} / (f/2) \quad (3.27) \end{aligned}$$

$$\leq R |B(m, n)|^2 / [f(\kappa_m, \omega_n)/2]$$

by the Cauchy-Schwarz inequality. The probability of "false alarm" (the size of the test) is independent of $\gamma_r(m, n)$ (chosen in advance) but the probability of detection (the power of the test) is quite sensitive to choice of $\gamma_r(m, n)$. At each point (m, n) let $\gamma_r - \beta_r = (r-1)x = kx$. Then by (3.27), the effective signal power density is reduced by the factor

$$\begin{aligned} P(R, x) &= \left[\frac{1}{R} \sum_{k=0}^{R-1} \cos kx \right]^2 + \left[\frac{1}{R} \sum_{k=0}^{R-1} \sin kx \right]^2 \\ &= \frac{1}{R^2} \left[\frac{1}{2} + \frac{\sin \left(R + \frac{1}{2} \right) x}{2 \sin x/2} - \cos Rx \right]^2 + \frac{1}{R^2} \left[\frac{\cos x/2 - \cos \left(R + \frac{1}{2} \right) x}{2 \sin x/2} - \sin Rx \right]^2 \end{aligned}$$

(See e.g., Tolstov [41], p. 98.) After straightforward manipulation, this becomes

$$P(R, x) = \frac{1}{2R^2} (1 - \cos Rx) \operatorname{csc}^2 x/2. \quad (3.28)$$

For fixed R , $P(R, x)$ is an even function of x , monotonically decreasing for $0 \leq x \leq \pi/2R$, $P(R, x) \geq \operatorname{csc}^2(\pi/4R)/2R^2 \geq 8/\pi^2$, and $\lim_{R \rightarrow \infty} P(R, \pi/2R) = 8/\pi^2$. Recall that $\beta_r(m, n) = 2\pi \delta_{jf}(r-1)$ where $|\delta_{jf}| \leq 1/2$. Let $\gamma_1(m, n) = \beta_1(m, n) = 0$. For all R and all $\delta_{jf} \in [-1/2, 1/2]$, there exists an integer $k \in [-R, R]$ such that $2R \delta_{jf} - 1/2 \leq k \leq 2R \delta_{jf} + 1/2$. For this k , if $\gamma_r = k\pi(r-1)/R$ for $r > 1$, then

$$|x| = \frac{|\gamma_r - \beta_r|}{r-1} = \frac{\pi}{R} |k - 2R\delta_{jf}| \leq \pi/2R.$$

The signal power, and hence the signal to noise (power) ratio, will be reduced by a factor of at most $8/\pi^2 > .8$ (at most 1 dB), compared to the ideal situation of known $\beta_r(m, n)$.

If we choose $\gamma_r = k\pi(r-1)/R$ for the $k \in [-R, R]$ which maximizes $|\hat{B}(m, n)|^2$ (see (3.24)), the probability of false alarm will of course be increased. We can compensate for this by choosing the nominal level of the test, α , low enough so that an adjusted level, α' , is as desired. The power (in both the statistician's sense and the physicist's sense) remains as before, including the "penalty" factor of $8/\pi^2$ for quantizing the analysis. For each value of k , the statistic

$$\mathcal{F}_k(m, n) = \frac{R |\hat{B}_k(m, n)|^2}{\sum_{r=1}^R |Y_{rk}''(m, n) - \hat{B}_k(m, n)|^2 / (R-1)},$$

where $\hat{B}_k(m, n)$ is given by (3.24) with $\gamma_r = k\pi(r-1)/R$, and $Y_{rk}''(m, n) = Y_r(m, n)e^{-i\gamma_r(m, n)}$, has asymptotically the F distribution with 2 and $2(R-1)$ degrees of freedom under the null hypothesis. Under the alternate hypothesis, $\mathcal{F}_k(m, n)$ has the non-central F distribution with the same degrees of freedom and non-centrality parameter given by (3.27) and bounded below by

$$\delta_k^2(m, n) \geq (8/\pi^2)R|B(m, n)|^2/[f(\kappa_m, \omega_n)/2].$$

Let $\mathcal{F}'(m, n)$ be the corresponding statistic for the k which maximizes $|\hat{B}(m, n)|^2$. If the \mathcal{F}_k were independent, and if $\mathcal{F}' = \max_{k \in [-R, R]} (\mathcal{F}_k)$ (neither of which is claimed), then we would have

$$\begin{aligned} \alpha' &= P[\mathcal{F}' > F_{\alpha; \nu_1, \nu_2}] \\ &= P[\max(\mathcal{F}_{-R}, \dots, \mathcal{F}_R) > F_{\alpha; \nu_1, \nu_2}] \\ &= 1 - P[\mathcal{F}_{-R} \leq F_{\alpha; \nu_1, \nu_2}, \dots, \mathcal{F}_R \leq F_{\alpha; \nu_1, \nu_2}] \\ &= 1 - (1 - \alpha)^{2R+1}. \end{aligned}$$

The required low adjusted test levels, α' , thus require, a fortiori, extension of F tables to even lower levels, α . Calculations using the computer program mentioned in section 3.3 revealed that acceptable probabilities of detection still exist, even at the low adjusted test levels (false alarm probabilities).

3.5 Simulated Tests of Signals with Unknown Epochs

That some limited success can be achieved with the above procedure is indicated by computer simulation. As in section 3.3, simulation was performed in the wavenumber-frequency domain, using (3.21)-(3.26). Fig. 3.5 is a typical computer printout of the results of one run, assuming a white Gaussian noise process with $f(\kappa_m, \omega_n) \equiv 1$. The notation is the same as that of Fig. 3.1, and the identical pseudo-random "noise" sequence was used. As before, "*" identifies those cells in which the null hypothesis was not true, with the signal to noise ratio the

same as in Fig. 3.1. $|\hat{B}_k(m,n)|^2$ was computed for each of the 17 values of k in $[-8,8]$, for each of the 256 cells, and $\mathcal{F}'(m,n)$ computed for each of the largest $|\hat{B}_k(m,n)|^2$. A transpose of the matrix ($\mathcal{F}'(m,n)$) is shown in the figure. The ">" symbol identifies those \mathcal{F}' which fall in the rejection region of a test of size $\alpha' = 1 - (1 - \alpha)^{17} = 10^{-4}$. (None did in this run. See Fig. 3.6.)

Theoretical probabilities and observed relative frequencies are tabulated at the bottom of the figure. "NOM.ALPHA" represents the nominal α , with $.4 \geq \alpha \geq 5.9 \times 10^{-7}$, "MAX.P(FA)" represents the level of the test, $\alpha' = 1 - (1 - \alpha)^{17}$, with $1 \geq \alpha' \geq 10^{-5}$, the "REL.FR.FA" indicates the relative frequency of type I errors at each of the above test levels. "NOM.P(DT)" represents the probability of detection for known $\beta_r(m,n)$ at each of the above test levels, calculated from the $F'_{2,14;64}$ distribution, while "PR.D:-1 DB" was calculated with a noncentrality parameter of 50.8, corresponding to a -19.05 dB signal and "PR.D:-2 DB" was calculated with a noncentrality parameter of 40.32, corresponding to a -20.07 dB signal. "REL.FR.DT" indicates the relative frequency of detection obtained.

Fig. 3.6 is a portion, including the tabulation of probabilities and frequencies, of a print-out of 100 similar runs in succession. Although the type I errors are close to the expected values, the observed relative frequencies of detection are lower than expected, but still within an acceptable range.

It must be noted that this approach assumes that the signal components are sufficiently stable in frequency to warrant R "replications" (as well as that the noise is stationary during the observation time). If this is the case, increasing N , the number of time samples, with consequent increased frequency resolution (and fewer "replications") may be desirable. In fact, if a single $M \times RN$ transform is feasible, the version of the problem of unknown epochs considered in this section disappears. In that case, R adjacent frequency "columns" yield the desired replications. If the size of the transform is limited, as it might be, for example, if the analysis must be in "real time," or if the analysis is on already transformed data, this approach may be useful. It must, of course, be compared with alternate techniques. If successive realizations result from observations at different spatial points (different arrays) the phase difference between realizations is completely unknown, and may be eliminated by the procedure considered in the next chapter.

SIGNALS WITH UNKNOWN EPOCHS, SPECTRAL DENSITY=1.0

SIMULATED ARRAY= 8 X 64 WITH 8 REPS/RUN (8 X 32 COMPLEX VARIATES)
 INIT. N: 3388 1062 3389 1062 P: 3391 1062 3392 1062

23 SIGNAL COMPONENTS: S/N=0.01566 (-18.05 DB)

N\M	F' (M,N)							
	1	2	3	4	5	6	7	8
1	3.37	2.86	4.12	7.25	5.26	4.17	3.92	5.01
2	2.96	4.17	3.11	20.00*	10.76	2.34	3.84	2.97
3	4.41	8.82	6.53	3.94	3.62	7.48	3.16	3.24
4	7.32	5.64	3.36	3.92	3.79	4.93	2.42	3.05
5	6.11	3.57	4.46	2.04	29.74*	3.58	3.01	2.66
6	6.42	4.48	4.54	3.57	13.55	5.83	1.94	3.03
7	3.44	2.56	4.17	4.00	24.18*	3.52	3.98	3.64
8	2.51	3.83	4.43	3.48	1.95	4.30	5.90	8.86
9	5.03	1.74	19.99*	2.65	3.24	21.45*	2.50	3.69
10	3.49	7.05	6.49	4.39	2.62	3.80	2.71	4.37
11	3.80	2.94	9.10	5.41	7.14	3.10	9.66	6.35
12	3.43	2.42	23.72*	3.86	2.79	3.52	4.56	3.82
13	5.74	3.64	2.80	4.82	22.63*	7.10	4.68	4.08
14	4.35	4.51	7.45	3.29	2.69	16.20*	3.16	3.25
15	9.21	5.03	3.19	3.64	2.13	5.22	4.19	5.45
16	3.90	2.18	28.81*	3.31	3.58	5.33	6.54	4.41
17	4.39	6.60	2.87	3.91	3.97	2.78	2.80	2.75
18	3.60	2.77	5.34	3.13	9.36	4.18	20.49*	2.35
19	4.46	2.00	12.72*	10.04	3.42	4.87	2.27	5.06
20	5.01	4.28	4.53	4.30	4.41	13.98*	2.99	7.18
21	3.74	4.81	2.37	3.95	2.63	3.54	3.07	3.11
22	2.32	4.83	3.34	2.14	3.23	4.26	24.53*	3.98
23	4.10	11.32*	5.15	2.63	4.41	3.89	2.27	3.22
24	2.89	3.20	2.55	2.29	3.12	7.80	4.21	5.66
25	4.86	7.21	2.66	10.32	6.09	2.64	1.69	4.87
26	18.02*	8.15	3.23	18.39*	3.48	28.66*	5.19	15.29*
27	2.07	3.80	4.41	13.64	6.09	3.75	3.00	5.05
28	9.11	5.18	2.50	4.16	4.79	3.34	4.63	3.66
29	4.24	4.13	6.58	3.71	8.10*	5.53	3.78	20.63*
30	24.72*	8.14	2.36	2.27	8.87	6.05	3.18	4.37
31	3.43	4.05	2.54	3.65	5.44	3.87	3.08	5.26
32	2.29	4.10	8.56	24.84*	3.84	4.10	19.36*	3.18

PROB. FALSE ALARM (TYPE I ERROR) 233 SAMPLES

NOM.ALPHA:	.40	.30	.20	.10	.05	.01	.001	6E-5	5.9E-6	5.9E-7
MAX.P(FA):	1.00	1.00	.98	.83	.58	.16	.017	.0010	.00010	.000010
REL.FR.FA:	1.00	1.00	0.99	0.84	0.56	0.13	0.009	0.0000	0.00000	0.000000

PROB. DETECTION (POWER OF TEST) 23 SAMPLES

NOM.P(DT):	1.00	1.00	1.00	1.00	1.00	1.00	0.99	0.86	0.55	0.24
PR.D:-1DB:	1.00	1.00	1.00	1.00	1.00	1.00	0.96	0.70	0.36	0.13
PR.D:-2DB:	1.00	1.00	1.00	1.00	1.00	0.99	0.89	0.52	0.21	0.06
REL.FR.DT:	1.00	1.00	1.00	1.00	1.00	1.00	0.91	0.43	0.00	0.00

Fig. 3.5—Simulation of Modified Likelihood Ratio Test: Results of One Run

SIGNALS WITH UNKNOWN EPOCHS, SPECTRAL DENSITY=1.0

SIMULATED ARRAY= 8 X 64 WITH 8 REPS/RUN (8 X 32 COMPLEX VARIATES)
INIT. N: 1751 11922 1752 11922 P: 1753 11922 1754 11922

23 SIGNAL COMPONENTS: S/N=0.01566 (-18.05 DB)

[(M,N,F'): F'(M,N)>F(5.9E-5;2,14)]

RUN	M, N:	F'	M, N:	F'	M, N:	F'	M, N:	F'	M, N:	F'
1	*5, 7	21.92	*3, 16	25.04	*7, 18	48.05>	*3, 19	33.95>	*6, 20	23.66
1	*7, 22	64.67>	*1, 26	84.97>	*8, 29	22.13				
2	*4, 2	60.49>	*5, 7	22.55	*3, 9	24.67	*6, 9	35.81>	*3, 16	54.13>
2	*7, 22	24.29	*1, 26	26.52	*4, 26	39.40>	*6, 26	21.44	*5, 29	22.45
2	*8, 29	32.19>	*1, 30	60.93>						
3	*4, 2	30.16	*5, 5	22.67	*5, 7	38.36>	*3, 9	22.12	*3, 12	59.07>
3	*7, 18	21.92	*3, 19	22.72	*6, 20	26.43	*7, 22	25.66	*7, 32	31.45
4	*4, 2	35.76>	*5, 5	48.30>	*3, 9	39.85>	*5, 13	23.42	*6, 14	22.58
4	*7, 18	42.56>	*3, 19	21.67	*7, 22	23.69	*2, 23	22.97	*1, 26	66.24>
4	*6, 26	29.56	*8, 26	40.58>	*8, 29	21.34	*1, 30	37.35>	*4, 32	29.06
5	*5, 5	24.96	*5, 7	33.36>	*6, 9	36.21>	*6, 14	34.67>	*3, 16	30.02
5	*3, 19	22.38	*4, 26	44.25>	*5, 29	28.23	*4, 32	25.55		
6	*4, 2	38.91>	*5, 5	34.13>	*3, 12	64.82>	*5, 13	21.89	*3, 16	24.08
6	1, 23	25.36	*2, 23	23.43	*4, 26	22.06	*5, 29	21.15	*1, 30	21.90
6	*4, 32	30.86	*7, 32	27.80						
96	*7, 18	33.65>	*6, 20	42.70>	*1, 26	27.63	*4, 26	32.31>	*5, 29	62.36>
96	*7, 32	24.15								
97	*5, 7	26.76	1, 13	30.26	*3, 16	34.34>	*6, 20	30.21	*7, 22	21.69
97	*2, 23	23.39	*8, 26	44.70>	*5, 29	22.42	*8, 29	25.74	*1, 30	22.03
97	*4, 32	39.17>	*7, 32	27.22						
98	*3, 9	22.51	*6, 9	46.02>	*3, 12	25.84	*3, 19	26.94	*2, 23	32.44>
98	*6, 26	28.08	*8, 26	30.36	*8, 29	24.11	*1, 30	24.57	*7, 32	21.24
99	*3, 9	103.84>	*6, 9	52.38>	*3, 16	32.18>	*7, 18	28.71	*3, 19	26.33
99	*7, 22	26.07	*2, 23	27.08	*5, 29	30.59	*7, 32	24.65		
100	*5, 13	22.66	*3, 19	73.12>	*6, 20	25.00	*7, 22	24.16	*2, 23	36.10>
100	*4, 26	32.51>	*4, 32	35.66>						

PROB. FALSE ALARM (TYPE I ERROR) 23300 SAMPLES

NOM. ALPHA:	.40	.30	.20	.10	.05	.01	.001	6E-5	5.9E-6	5.9E-7
MAX. P(FA):	1.00	1.00	.98	.83	.58	.16	.017	.0010	.00010	.000010
REL. FR. FA:	1.00	1.00	1.00	0.87	0.57	0.14	0.012	0.0006	0.00004	0.000000

PROB. DETECTION (POWER OF TEST) 2300 SAMPLES

NOM. P(DT):	1.00	1.00	1.00	1.00	1.00	1.00	0.99	0.86	0.55	0.24
PR. D: -1DB:	1.00	1.00	1.00	1.00	1.00	1.00	0.96	0.70	0.36	0.13
PR. D: -2DB:	1.00	1.00	1.00	1.00	1.00	0.99	0.89	0.52	0.21	0.06
REL. FR. DT:	1.00	1.00	1.00	1.00	1.00	1.00	0.91	0.46	0.17	0.06

Fig. 3.6—Simulation of Modified Likelihood Ratio Test:
Summary of 100 Runs

4. AN AD HOC TEST FOR SIGNALS WITH UNKNOWN EPOCHS

When the epoch or phase of a signal varies between realizations, the identical signal is not common to all observations and no true replications are possible. Classical techniques involving averaging cannot be extended to this situation without difficulties. As in section 3.4, we have

$$y_r(x,t) = s_r(x,t) + n_r(x,t) , \quad (4.1)$$

$x = 0, 1, \dots, M - 1; t = 0, 1, \dots, N - 1; r = 1, \dots, R$, and

$$Y_r(m,n) = S_r(m,n) + \epsilon_r(m,n) \quad (4.2)$$

$m = 0, 1, \dots, M - 1; n = 0, 1, \dots, N - 1; r = 1, \dots, R$, in place of (3.1) and (3.2). If $S_r(m,n) \neq S_{r'}(m,n)$ when $r \neq r'$, observation of one provides no information concerning the other, so that averaging over r may not be desirable.

One approach to the problem involves consideration of a single $M \times RN$ space-time series. Various solutions in terms of orthogonal expansions of the signal and noise functions are possible, see, e.g., Selin [35], Helstrom [16], Wainstein and Zubakov [43]. For some problems of practical interest this array may be too large for the discrete Fourier transform (DFT) using existing computer technology. If the transform is feasible, smoothing over R adjacent frequency "columns" may produce consistent estimators.

M one-dimensional time series of N points with a common signal may be obtained by incorporating the time delay corresponding to a particular direction of arrival into each spatial sample. A separate analysis for each direction of interest using the one-dimensional DFT is then possible. (See Shumway [37].) This approach provides a one-dimensional concentration of information in the frequency domain, but does not permit any systematic use of information from analyses at nearby directions of arrival. Furthermore, unless M series of length RN are considered, R repetitions of the "experiment" provide the same problem of phase difference as in the two-dimensional approach. The additional repetitions may be used to provide estimators of the spectral mass function of a stochastic signal and spectral density function of

the noise for use in the empirical Bayes method (see Shumway and Saikia [38], Saikia [32], or Hoch [18]), but this does not seem to be the optimum use of current data.

In section 3.4 we attempted to make reasonable estimates of the unknown epochs and to correct for them. In this chapter we eliminate the unknown parameter and consider a test based on those aspects of the signals which are common to all realizations.

4.1 Distribution of the Test Statistic

From (3.21), we have

$$S_r(m,n) = B(m,n)e^{i\beta_r(m,n)} , \quad (4.3)$$

where $B(m,n) = \sqrt{MN} A_j e^{-i\phi_j/2}$ when $m = k_j$ and $n = f_j$ for some $j \in \{1, \dots, J\}$, and is zero otherwise, and $\beta_r(m,n)$ is an unknown which depends on $r = 1, \dots, R$. For all (m,n) , $S_r(m,n)$ averaged over the unknown $\beta_r(m,n)$ vanishes:

$$\frac{1}{2\pi} \int_0^{2\pi} S_r d\beta = \frac{B}{2\pi} \int_0^{2\pi} e^{i\beta_r} d\beta_r = 0 ,$$

but

$$|S_r(m,n)|^2 = |B(m,n)|^2$$

is independent of r . Thus if β_r is eliminated, a sample of size R provides R times the mean information concerning $|B(m,n)|^2$ as in a single observation. (Kullback [22], p. 13). The hypothesis $H_0: S_r(m,n) = 0, r = 1, \dots, R$ may be replaced by the equivalent hypothesis $H_0: |B(m,n)|^2 = 0$. For a deterministic signal, or a conditional model, $Y_r(m,n) = Y_{rR}(m,n) - iY_{rI}(m,n)$ is asymptotically distributed as $N(0, f(\kappa_m, \omega_n))$ under H_0 and as $N(S_r(m,n), f(\kappa_m, \omega_n))$ under H_1 . Hence $2f^{-1}(\kappa_m, \omega_n)|Y_r(m,n)|^2$ has the central chi-square distribution with two degrees of freedom under H_0 and the noncentral chi-square distribution with two degrees of freedom and noncentrality parameter $2f^{-1}(\kappa_m, \omega_n)|B(m,n)|^2$ under H_1 . Letting

$$\overline{|Y(m,n)|^2} = R^{-1} \sum_{r=1}^R |Y_r(m,n)|^2 ,$$

we have

$$U(m,n) = \frac{R|Y(m,n)|^2}{\frac{f(\kappa_m, \omega_n)}{2}} \sim \begin{cases} \chi_{2R}^2(0) & \text{under } H_0 \\ \chi_{2R}^2(2Rf^{-1}(\kappa_m, \omega_n)|B(m,n)|^2) & \text{under } H_1. \end{cases} \quad (4.4)$$

This statistic depends on the unknown spectral density $f(\kappa_m, \omega_n)$. In some situations, analysis of variance applied to prior data may be used to obtain an estimator of $f(\kappa_m, \omega_n)$, as in the empirical Bayes approach [38,32,18]. In many applications, however, the assumption of stationarity is valid only over short time periods, so that appropriate prior data may not be available. If $f(\kappa_m, \omega_n)$ varies slowly, the asymptotic independence of $Y_r(m,n)$ and $Y_r(m',n')$ for $m \neq m'$ or $n \neq n'$ suggests using data from adjacent cells. One may either estimate $f(\kappa_m, \omega_n)$ in the spirit of empirical Bayes, or form an independent chi-square variable to approximately "Studentize" $U(m,n)$. Let $\mu \ll M$ and $\nu \ll N$, let

$$\Omega(m,n;\mu,\nu) = \{ (\zeta, \xi) : m - \mu \leq \zeta \leq m + \mu, n - \nu \leq \xi \leq n + \nu, (\zeta, \xi) \neq (m,n) \}, \quad (4.5)$$

and let $H_i(m,n)$, $i = 0, 1$ be the null and alternate hypotheses respectively for the (m,n) th cell. (When the signal components are not members of the basis set used in the DFT, adjacent cells as well as (m,n) itself must be excluded from Ω . See the discussion following (3.19).)

If $H_0(\zeta, \xi)$ is true for all $(\zeta, \xi) \in \Omega(m,n;\mu,\nu)$,

$$V(m,n) = \sum_{(\zeta, \xi) \in \Omega} U(\zeta, \xi)$$

has the central chi-square distribution with $4R(\mu + 2\mu\nu + \nu)$ degrees of freedom, and is asymptotically independent of $U(m,n)$. Under these assumptions,

$$\mathcal{F}(m,n) = 2(\mu + 2\mu\nu + \nu) \frac{U(m,n)}{V(m,n)} \quad (4.6)$$

has approximately the central F distribution with $2R$ and $4R(\mu + 2\mu\nu + \nu)$ degrees of freedom under $H_0(m,n)$, and the noncentral F distribution with these degrees of freedom and noncentrality parameter $2Rf^{-1}(\kappa_m, \omega_n)|B(m,n)|^2$ under $H_1(m,n)$.

If $H_0(m,n)$ is true but $H_1(\zeta, \xi)$ is true for some $(\zeta, \xi) \in \Omega(m,n;\mu,\nu)$, then $1/\mathcal{F}(m,n)$ has a noncentral F distribution with $\nu_1 = 4R(\mu + 2\mu\nu + \nu)$ and $\nu_2 = 2R$ degrees of freedom. The false alarm probability (type I error) is then

$$P[\mathcal{F}(m,n) > F_{\alpha;\nu_2,\nu_1}] = P\left[\frac{1}{\mathcal{F}(m,n)} < F_{1-\alpha;\nu_1,\nu_2}\right] < \alpha \quad (4.7)$$

i.e., less than the nominal false alarm probability α . If $H_1(m,n)$ is true and $H_1(\zeta,\xi)$ is also true for some $(\zeta,\xi) \in \Omega(m,n;\mu,\nu)$, then the probability of detection will also be decreased, since both $U(m,n)$ and $V(m,n)$ will have a noncentral chi-square distribution. It happens sufficiently often in practice to be of interest, however, that signal components are isolated from each other in wavenumber and in frequency, so that for sufficiently small μ and ν ,

$$H_1(m,n) \Rightarrow H_0(\zeta,\xi), \forall (\zeta,\xi) \in \Omega(m,n;\mu,\nu) . \quad (4.8)$$

4.2 Simulated Examples

A computer simulated test of this procedure has been made. Each signal component was confined to a single (m,n) cell in the wavenumber-frequency space, and was isolated from other signal components in accordance with (4.8). To make room for more signal components in this relatively small (8×32) array, we take $\mu = \nu = 1$ in (4.5), and assume the data to be periodically continued in m and n .

Fig. 4.1 is a typical computer printout of the results of one run of this simulation. Eight "replications" of the 8×32 data array were generated in accordance with (4.2), assuming a white Gaussian noise process with $f(\kappa_m, \omega_n) \equiv 1$. The figure shows a transpose of the $(\mathcal{F}(m,n))$ matrix whose elements are given by (4.6), and have 16 and 128 degrees of freedom. Signal components with signal to noise ratio, defined by (3.13), of 0.01566 or -18.05 dB were added to the noise in 16 of the cells, identified by "*". The resulting noncentrality parameter is 64. The ">" symbol identifies those \mathcal{F} which fall in the rejection region of a test of size $\alpha = 10^{-6}$. Most entries in the table, having neither symbol, indicate correct rejection. An entry with an asterisk alone, as in (5,5) indicates a type II error (miss) at the level $\alpha = 10^{-6}$ ($F_{10^{-6};16,128} = 4.32$). A type I error (false alarm) would be indicated by ">" alone if there were any; "*>" indicates correct detection.

Theoretical probabilities were calculated using the program mentioned in section 3.3. For small type I errors the power of this test is greater than that of the procedure of Chapter 3, even in the case where the frequency difference and hence the difference in phase between realizations is zero. (Compare the theoretical probabilities in Fig. 4.1 with those of Fig. 3.1.) This does not violate the optimality of the T^2 test (Anderson [1], Theorem 5.5.3, p. 116) since this test depends on $|\overline{Y(m,n)}|^2$ rather than $\overline{Y(m,n)}$. Theoretical probabilities and observed relative frequencies are tabulated at the bottom of Fig. 4.1. There are 240 cells in which $H_0(m,n)$ is true. Of these, 112 are isolated, that is $H_0(\zeta,\xi)$ is true for all $(\zeta,\xi) \in \Omega(m,n;1,1)$.

AD HOC TEST
 SPECTRAL DENSITY = 1.0
 SIMULATED ARRAY= 8 X 64 WITH 8 REPS/RUN , (8 X 32 COMPLEX VARIATES)
 INIT. N: 3388 1062 3389 1062 P: 3391 1062 3392 1062

16 SIGNAL COMPONENTS: S/N=0.01566 (-18.05 DB)

NAM	F (M,N)							
	1	2	3	4	5	6	7	8
1	1.49	1.19	0.46	0.19	0.80	1.21	1.04	0.85
2	0.55	0.89	1.34	1.79	1.00	1.09	0.62	0.76
3	1.41	1.24	1.00	0.57	1.02	0.98	0.90	0.91
4	0.99	0.53	1.86	0.34	1.15	0.81	0.61	0.74
5	1.95	0.72	0.79	0.61	4.31*	0.54	1.48	0.95
6	1.40	0.41	1.63	0.85	0.52	1.01	0.78	0.57
7	0.93	1.75	0.55	0.60	0.62	1.20	1.35	0.69
8	0.96	0.93	0.35	0.91	0.80	0.49	0.28	2.00
9	0.56	0.49	5.69*>	0.49	0.74	6.65*>	0.36	1.31
10	0.98	0.73	0.73	0.50	0.21	1.15	0.60	1.49
11	0.90	0.84	0.61	0.46	1.13	0.83	0.60	0.66
12	0.29	0.62	7.56*>	0.47	0.50	1.03	0.64	2.15
13	1.06	0.40	0.31	0.70	0.83	0.87	0.84	1.27
14	1.25	0.60	0.84	1.16	0.99	3.59*	0.85	1.21
15	0.99	0.91	0.73	0.63	0.66	0.22	0.84	0.83
16	0.80	1.13	4.13*	0.61	1.13	0.56	0.97	1.24
17	0.68	0.36	1.11	0.76	1.08	0.76	0.67	0.59
18	0.78	0.76	0.61	0.71	0.85	0.56	5.67*>	1.10
19	0.99	0.79	3.77*	0.98	1.11	0.45	0.41	0.49
20	0.62	1.27	0.29	0.70	0.53	1.15	1.50	1.58
21	0.57	0.97	1.33	0.77	2.00	0.44	0.42	1.07
22	0.37	0.95	0.56	0.38	1.16	0.47	6.08*>	0.49
23	0.70	5.08*>	0.59	1.61	0.53	1.10	0.39	0.72
24	0.47	0.97	0.71	1.33	0.38	1.08	1.07	1.84
25	0.79	0.41	0.66	0.53	1.02	0.87	1.00	0.50
26	3.18*	1.18	0.35	5.50*>	0.81	0.87	0.79	0.57
27	0.56	0.97	0.49	0.43	0.89	0.48	1.17	1.26
28	0.36	0.96	2.18	0.33	0.34	0.96	0.91	0.39
29	0.54	1.16	0.71	0.91	5.36*>	0.59	0.51	6.79*>
30	0.66	1.14	0.95	0.85	0.44	0.61	0.78	0.42
31	0.70	1.11	0.57	0.44	0.55	0.68	0.98	0.81
32	1.49	1.15	0.44	6.76*>	0.45	0.55	3.69*	0.37

PROB. FALSE ALARM (TYPE I ERROR) 240 SAMPLES (112 ISOLATED)

ALPHA: .40 .30 .20 .10 .05 .01 .0010 .00010 .000010 .0000010
 ISO.FA: 0.41 0.28 0.21 0.11 0.08 0.02 0.0000 0.00000 0.000000 0.0000000
 TOT.FA: 0.24 0.15 0.10 0.05 0.04 0.01 0.0000 0.00000 0.000000 0.0000000

PROB. DETECTION (POWER OF TEST) 16 SAMPLES

PR(D): 1.00 1.00 1.00 1.00 1.00 1.00 0.99 0.95 0.85 0.71
 FR(D): 1.00 1.00 1.00 1.00 1.00 1.00 1.00 0.94 0.75 0.62

Fig. 4.1—Simulation of Ad Hoc Test: Results of One Run, White Noise

The relative frequency of false alarm for these is shown in the row labeled "ISO.FA:", and the total relative frequency of false alarm for all 240 is shown in the row labeled "TOT.FA:". "PR(D):" and "FR(D):" refer to the probability and relative frequency of detection, respectively, both at the levels indicated by the label "ALPHA:" above for the 16 cells for which $H_1(m,n)$ is true.

Fig. 4.2 is a portion of the printout of 100 similar runs in succession. Here, to avoid excessive data printing, the run number, coordinates and \mathcal{F} value are printed for only those (m,n) for which $\mathcal{F}(m,n)$ indicates rejection at $\alpha = 10^{-5}$, with the symbol ">" indicating rejection at $\alpha = 10^{-6}$ as well. $H_1(m,n)$ is indicated by $*m,n$. All the entries shown in the figure indicate correct detection, most at the level $\alpha = 10^{-6}$.

Theoretical probabilities and observed relative frequencies are again tabulated at the bottom of the figure, with the same notation as in Fig. 4.1. There are now 24000 samples for which H_0 is true, with 11200 of them isolated, and 1600 samples for which H_1 is true. The results show good agreement with the theory.

Some results of simulation with non-white noise are shown in Figs. 4.3 and 4.4. The noise spectral density was

$$f(\kappa, \omega) = 1 + \cos\left(\kappa + \frac{\pi}{4}\right) \cos(2\omega)/4.$$

Six signal components with the same signal to noise ratio as before (-18.05 dB) were added, two each in regions of low ($f = 0.75$), medium ($f = 1.0$) and high ($f = 1.25$) noise spectral density. There are indicated by the symbols "#", "*" and "↑", respectively. The respective noncentrality parameters are 85.33, 64 and 51.2. Fig. 4.3 is a computer printout of a single run, and Fig. 4.4 is a portion of the printout of 100 successive runs. The notation is that of Figs. 4.1 and 4.2, except that the probabilities and relative frequencies of detection are listed separately for signals in each of the three types of noise regions. The agreement is satisfactory.

AD HOC TEST
SPECTRAL DENSITY = 1.0

SIMULATED ARRAY= 8 X 64 WITH 8 REPS/RUN , (8 X 32 COMPLEX VARIATES)
INIT. N: 1751 11922 1752 11922 P: 1753 11922 1754 11922

16 SIGNAL COMPONENTS: S/N=0.01566 (-18.05 DB)

[(M,N,F): F(M,N)>F(.00001;16,128)]

RUN	M, N: F	M, N: F					
1	*5, 5 4.34>	*3, 9 6.54>	*3, 12 6.67>	*6, 14 4.94>	*3, 16 6.05>		
1	*7, 18 4.54>	*3, 19 5.75>	*7, 22 6.38>	*2, 23 5.62>	*1, 26 4.29		
1	*4, 26 8.76>	*5, 29 5.41>	*8, 29 6.54>	*4, 32 6.72>	*7, 32 5.99>		
2	*5, 5 4.27	*3, 9 6.51>	*6, 9 5.24>	*3, 12 5.50>	*6, 14 5.75>		
2	*7, 18 6.20>	*3, 19 4.63>	*7, 22 4.27	*2, 23 7.48>	*1, 26 5.63>		
2	*4, 26 5.80>	*8, 29 5.71>	*7, 32 7.84>				
3	*5, 5 8.94>	*3, 9 5.70>	*3, 12 4.35>	*6, 14 5.13>	*3, 16 5.00>		
3	*7, 18 5.47>	*3, 19 6.70>	*7, 22 5.69>	*2, 23 4.38>	*1, 26 4.92>		
3	*4, 26 6.10>	*5, 29 6.84>	*4, 32 6.41>				
4	*5, 5 5.56>	*3, 9 4.82>	*6, 9 5.25>	*3, 12 6.86>	*6, 14 5.51>		
4	*3, 16 6.26>	*7, 18 5.58>	*3, 19 4.16	*7, 22 4.10	*2, 23 4.33>		
4	*1, 26 6.90>	*8, 29 5.68>	*4, 32 6.13>	*7, 32 5.56>			
5	*5, 5 6.16>	*3, 9 4.64>	*6, 9 4.69>	*6, 14 5.44>	*3, 16 4.42>		
5	*3, 19 5.23>	*7, 22 5.65>	*2, 23 5.08>	*1, 26 5.30>	*4, 26 5.15>		
5	*5, 29 7.71>	*8, 29 5.39>	*7, 32 4.86>				
6	*5, 5 6.11>	*3, 9 4.85>	*6, 9 5.17>	*3, 12			
						*1, 26 7.23>	
98	*4, 26 4.04	*5, 29 4.85>	*8, 29 4.33>	*4, 32 4.04	*7, 32 7.54>		
99	*5, 5 4.41>	*3, 9 5.27>	*6, 9 6.14>	*3, 12 6.87>	*6, 14 5.45>		
99	*3, 16 3.82	*7, 18 6.78>	*3, 19 4.23	*7, 22 5.10>	*2, 23 5.13>		
99	*1, 26 4.68>	*4, 26 4.40>	*5, 29 6.85>	*8, 29 5.18>	*4, 32 5.53>		
99	*7, 32 5.90>						
100	*5, 5 5.40>	*3, 9 6.09>	*3, 12 5.10>	*7, 18 6.54>	*3, 19 5.40>		
100	*7, 22 7.10>	*2, 23 6.64>	*1, 26 4.61>	*5, 29 4.56>	*8, 29 5.95>		
100	*4, 32 6.62>						

PROB. FALSE ALARM (TYPE I ERROR) 24000 SAMPLES (11200 ISOLATED)

ALPHA: .40 .30 .20 .10 .05 .01 .0010 .00010 .000010 .0000010
ISO.FA: 0.40 0.30 0.20 0.10 0.05 0.01 0.0003 0.00000 0.000000 0.0000000
TOT.FA: 0.23 0.16 0.10 0.05 0.02 0.00 0.0001 0.00000 0.000000 0.0000000

PROB. DETECTION (POWER OF TEST) 1600 SAMPLES

PR(D): 1.00 1.00 1.00 1.00 1.00 1.00 0.99 0.95 0.85 0.71
FR(D): 1.00 1.00 1.00 1.00 1.00 1.00 0.99 0.93 0.84 0.72

Fig. 4.2—Simulation of Ad Hoc Test: Summary of 100 Runs, White Noise

AD HOC TEST
SPECTRAL DENSITY = $F(K,W)=1+.25*\text{COS}(K+PI/4)*\text{COS}(2W)$

SIMULATED ARRAY= 8 X 64 WITH 8 REPS/RUN , (8 X 32 COMPLEX VARIATES)
INIT. N: 12559 13034 12559 13034 P: 12561 13034 12561 13034

6 SIGNAL COMPONENTS: S/N=0.01566 (-18.05 DB)

N\M	F(M,N)							
	1	2	3	4	5	6	7	8
1	1.79	0.74	0.87	0.69	0.60	0.43	0.54	0.40
2	0.81	0.61	0.95	1.45	0.82	1.45	1.17	1.50
3	1.13	0.94	1.15	1.34	0.97	1.16	1.22	1.00
4	0.64	0.40	1.24	0.76	0.32	0.59	1.25	0.92
5	1.25	0.92	1.44	0.46	6.76*>	0.44	1.47	1.18
6	1.16	0.85	1.69	0.47	0.55	0.33	0.93	0.69
7	1.08	0.78	1.47	1.05	1.45	1.45	0.74	0.86
8	1.39	0.62	0.85	0.75	0.54	0.96	1.24	0.93
9	0.90	0.88	1.83	0.74	2.03	0.33	0.85	1.02
10	0.90	0.89	1.04	0.67	1.28	0.58	1.30	1.09
11	1.50	1.59	1.16	1.74	0.63	0.77	0.65	0.71
12	0.45	0.55	0.48	0.90	0.37	6.03*>	0.77	0.46
13	1.86	1.34	0.72	1.50	0.51	0.65	0.52	1.11
14	0.62	1.34	0.62	1.08	1.10	0.89	1.06	1.64
15	0.97	0.66	0.89	0.52	1.10	1.26	1.05	0.79
16	1.21	0.45	5.21#>	0.61	1.56	0.77	0.99	0.76
17	0.69	0.41	0.56	0.47	0.59	0.77	1.11	1.54
18	1.20	2.12	0.64	1.19	0.70	1.46	1.12	0.80
19	0.70	1.45	0.61	0.77	1.28	1.80	0.93	0.59
20	1.07	0.43	0.92	1.40	1.30	0.40	0.62	1.24
21	1.30	1.26	0.99	1.00	0.75	1.53	1.08	1.00
22	0.71	0.88	1.14	1.01	0.82	0.66	1.17	0.93
23	1.08	0.74	0.81	0.71	0.83	0.78	0.69	0.40
24	1.69	0.60	3.03†	1.25	0.84	0.99	4.77#>	0.85
25	0.78	0.83	0.92	0.96	0.95	0.43	0.61	0.50
26	0.72	1.21	0.95	0.61	1.22	1.12	1.00	0.87
27	0.69	1.36	0.73	0.96	1.23	1.06	0.92	1.34
28	0.89	1.13	1.40	0.75	0.92	0.72	1.95	0.83
29	0.60	0.79	1.80	0.77	0.72	0.69	0.45	0.97
30	1.85	0.42	1.09	0.68	1.13	1.71	0.96	1.30
31	1.02	1.00	1.01	0.81	1.22	0.48	0.67	0.94
32	0.94	0.48	0.98	0.96	1.59	0.63	5.30†>	0.66

PROB. FALSE ALARM (TYPE I ERROR) 250 SAMPLES (202 ISOLATED)

ALPHA: .40 .30 .20 .10 .05 .01 .0010 .00010 .000010 .0000010
ISO.FA: 0.42 0.31 0.19 0.09 0.05 0.00 0.00000 0.000000 0.0000000 0.00000000
TOT.FA: 0.34 0.25 0.16 0.08 0.04 0.00 0.00000 0.000000 0.0000000 0.00000000

PROB. DETECTION (POWER OF TEST) 2 SAMPLES EACH

PR(D#): 1.00 1.00 1.00 1.00 1.00 1.00 1.00 1.00 0.98 0.94
FR(D#): 1.00 1.00 1.00 1.00 1.00 1.00 1.00 1.00 1.00 1.00
PR(D*): 1.00 1.00 1.00 1.00 1.00 1.00 0.99 0.95 0.85 0.71
FR(D*): 1.00 1.00 1.00 1.00 1.00 1.00 1.00 1.00 1.00 1.00
PR(D†): 1.00 1.00 1.00 1.00 1.00 0.99 0.94 0.82 0.64 0.44
FR(D†): 1.00 1.00 1.00 1.00 1.00 1.00 1.00 0.50 0.50 0.50

Fig. 4.3—Simulation of Ad Hoc Test: Results of One Run, Nonwhite Noise

AD HOC TEST
SPECTRAL DENSITY = $F(K,W)=1+.25*\text{COS}(K+\text{PI}/4)*\text{COS}(2W)$

SIMULATED ARRAY= 8 X 64 WITH 8 REPS/RUN , (8 X 32 COMPLEX VARIATES)
INIT. N: 4259 13973 4259 13973 P: 4261 13973 4262 13973

6 SIGNAL COMPONENTS: S/N=0.01566 (-18.05 DB)

[(M,N,F): F(M,N)>F(.00001;16,128)]

RUN	M, N:	F								
1	*5, 5	7.82>	*6, 12	3.88	#3, 16	7.10>	#7, 24	5.63>		
2	*5, 5	4.87>	*6, 12	3.94	#3, 16	4.89>	†3, 24	3.97	#7, 24	4.39>
2	†7, 32	3.97								
3	*5, 5	4.97>	*6, 12	4.22	#3, 16	4.48>	†3, 24	4.63>	#7, 24	7.75>
3	†7, 32	4.14								
4	*5, 5	3.88	*6, 12	5.86>	#3, 16	6.27>	†3, 24	5.22>	#7, 24	8.36>
4	†7, 32	4.60>								
5	*5, 5	8.42>	*6, 12	4.26	#3, 16	4.92>	†3, 24	4.78>	#7, 24	6.08>
6	#3, 16	4.95>	#7, 24	6.80>	†7, 32	5.69>				
7	*5, 5	5.95>	*6, 12	4.29	†3, 24	3.93	#7, 24	7.26>		
8	*5, 5	4.17	*6, 12	4.37>	#3, 16	5.79>	†3, 24	5.96>	#7, 24	4.98>
9	*6, 12	4.00	#3, 16	6.63>	†3, 24	8.20>	#7, 24	5.75>		
10	*5, 5	5.24>	*6, 12	4.90>	#3, 16	5.49>	†3, 24	4.41>	#7, 24	5.26>
10	†7, 32	4.98>								
				5.59>	#7, 24	5.93>				
94	*6, 12	5.96>	#3, 16	5.58>	†3, 24	4.35>	#7, 24	8.19>	†7, 32	4.84>
95	*5, 5	6.29>	*6, 12	5.25>	#3, 16	4.60>	#7, 24	4.55>	†7, 32	4.02
96	*6, 12	4.04	#3, 16	5.96>	†3, 24	5.85>	#7, 24	7.04>	†7, 32	5.19>
97	*6, 12	4.76>	#3, 16	4.36>	†3, 24	5.29>	#7, 24	6.45>	†7, 32	3.90
98	*5, 5	7.14>	*6, 12	4.91>	#3, 16	4.02	†3, 24	6.81>	#7, 24	5.61>
98	†7, 32	5.93>								
99	*5, 5	6.32>	*6, 12	6.05>	#3, 16	6.05>	†3, 24	5.63>	#7, 24	5.82>
100	*5, 5	4.13	*6, 12	5.68>	#3, 16	4.12	†7, 32	5.31>		

PROB. FALSE ALARM (TYPE I ERROR) 25000 SAMPLES (20200 ISOLATED)

ALPHA: .40 .30 .20 .10 .05 .01 .0010 .00010 .000010 .0000010
ISO.FA: 0.40 0.30 0.20 0.10 0.05 0.01 0.0009 0.00010 0.000000 0.0000000
TOT.FA: 0.34 0.25 0.17 0.08 0.04 0.01 0.0008 0.00008 0.000000 0.0000000

PROB. DETECTION (POWER OF TEST) 200 SAMPLES EACH

PR(D#):	1.00	1.00	1.00	1.00	1.00	1.00	1.00	1.00	0.98	0.94
FR(D#):	1.00	1.00	1.00	1.00	1.00	1.00	1.00	1.00	0.97	0.85
PR(D*):	1.00	1.00	1.00	1.00	1.00	1.00	0.99	0.95	0.85	0.71
FR(D*):	1.00	1.00	1.00	1.00	1.00	1.00	0.99	0.98	0.88	0.72
PR(D†):	1.00	1.00	1.00	1.00	1.00	0.99	0.94	0.82	0.64	0.44
FR(D†):	1.00	1.00	1.00	1.00	1.00	1.00	0.97	0.88	0.75	0.57

Fig. 4.4—Simulation of Ad Hoc Test: Summary of 100 Runs, Nonwhite Noise

5. ANALYSIS OF VARIANCE AND METHODS OF MULTIPLE COMPARISON

The model represented by (3.1),

$$y_r(x, t) = s(x, t) + n_r(x, t) , \quad (5.1)$$

$x = 0, 1, \dots, M - 1; t = 0, 1, \dots, N - 1; r = 1, \dots, R$, is a special case of a two-dimensional extension of a general linear model considered by Shumway [36]

$$y_r(x, t) = \sum_{j=1}^J \sum_{u=-\infty}^{\infty} \sum_{v=-\infty}^{\infty} X_{rj}(x-u, t-v) \beta_j(u, v) + n_r(x, t) . \quad (5.2)$$

Here $\{X_{rj}(x, t), r = 1, \dots, R, j = 1, \dots, J\}$ is an $R \times J$ matrix function of fixed space and time invariant observables and $\{\beta_j(x, t), j = 1, \dots, J\}$ is a $J \times 1$ vector of regression functions. In the present application, the regression functions are the signals (3.9)

$$s_j(x, t) = A_j \cos (\kappa_j x + \omega_j t - \phi_j) . \quad (5.3)$$

As in previous chapters, the error series $n_r(x, t)$ is assumed to be a realization of a two-dimensional zero mean wide-sense stationary noise process.

The transformed observations are given by (3.12):

$$Y_r(m, n) = B(m, n) + \epsilon_r(m, n) \quad (5.4)$$

when $(m, n) \in Q$, where $B(m, n) = \sqrt{MN} A_j e^{-i\phi_j/2}$ when $m = k_j$ and $n = f_j$ for some $j \in \{1, \dots, J\}$, and is zero otherwise. Since the variance of $\epsilon_r(m, n)$ is $f(\kappa_m, \omega_n) + O(M^{-1}) + O(N^{-1})$ as has been shown in Chapter 2, if $f(\kappa_m, \omega_n)$ is constant ("white noise") and if the signals are common to all R realizations, then the assumptions underlying the analysis of variance (Scheffé [33], p. 55, p. 106) are asymptotically satisfied by the real and imaginary parts of (5.4).

5.1 The One-Way Layout, Common Signal Case

As in previous chapters, we consider the transformed array relabeled to yield $M'N'$ asymptotically independent complex variables, and again drop the primes. Consider first the case $\phi_j = 0, j = 1, \dots, J$, and for $r = 1, \dots, R$, let

$$\mathbf{U}_r = (Y_{rR}(1,1), \dots, Y_{rR}(1,N), Y_{rR}(2,1), \dots, Y_{rR}(2,N), \dots, Y_{rR}(M,1), \dots, Y_{rR}(M,N))', \quad (5.5)$$

$$\boldsymbol{\beta} = (B(1,1), \dots, B(1,N), B(2,1), \dots, B(2,N), \dots, B(M,1), \dots, B(M,N))', \quad (5.6)$$

and

$$\mathbf{e}_r = (\epsilon_{rR}(1,1), \dots, \epsilon_{rR}(1,N), \epsilon_{rR}(2,1), \dots, \epsilon_{rR}(2,N), \dots, \epsilon_{rR}(M,1), \dots, \epsilon_{rR}(M,N))'. \quad (5.7)$$

Then for each r the $M \times N$ matrix of observations $\{Y_{rR}(m,n), m = 1, \dots, M, n = 1, \dots, N\}$ has been "strung out" into a $MN \times 1$ (column) vector \mathbf{U}_r . Letting $\mathbf{U}' = (\mathbf{U}'_1, \dots, \mathbf{U}'_R)$ and $\mathbf{e}' = (\mathbf{e}'_1, \dots, \mathbf{e}'_R)$ we have

$$\mathbf{U} = \mathbf{X}\boldsymbol{\beta}' + \mathbf{e},$$

with \mathbf{X} given below.

The problem is now in the form considered by Scheffé [33], Chapter 3, with the $MN \times MNR$ matrix

$$\mathbf{X} = \begin{pmatrix} 1 & 1 & \cdots & 1 & 0 & 0 & \cdots & 0 & 0 & 0 & \cdots & 0 & 0 & 0 & \cdots & 0 \\ 0 & 0 & \cdots & 0 & 1 & 1 & \cdots & 1 & 0 & 0 & \cdots & 0 & 0 & 0 & \cdots & 0 \\ & & & \vdots & & & & \vdots & & & & \cdots & & & & \vdots \\ & & & \vdots & & & & \vdots & & & & \cdots & & & & \vdots \\ 0 & 0 & \cdots & 0 & 0 & 0 & \cdots & 0 & 1 & 1 & \cdots & 1 & & & & & \end{pmatrix}$$

of rank MN , so that all parametric functions are estimable (Scheffé [33], p. 56). The test statistic

$$\mathcal{F} = \frac{\frac{SS_H}{(MN-1)}}{\frac{SS_e}{MN(R-1)}}, \quad (5.8)$$

has the central F distribution with $MN - 1$ and $MN(R - 1)$ degrees of freedom under the null hypothesis, where

$$SS_H = R \sum_{m=1}^M \sum_{n=1}^N [Y_{\cdot R}(m,n) - \bar{Y}_R]^2 ,$$

$$\bar{Y}_R = \frac{1}{MN} \sum_{m=1}^M \sum_{n=1}^N Y_{\cdot R}(m,n) ,$$

and

$$SS_e = \sum_{m=1}^M \sum_{n=1}^N \sum_{r=1}^R [Y_{rR}(m,n) - Y_{\cdot R}(m,n)]^2 .$$

Here the dot replacing a subscript has the usual meaning of average. Let

$$B_{..} = \frac{1}{MN} \sum_{m=1}^M \sum_{n=1}^N B(m,n)$$

Under the alternate hypothesis, \mathcal{F} has the noncentral F distribution with noncentrality parameter δ given by

$$\sigma^2 \delta^2 = R \sum_{m=1}^M \sum_{n=1}^N [B(m,n) - B_{..}]^2 ,$$

where $\sigma^2 = f(\kappa_m, \omega_n)/2$. As in (3.9), we consider J signal components. Let

$$B(m,n) = B \sum_{j=1}^J \delta_{mk_j} \delta_{nf_j} , \quad (5.9)$$

where k_j and f_j are the coordinates of the signal components. Then

$$B_{..} = \frac{B}{MN} \sum_{m=1}^M \sum_{n=1}^N \sum_{j=1}^J \delta_{mkj} \delta_{nfj} = \frac{BJ}{MN},$$

so that

$$\begin{aligned} \sigma^2 \delta^2 &= R \sum_{m=1}^M \sum_{n=1}^N \left[B \sum_{j=1}^J \delta_{mkj} \delta_{nfj} - \frac{BJ}{MN} \right]^2 \\ &= \frac{RJB^2(MN - J)}{MN}. \end{aligned} \quad (5.10)$$

Computer simulation has met with excellent agreement and some results will be shown later. Since the theory is well established (cf. Scheffé [33], *ibid.*) this simulation serves merely as a check of the simulation procedure itself and the F -distribution calculations. The only unusual features are the degrees of freedom. As in previous chapters, an 8×32 array with 8 observations per cell was used. This results in $MN - 1 = 255$ and $MN(R - 1) = 1792$ degrees of freedom. To calculate the upper alpha points, F_{ν_1, ν_2} was approximated by

$$Z = \frac{1}{2} \ln F_{\nu_1, \nu_2} \sim N(\mu_1, \mu_2), \quad (5.11)$$

where $\mu_1 = (\nu_2^{-1} - \nu_1^{-1})/2$ and $\mu_2 = (\nu_1^{-1} + \nu_2^{-1})/2$. (cf. Kendall and Stuart [21], p. 379). The noncentral $F'_{\nu_1, \nu_2; \delta}$ was approximated by

$$F'_{\nu_1, \nu_2; \delta} \approx c\nu_1^{-1} \tilde{\nu}_1 F_{\tilde{\nu}_1, \nu_2}, \quad (5.12)$$

where $c\tilde{\nu}_1 = \nu_1 + \delta^2$ and $c^2\tilde{\nu}_1 = \nu_1 + 2\delta^2$ (Scheffé [33], p. 414).

5.2 Robustness of the F -Test

With the same considerations as in section 3.4, we have from (3.21) for signals with unknown epochs

$$Y_r(m, n) = S_r(m, n) + \epsilon_r(m, n) \quad (5.13)$$

when $(m, n) \in Q$, where $S_r(m, n) = B(m, n)e^{i\beta_r(m, n)}$ as in (4.3). Let

$$U_r(m,n) = |Y_r(m,n)|^2, \quad (5.14)$$

and let

$$\begin{aligned} Z_r(m,n) &= \frac{1}{2\pi} \int_0^{2\pi} U_r(m,n) d\beta_r \\ &= \frac{1}{2\pi} \int_0^{2\pi} \{ |S_r(m,n)|^2 + 2\Re[S_r(m,n)\epsilon_r^*(m,n)] + |\epsilon_r(m,n)|^2 \} d\beta_r \\ &= |B(m,n)|^2 + |\epsilon_r(m,n)|^2, \end{aligned} \quad (5.15)$$

with the dependence on β_r vanishing as in section 4.1.

Let $\mu(m,n) = |B(m,n)|^2$ (which is zero unless $m = k_j$ and $n = f_j$ for some $j \in \{1, \dots, J\}$) and let

$$\nu_r(m,n) = |\epsilon_r(m,n)|^2 \quad (5.16)$$

Then (5.15) becomes

$$Z_r(m,n) = \mu(m,n) + \nu_r(m,n), \quad (5.17)$$

which has the same form as (5.4). Now, however, $2\nu_r(m,n)/f(\kappa_m, \omega_n)$ is asymptotically distributed as a chi-square variable with two degrees of freedom, by Theorem 2.2.

There have been many investigations of the effect of non-normality on the type I error of the F -test, and some on the effect on the power of the test. See Scheffé [33], Chapter 10, Srivastava [39], Donaldson [7], and the recent paper by Tiku [40] and the references contained therein. In the present case, robustness of the test to type I errors is illustrated in Fig. 5.1 which shows both sides of the empirical distributions resulting from 1000 replications of a simulation of (5.4) (normal population) and (5.17) (chi-square population) under the null hypothesis. Each replication simulated an 8×32 array with 8 observations per cell. A chi-square test and a Kolmogorov-Smirnov test of these empirical distributions both show that neither of them differs significantly from the central F distribution with 255 and 1792 degrees of freedom. The computed chi-square values with 19 degrees of freedom are indicated by “ $X \uparrow 2(19)$ ”; $\sqrt{1000}$ times the computed Kolmogorov-Smirnov values are indicated by “ $K - S \times 31.62$.”

ONE-WAY ANALYSIS OF VARIANCE
SPECTRAL DENSITY=2.0

255, 1792 DF PN INI1.= 303.4300 1000 RUNS

N(0,1) POPULATION, H0 TRUE

AV. Y...= .001660 , AV. MSE= 1.000129

ALPHA:	0.50	0.40	0.30	0.20	0.10	0.05	.025	0.01	.001	E-4
NO.>F:	.50	.39	.31	.20	.10	.05	.02	.01	0.	0.
NO.<F:	.49	.39	.29	.20	.11	.06	.03	.01	.00	.00

X²(19)= 21.4000 K-S X 31.62= .47

CHI-SQUARE (2) POPULATION, H0 TRUE

AV. Y...= 2.001504 , AV. MSE= 3.995411

ALPHA:	0.50	0.40	0.30	0.20	0.10	0.05	.025	0.01	.001	E-4
NO.>F:	.50	.40	.31	.20	.09	.05	.02	.01	.00	0.
NO.<F:	.50	.38	.29	.19	.11	.05	.02	.01	.00	0.

X²(19)= 21.0800 K-S X 31.62= .54

Fig. 5.1--Empirical Distribution of the Test Statistic with Normal and Chi-square Populations

Monte Carlo methods were also employed to determine the power of the test of the model represented by (5.17). Again, an 8×32 array with 8 observations per cell was simulated, with 100 replications per point. One signal component was included, and its signal to noise ratio (3.13) was varied. Some results are shown in Fig. 5.2, where power is plotted as a function of signal to noise ratio, S/N . The solid curves are computed for the normal distribution using (5.12). The + sign indicates simulation of (5.4) with a normal population, while the ---x---x curve is the result of simulation of (5.17), with $\nu_r(m, n)$ distributed as $f(\kappa_m, \omega_n)/2$ times a chi-square variable with two degrees of freedom, with $f(\kappa_m, \omega_n) \equiv 1$. These results imply that as the level of the test is decreased, the power of the test with a chi-square population does not decrease as rapidly as that with a normal population. At very low test levels the power of the test using (5.17) is greater than that using (5.4) at all signal to noise ratios.

The integration indicated in (5.15) disposes of the cross-product term and the dependence on $r = 1, \dots, R$. Since such integration cannot be carried out in practice, the test was also simulated for $U_r(m, n)$, given by (5.14). The results, indicated by ---o---o in Fig. 5.2, generally fall between the other two curves. The cross-product term, with its dependence on r , acts as additional noise and decreases the power slightly when the signal to noise ratio is high. For very weak signals and low test levels, the power may be increased slightly.

As a check on the computation, a case similar to those studied by Donaldson [7] was considered. Donaldson used Monte Carlo techniques to compute the power of the F -test with normal, exponential, and lognormal populations. All of his distributions had a mean of 10 and a variance of 100 under the null hypothesis. Since this is not possible with $N(0, f/2)$ and $(f/2)\chi_2^2$ populations, I can only qualitatively match his results under the conditions of this section. One thousand replications of a simulated 2×2 array with 4 observations per cell were taken for each point, with $f(\kappa_m, \omega_n) \equiv 200$. The resulting curves, shown in Fig. 5.3a are similar to the curves of Donaldson's Fig. 2. Here power is plotted against ϕ , where

$$\phi = \left[R \sum_{j=1}^I \frac{(\mu_j - \mu)^2}{I\sigma_e^2} \right]^{1/2} \quad (5.18)$$

is used by Donaldson to indicate the degree of inequality between means. In (5.18), $I=MN$, μ is the grand mean of all cell populations, μ_j is the mean of the j th population and σ_e^2 is the population variance, estimated by $SS_e/[I(R-1)]$. The difference between Fig. 5.3a and Donaldson's Fig. 2 can be attributed to the differences in these parameters. The same data are plotted in Fig. 5.3b as a function of signal to noise ratio in decibels, rather than the empirical parameter ϕ . The relative positions of the two curves in the region of strong signals is reversed, with the resemblance to Fig. 5.2 obvious.

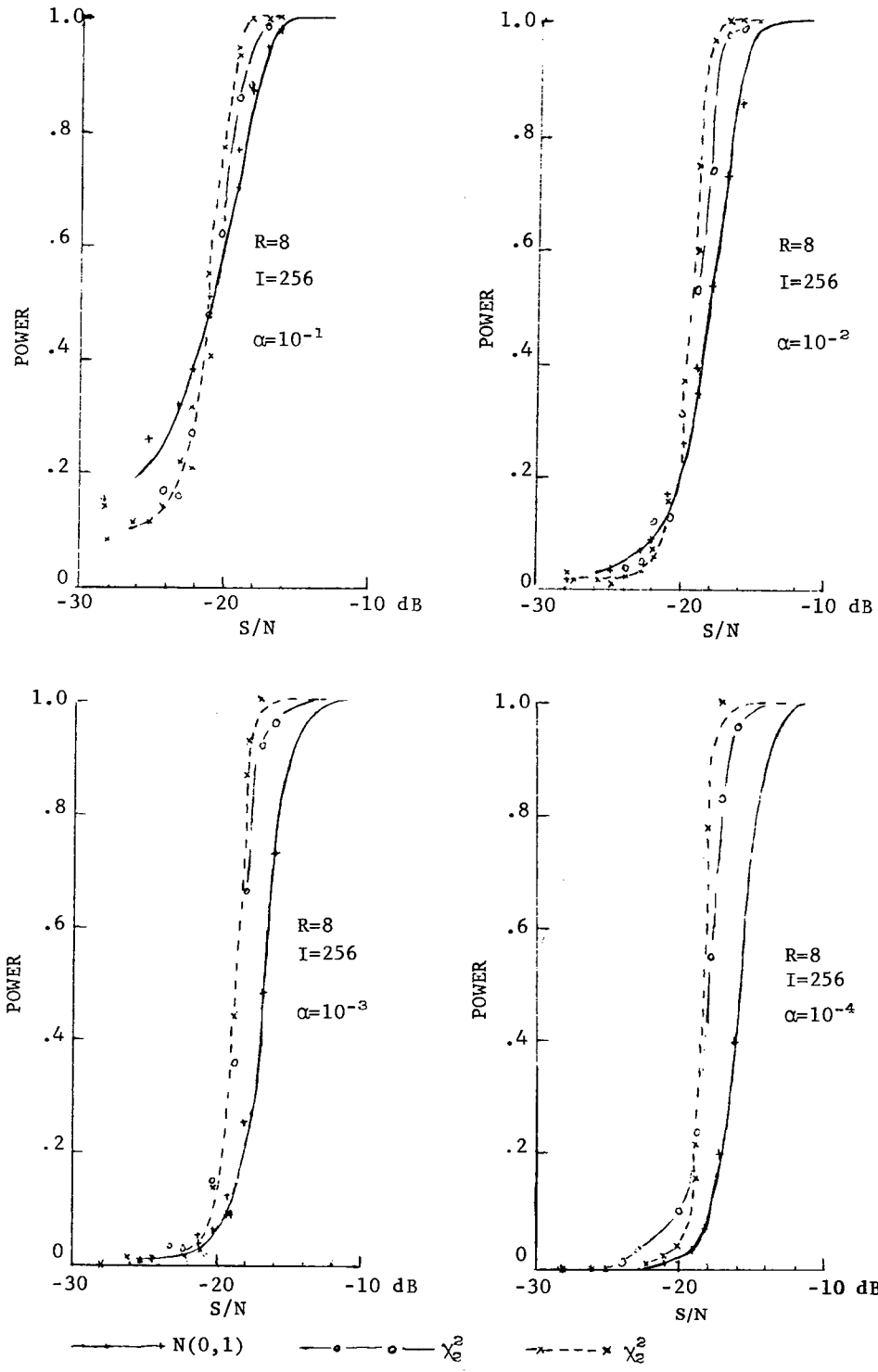
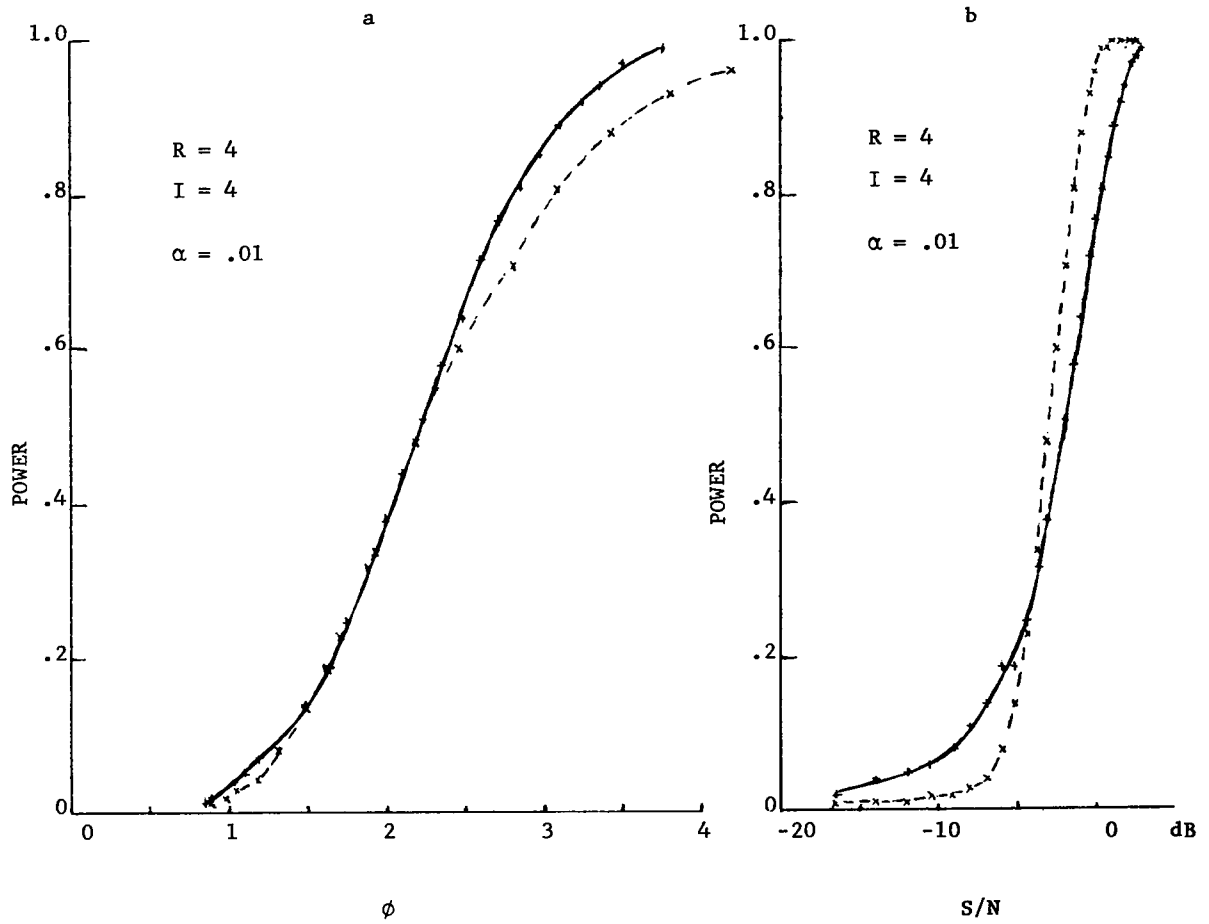


Fig. 5.2—Power Curves

Fig. 5.3—Power Curves for the case $M=N=2$, $R=4$

Non-constant spectral density ("nonwhite noise") means unequal cell variances. Scheffé [33], p. 343 shows that the type I errors will be increased. Moderate robustness to unequal variances with normal populations is indicated by Figs. 5.4 and 5.5. As in Fig. 5.1, these figures show the empirical distributions resulting from 1000 replications of a simulation of an 8×32 array with 8 observations per cell of (5.4)(normal population) and of (5.17) (chi-square population) under the null hypothesis. In Fig. 5.4, $f(\kappa, \omega) = 1 + .025 \cos(\kappa + \pi/4) \cos(2\omega)$. Both the chi-square and Kolmogorov-Smirnov tests indicate that neither of the empirical distributions differs significantly from the central F distribution with 255 and 1792 degrees of freedom. In Fig. 5.5, $f(\kappa, \omega) = 1 + .1 \cos(\kappa + \pi/4) \cos(2\omega)$. Here the empirical distribution with a normal population remains indistinguishable from the central F distribution. Both the chi-square and the Kolmogorov-Smirnov tests show, however, that the differences between the empirical distribution from a chi-square population with unequal variances and the central F distribution are highly significant. The differences appear to be mainly at large values of alpha. Further simulation, not shown, indicates that the test with normal populations is insensitive to unequal variances at least to the extent caused by the spectral density given by (3.15) and used again in Chapter 4, namely $f(\kappa, \omega) = 1 + .25 \cos(\kappa + \pi/4) \cos(2\omega)$.

5.3 Multiple Comparisons

As with any application of analysis of variance, rejection of the null hypothesis can be followed by tests of multiple comparisons to determine the statistical significance of the sources of variation revealed by the data. See Scheffé [34,33], p. 68, Gabriel [10], and their references. Specifically, determination of the subgroup of cells in the wavenumber-frequency space contributing to rejection of the null hypothesis is equivalent to detection of the corresponding signal components. We consider estimable functions of cell means

$$\Psi = \sum_{m=0}^{M-1} \sum_{n=0}^{N-1} c(m,n)B(m,n) \quad (5.19)$$

and, in particular, contrasts, where

$$\sum_{m=0}^{M-1} \sum_{n=0}^{N-1} c(m,n) = 0 \quad (5.20)$$

The function Ψ is estimated by

ONE-WAY ANALYSIS OF VARIANCE
 SPECTRAL DENSITY=1.00[1+.025 COS(K+PI/4) COS(2W)]

255, 1792 DF PN INIT.= 324.5172 1000 RUNS

N(0,1) POPULATION, H0 TRUE

AV. Y...= .000227 , AV. MSE= .499630

ALPHA:	0.50	0.40	0.30	0.20	0.10	0.05	.025	0.01	.001	E-4
NO.>F:	.50	.41	.31	.21	.10	.05	.03	.01	.00	0.
NO.<F:	.50	.41	.30	.23	.10	.05	.03	.01	0.	0.

X²(19)= 21.2000

K-S X 31.62= .85

CHI-SQUARE (2) POPULATION, H0 TRUE

AV. Y...= 1.000689 , AV. MSE= 1.001621

ALPHA:	0.50	0.40	0.30	0.20	0.10	0.05	.025	0.01	.001	E-4
NO.>F:	.53	.43	.34	.22	.11	.05	.02	.01	.00	0.
NO.<F:	.47	.39	.29	.19	.10	.05	.02	.01	.00	0.

X²(19)= 15.3200

K-S X 31.62= .92

Fig. 5.4—Empirical Distribution of the Test Statistic with Normal and Chi-square Populations, Nonwhite Noise

ONE-WAY ANALYSIS OF VARIANCE
 SPECTRAL DENSITY=1.00[1+.1 COS(K+PI/4) COS(2W)]

255, 1792 DF PN INIT.= 408.5172 1000 RUNS

N(0,1) POPULATION, H0 TRUE

AV. Y...= .000059 , AV. MSE= .500905

ALPHA:	0.50	0.40	0.30	0.20	0.10	0.05	.025	0.01	.001	E-4
NO.>F:	.50	.41	.32	.21	.11	.05	.03	.02	.00	0.
NO.<F:	.50	.41	.31	.21	.11	.06	.03	.01	.00	0.

X²(19)= 8.7200 K-S X 31.62= .32

CHI-SQUARE (2) POPULATION, H0 TRUE

AV. Y...= 1.001109 , AV. MSE= 1.003052

ALPHA:	0.50	0.40	0.30	0.20	0.10	0.05	.025	0.01	.001	E-4
NO.>F:	.59	.49	.37	.24	.14	.07	.03	.01	.00	0.
NO.<F:	.41	.30	.22	.14	.07	.03	.01	.00	.00	0.

X²(19)= 59.8000 K-S X 31.62= 3.13

Fig. 5.5—Empirical Distribution of the Test Statistic with Normal and Chi-square Populations, Nonwhite Noise

$$\hat{\Psi} = \sum_{m=0}^{M-1} \sum_{n=0}^{N-1} c(m,n)Y.(m,n) \quad (5.21)$$

in the case of signals common to all realizations, and by

$$\hat{\Psi} = \sum_{m=0}^{M-1} \sum_{n=0}^{N-1} c(m,n)U.(m,n) \quad (5.22)$$

when the signal epoch varies with realization, where $U_r(m,n)$ is given by (5.14). In the first case, the variance of $\hat{\Psi}$ is given by

$$\begin{aligned} V = \text{var}(\hat{\Psi}) &= \sum_{m=0}^{M-1} \sum_{n=0}^{N-1} c^2(m,n) \text{var}[Y.(m,n)] \\ &= \frac{fC}{R}, \end{aligned} \quad (5.23)$$

where

$$C = \sum_{m=0}^{M-1} \sum_{n=0}^{N-1} c^2(m,n),$$

and is estimated by $\hat{V} = s^2 C/R$, where $s^2 = MS_e$. Following Scheffé [33], we say that $\hat{\Psi}$ is significantly different from zero if and only if $|\hat{\Psi}|^2 > S^2 \hat{V}$, where $S^2 = (MN-1)F_{\alpha; MN-1, MN(R-1)}$

Multiple comparisons were simulated along with the analysis of variance for both the normal population ($Y_r(m,n)$) and the chi-square population ($U_r(m,n)$). The sum of all cell means which exceeded a preset "threshold" was considered as an estimable function. Contrasts were formed between all cell means which exceeded (the same) preset threshold and all other cell means. It was found possible with a signal to noise ratio of 0.015 (-18 dB) to set the threshold so that it was exceeded by few if any means of cells in which the null hypothesis was true. Some results will be shown in Table 6.1, where the power of various tests will be compared. The power depends, of course, on the number of signal components as well as the signal to noise ratio of each component. The power is very low for a single (-18 dB)

signal component, but can be unity at test levels down to $\alpha = 10^{-6}$ if the number of signal components is large.

For the normal population, little difference at all test levels was found between the power of the test using this estimable function and that using this contrast. For the chi-square population (treated as if it were normal) the test of this estimable function was more powerful at all test levels than that of this contrast.

5.4 *The Two-Way Layout*

Since the models under consideration result in a two-dimensional array of data, it seems natural to consider analysis of variance of a two-way layout. Here, however, a significant row effect ("wavenumber effect") or column effect ("frequency effect") has a physically meaningful interpretation only under certain unusual circumstances. It may happen that the hypothesis of no interactions is rejected, but the hypotheses of no main effects are accepted. In this case we conclude that there must be differences in the main effects, but that the data are insufficient to reveal these differences when the effect of the levels of one factor are averaged over the levels of the other. (Scheffé [33], p. 94.) A significant interaction may be interpreted as detection of a two-dimensional plane wave with wavenumber and frequency components corresponding to those responsible for the interaction.

The power of the interaction test of the two-way layout has also been calculated and the test simulated. Some results will be presented in Table 6.1, where they may be compared with those of the one-way layout and with other tests. In general the one-way layout produces a slightly more powerful test both for the normal and the chi-square populations. In all of the two-way layout results shown in the table there was not more than one signal component in each row and in each column. With more than one component in a row or column, the power of the interaction test decreases. Thus the one-way layout is clearly preferable.

6. SUMMARY AND CONCLUSIONS

Several techniques for testing hypotheses concerning multidimensional stationary stochastic processes have been developed. These were applied to the two-dimensional discrete finite Fourier transforms of space-time series. The justification for this is the asymptotic normality and independence of the transformed variables.

It was shown that the correlation between the real and imaginary parts of a transformed $M \times N$ space-time series is $O(M^{-1}) \cdot O(N^{-1})$, and that the variance of each is equal to $(1/2)f(\kappa, \omega) + O(M^{-1}) + O(N^{-1})$, where $f(\kappa, \omega)$ is the spectral density. The limiting joint distribution of a collection of transformed variables was shown to be that of mutually independent normally distributed random variables. It follows that the joint distribution of a collection of periodograms, defined as the squared modulus of the transformed variables, tends to that of mutually independent chi-square variates.

In addition to transforming a multivariate problem in the space-time domain into a univariate problem in the wavenumber-frequency domain, the discrete finite Fourier transform also concentrates the information for discrimination between hypotheses for a class of processes of considerable practical interest.

When the space-time series under consideration consists of two-dimensional signal functions imbedded in and common to all realizations of a stationary noise process, a likelihood ratio test can be applied in the transformed domain. If the signal model includes an unknown epoch or phase which varies from realization to realization, no true replications are possible, and the test must be modified. If one is willing to pay the price of increased computation and increased errors of both kinds, the modified test has reasonable power at acceptably low test levels. However, an ad hoc test is at least as powerful at all test levels and is considerably more powerful at very low levels.

The ad hoc test is based on the asymptotic distribution of averaged two-dimensional periodograms. The test statistic is "Studentized" by use of data from neighboring cells to eliminate the unknown spectral density. Thus it requires that the signal components be isolated from each other in wavenumber and in frequency, a case which occurs sufficiently often to be of interest.

Analysis of variance has been applied to the two-dimensional wavenumber-frequency variables, both as a one-way layout and as a two-way layout. Since the row and column effects of the

two-way layout have meaningful physical interpretations only under unusual circumstances, the one-way layout seems a priori to be preferable. It is in fact at least slightly more powerful than the test for interactions in the two-way layout in all cases considered, and clearly more powerful when there are many signal components in a single row or column.

Unlike the ad hoc test which considers each cell separately, the power of the analysis of variance test depends upon the relative number of signal components in the wavenumber-frequency matrix. With more than two components, the power of the analysis of variance test of the entire array exceeds that of the ad hoc test for each component. As with any application of analysis of variance, rejection of the null hypothesis can be followed by multiple comparisons to determine the source of the rejection.

An estimable function consisting of the sum of all cell means which exceed a preset "threshold" was found to produce a test slightly more powerful than that yielded by contrasting all such cell means with all other cell means. With the test conditions used in the simulation, it was found possible to set the threshold so that it was seldom exceeded by cell means for which the null hypothesis was valid.

When signals have varying epochs or phases, the two-dimensional periodogram is independent of this unknown parameter. Analysis of variance and multiple comparisons have been applied to the periodogram in this case. The tests were found to be robust to errors of both kinds with this non-normal (i.e., chi-square) population.

Table 6.1 shows a comparison of the power of some of the tests considered. In it, all simulated tests were of an 8×32 wavenumber-frequency array with 8 observations per cell. This represents an approximately 8×64 array of space-time observations. All signal components had a signal to noise ratio of 0.0156 or -18 dB, and the noise spectral density was identically unity. There were 2300 samples in each simulation of the first two tests, 1600 in the third, and 100 in each of the others. The same pseudo-random sequence was used to simulate tests 1-3, and the same sequence was used for corresponding items in tests 4-11.

The analysis of variance tests with normal populations were found to be reasonably robust to non-constant spectral density (unequal cell variances). With chi-square populations, only a very modest inequality in variances could be tolerated with acceptable type I errors.

For many signal components, each common to all realizations, the analysis of variance and multiple comparison tests seem to be preferable. When the signal component epochs or phases vary with realization the ad hoc test is better since it is more robust to non-constant spectral density. It requires the signal components to be isolated from each other, however, while analysis of variance does not.

Tests for the situation when these assumptions are not valid, in particular for non-stationary processes, remain for future work.

TABLE 6.1—Continued

$\alpha :$.5	.4	.3	.2	.10	.05	.01	10^3	10^4	10^5	10^{-6}
5. Two-Way Layout, Interaction Test											
1 signal component ^c	Pr: .99	.98	.96	.92	.82	.71	.45	.18	.06	.02	.005
	Fr: .97	.95	.93	.90	.84	.78	.53	.25	.11	.05	--
2 signal components ^c	Pr: 1.0	1.0	1.0	1.0	1.00	.99	.96	.83	.62	.39	.19
	Fr: 1.0	1.0	1.0	1.0	.99	.98	.95	.78	.56	.36	--
3 signal components ^c	Pr: 1.0	1.0	1.0	1.0	1.0	1.0	1.0	1.00	.98	.92	.81
	Fr: 1.0	1.0	1.0	1.0	1.0	1.0	1.0	.99	.98	.93	--
4 signal components ^c	Pr: 1.0	1.0	1.0	1.0	1.0	1.0	1.0	1.0	1.00	1.00	.99
	Fr: 1.0	1.0	1.0	1.0	1.0	1.0	1.0	1.0	1.00	.98	--
III. ANOVA, chi-square ^f											
6. One-Way Layout											
1 signal component ^c	Fr: .99	.98	.98	.98	.95	.93	.84	.70	.58	.44	.37
2 signal components ^c	Fr: 1.00	1.00	1.00	1.00	1.00	.99	.98	.96	.94	.93	.86
3 signal components ^c	Fr: 1.00	1.00	1.00	1.00	1.00	1.00	1.00	1.00	1.00	1.00	1.00
4 signal components ^c	Fr: 1.00	1.00	1.00	1.00	1.00	1.00	1.00	1.00	1.00	1.00	1.00

TABLE 6.1—Continued

$\alpha :$.5	.4	.3	.2	.10	.05	.01	10^{-3}	10^{-4}	10^{-5}	10^{-6}
7. Two-Way Layout, Interaction Test											
1 signal component ^c	Fr: 1.0	.98	.98	.98	.95	.91	.78	.69	.54	.40	.33
2 signal components ^c	Fr: 1.0	1.00	1.00	1.00	.99	.98	.97	.93	.93	.86	.78
3 signal components ^c	Fr: 1.0	1.00	1.00	1.00	1.00	1.00	1.00	1.00	1.00	1.00	1.00
4 signal components ^c	Fr: 1.0	1.00	1.00	1.00	1.00	1.00	1.00	1.00	1.00	1.00	1.00
IV. MULTIPLE COMPARISONS, $N(0, \sigma^2)$											
8. Contrast ^g											
4 signal components ^c	Fr: .49	.44	.37	.29	.18	.13	.04	.01	0	0	--
9. Estimable function ^h											
4 signal components ^c	Fr: .54	.46	.42	.34	.25	.14	.05	.01	0	0	--

TABLE 6.1—Continued

		α :	.5	.4	.3	.2	.10	.05	.01	10^{-3}	10^{-4}	10^{-5}	10^{-6}
V. MULTIPLE COMPARISONS, chi-square ^h													
10. Contrast ^g													
4 signal components ^c	Fr:	.74	.74	.72	.72	.72	.68	.67	.58	.54	.51	.48	.43
11. Estimable function ^h													
4 signal components ^c	Fr:	.83	.83	.83	.83	.80	.80	.80	.78	.78	.77	.75	.73

Notes:

- a. Tests of an 8 X 32 wavenumber-frequency array with 8 observations per cell. "Pr" and "Fr" indicate theoretical probabilities and empirical relative frequencies, respectively.
- b. Likelihood ratio with signals common to stationary noise processes.
- c. All signal components had a signal to noise ratio of 0.0156 or -18.05 dB, with $f(k, \omega) \equiv 1$.
- d. Modified likelihood ratio test for signals with unknown epochs.
- e. Ad hoc test for signals with unknown epochs.
- f. Simulated χ_2^2 variates were used under H_0 . Under H_1 the squared modulus of normal noise plus signal was used.
- g. All cell means which exceeded a preset "threshold" were contrasted with all other cell means.
- h. The sum of all cell means which exceeded a preset "threshold" was the estimable function of cell means.

GLOSSARY

Absolutely Continuous Function: A real-valued function f defined on $[a, b]$ is absolutely continuous on $[a, b]$ if, given $\epsilon > 0$, there is a $\delta > 0$ such that

$$\sum_{i=1}^n |f(x'_i) - f(x_i)| < \epsilon$$

for every finite collection $\{(x_i, x'_i)\}$ of nonoverlapping intervals with

$$\sum_{i=1}^n |x'_i - x_i| < \delta .$$

Epoch: Phase relative to an origin. See phase.

First Mean Value Theorem for Integrals: If $f(x)$ is continuous on $[a, b]$, then

$$\int_a^b f(x) dx = f(c)(b - a) ,$$

where $a < c < b$.

Frequency: A measure of the rate of repetition of a periodic function, equal to the reciprocal of the period.

Mean Value Theorem: If $f(x)$ is continuous on $[a, b]$ and differentiable on (a, b) , then $f(b) - f(a) = (b - a)f'(c)$, for some c between a and b .

Mean Value Theorem for a Function of Two Variables: If $f(x, y)$ is continuous and has continuous first partial derivatives for $x \in [a, b]$ and $y \in [c, d]$, then there exists ξ and η such that $f(b, d) - f(a, c) = (b - a)f_x(\xi, \eta) + (d - c)f_y(\xi, \eta)$ where f_x and f_y denote the partial derivatives of f with respect to x and y respectively, and $\xi \in (a, b)$, $\eta \in (c, d)$.

Noise: Error process, an undesired stochastic process.

Order Symbols O , o , \sim : $f(x) = O(g(x))$ if $f(x)/g(x)$ remains bounded as x tends to its limit. If $f(x)/g(x)$ tends to zero, then $f(x) = o(g(x))$, while if $f(x)/g(x)$ tends to unity, then $f(x) \sim g(x)$.

Phase: The angle $\kappa x + \omega t + \phi$ in a plane wave $s(x,t) = a \cos(\kappa x + \omega t + \phi)$. The epoch, initial phase, phase constant, or phase relative to an origin is ϕ , often called simply the phase.

Plane Wave: A wave in which the disturbance is constant over all points of a plane perpendicular to the direction of propagation.

Second Mean Value Theorem for Integrals: If $f(x)$ and $g(x)$ are both integrable on (a,b) and $f(x)$ is always of the same sign, then

$$\int_a^b f(x)g(x)dx = K \int_a^b f(x)dx ,$$

where $\inf g(x) \leq K \leq \sup g(x)$.

Signal: A function of space and/or time potentially conveying information.

Wave: A disturbance propagating as a function of space and time.

Wavenumber: A measure of the rate of (spatial) repetition of a spatially periodic function, equal to the reciprocal of the wavelength.

White Noise: An error process with constant spectral density.

REFERENCES

1. Anderson, T.W., *An Introduction to Multivariate Statistical Analysis*, Wiley, New York, 1958.
2. Anderson, T.W., *The Statistical Analysis of Time Series*, Wiley, New York, 1971.
3. Blackman, R.B. and Tukey, J.W., *The Measurement of Power Spectra*, Dover, New York, 1958.
4. Box, G.E.P. and Muller, M.E., *A Note on the Generation of Random Normal Deviates*, *Ann. Math. Statist.*, 29, 610-11, 1958.
5. Chernoff, H., *Large-Sample Theory: Parametric Case*, *Ann. Math. Statist.*, 27, 1-22, 1956.
6. Cramér, H. and Leadbetter, M.R., *Stationary and Related Stochastic Processes*, Wiley, New York, 1967.
7. Donaldson, T.S., *Robustness of the F-Test to Errors of Both Kinds and the Correlation between the Numerator and Denominator of the F-Ratio*, *J. Amer. Statist. Assoc.*, 63, 660-76, 1968.
8. Doob, J.L., *Stochastic Processes*, Wiley, New York, 1953.
9. Fejér, L., *Lebesguesche Konstanten und divergente Fourierreihen*, *J. reine angew. Math.*, 138, 22-53, 1910.
10. Gabriel, K.R., *Simultaneous Test Procedures—Some Theory of Multiple Comparisons*, *Ann. Math. Statist.*, 40, 224-50, 1969.
11. Goodman, N.R., *Statistical Analysis Based on a Certain Multivariate Complex Gaussian Distribution (An Introduction)*, *Ann. Math. Statist.*, 34, 152-77, 1963.
12. Gradshteyn, I.S. and Ryzhik, I.M., *Table of Integrals, Series, and Products*, Academic Press, New York, 1965.
13. Grenander, U. and Rosenblatt, M., *Statistical Analysis of Stationary Time Series*, Wiley, New York, 1957.

14. Hannan, E. J., *Time Series Analysis*, Methuen, London, 1960.
15. Hannan, E.J., *Multiple Time Series*, Wiley, New York, 1970.
16. Helstrom, C.W., *Statistical Theory of Signal Detection*, 2nd Edition, Pergamon Press, Oxford, 1968.
17. Hinich, M.J. and Shaman, P., *Parameter Estimation for an R-Dimensional Plane Wave Observed with Additive Independent Gaussian Errors*, Ann. Math. Statist., 43, 153-69, 1972.
18. Hoch, P., *Asymptotically Optimum Joint Estimation and Detection of Stochastic Signals in Noise*, unpublished D.Sc. Dissertation, The George Washington University, 1972.
19. Jenkins, G.M., *General Considerations in the Analysis of Spectra*, Technometrics, 3, 133-66, 1961.
20. Jenkins, G.M. and Watts, D.G., *Spectral Analysis and its Applications*, Holden-Day, San Francisco, 1968.
21. Kendall, M.G. and Stuart, A., *The Advanced Theory of Statistics*, Vol. 1, Griffin, London, 1963.
22. Kullback, S., *Information Theory and Statistics*, Dover, New York, 1968.
23. Kullback, S., *Topics in Statistical Information Theory*, unpublished typescript, The George Washington University, 1971.
24. Liggett, W.S., Jr., *On the Asymptotic Optimality of Spectral Analysis for Testing Hypotheses about Time Series*, Ann. Math. Statist., 42, 1348-58, 1971.
25. Loève, M., *Probability Theory*, Van Nostrand, New York, 1963.
26. Olshen, R.A., *Asymptotic Properties of the Periodogram of a Discrete Stationary Process*, J. Appl. Prob., 4, 508-28, 1967.
27. Pagano, M., *Some Asymptotic Properties of a Two-Dimensional Periodogram*, Tech. Rept. No. 146, Johns Hopkins U., 1970.
28. Parzen, E., *Mathematical Considerations in the Estimation of Spectra*, Technometrics, 3, 167-90, 1961.
29. Rayleigh, Baron (J.W. Strutt), *On the Resultant of a Large Number of Vibrations of the Same Pitch and of Arbitrary Phase*, Phil. Mag., X, 73-78, 1880. Reprinted in *Scientific Papers*, Vol. 1, 1869-1881, Cambridge, 1899.
30. Rosenblatt, M., *Random Processes*, Oxford, New York, 1962.

31. Royden, H.L., *Real Analysis*, Macmillan, New York, 1968.
32. Saikia, A., *Asymptotic Methods for Estimating the Mean of N Stationary Time Series*, unpublished Ph.D. Dissertation, The George Washington University, 1971.
33. Scheffé, H., *The Analysis of Variance*, Wiley, New York, 1959.
34. Scheffé, H., *Multiple Testing versus Multiple Estimation. Improper Confidence Sets. Estimation of Directions and Ratios*, Ann. Math. Statist., 41, 1-29, 1970.
35. Selin, I., *Detection Theory*, Princeton, N.J., 1965.
36. Shumway, R.H., *Applied Regression and Analysis of Variance for Stationary Time Series*, J. Amer. Statist. Assoc., 65, 1527-46, 1970.
37. Shumway, R.H., *On Detecting a Signal in N Stationarily Correlated Noise Series*, Technometrics, 13, 499-519, 1971.
38. Shumway, R.H. and Saikia, A., *An Empirical Bayes Approach to Stochastic Signal Estimation*, in press.
39. Srivastava, A.B.L., *Effect of Non-Normality on the Power of the Analysis of Variance Test*, Biometrika, 46, 114-22, 1959.
40. Tiku, M.L., *Power Function of the F-Test under Non-Normal Situations*, J. Amer. Statist. Assoc., 66, 913-16, 1971.
41. Tolstov, G.P., *Fourier Series*, Prentice-Hall, Englewood Cliffs, N.J., 1962.
42. Wahba, G., *On the Distribution of Some Statistics Useful in the Analysis of Jointly Stationary Time Series*, Ann. Math. Statist., 39, 1849-62, 1968.
43. Wainstein, L.A. and Zubakov, V.D., *Extraction of Signals from Noise*, Prentice-Hall, Englewood Cliffs, N.J., 1962.
44. Walker, A.M., *Some Asymptotic Results for the Periodogram of a Stationary Time Series*, J. Austral. Math. Soc., 5, 107-28, 512, 1965.
45. Walker, A.M., *On the estimation of a harmonic component in a time series with stationary independent residuals*, Biometrika, 58, 21-36, 1971.
46. Whittaker, E.T. and Watson, G.N., *A Course of Modern Analysis*, Macmillan, New York, 1944.
47. Wilks, S.S., *Mathematical Statistics*, Wiley, New York, 1962.

48. Yaglom, A.M., *An Introduction to the Theory of Stationary Random Functions*, Prentice-Hall, Englewood Cliffs, N.J., 1962.
49. Zygmund, A., *Trigonometric Series*, Vol. I, Cambridge, 1968.

DOCUMENT CONTROL DATA - R & D

(Security classification of title, body of abstract and indexing annotation must be entered when the overall report is classified)

1. ORIGINATING ACTIVITY (Corporate author) Naval Research Laboratory Washington, D.C. 20390		2a. REPORT SECURITY CLASSIFICATION Unclassified	
		2b. GROUP	
3. REPORT TITLE SOME APPROACHES TO TESTING HYPOTHESES FOR MULTIDIMENSIONAL STATIONARY STOCHASTIC PROCESSES			
4. DESCRIPTIVE NOTES (Type of report and inclusive dates) Interim report on a continuing problem.			
5. AUTHOR(S) (First name, middle initial, last name) David A. Swick			
6. REPORT DATE October 2, 1972		7a. TOTAL NO. OF PAGES 104	7b. NO. OF REFS 49
8a. CONTRACT OR GRANT NO. NRL Problem 81S02-35		9a. ORIGINATOR'S REPORT NUMBER(S) NRL Report 7466	
b. PROJECT NO. Project RF 52-552-403-6079		9b. OTHER REPORT NO(S) (Any other numbers that may be assigned this report)	
c.			
d.			
10. DISTRIBUTION STATEMENT Approved for public release; distribution unlimited.			
11. SUPPLEMENTARY NOTES		12. SPONSORING MILITARY ACTIVITY Office of Naval Research Department of the Navy Arlington, Virginia 22217	
13. ABSTRACT <p>The discrete finite Fourier transform of a multidimensional stationary stochastic process transforms a multivariate problem into an asymptotically univariate one. For a one- or two-dimensional process it is shown that, under stated conditions, the correlation between the real and imaginary parts of the transformed variables is</p> $\prod_{j=1}^n 0(T_j^{-1}),$ <p>and that the variance of each is equal to</p> $\frac{1}{2}f(\kappa, \omega) + \sum_{j=1}^n 0(T_j^{-1}),$ <p>where $f(\kappa, \omega)$ is the spectral density, T_j is the number of observations in the j^{th} dimension, and $n = 1$ or 2. The limiting joint distribution of a collection of two-dimensional periodograms, defined as the squared modulus of the transformed variables, is shown to be that of mutually independent chi-square variates. The discrete finite Fourier transform also concentrates the information for discrimination between hypotheses for a class of processes of interest.</p> <p>Several techniques for testing hypotheses concerning multidimensional stationary stochastic processes were developed. These were applied to the detection of two-dimensional plane-wave signals imbedded in a collection of independent identically distributed noise processes.</p> <p style="text-align: right;">(Continued) —</p>			

UNCLASSIFIED

14. KEY WORDS	LINK A		LINK B		LINK C	
	ROLE	WT	ROLE	WT	ROLE	WT
Discrete finite Fourier transform Multidimensional stationary stochastic processes Two-dimensional plane-wave signals Signal detection Hypothesis testing Analysis of variance						

When the signals are common to all realizations, a likelihood ratio test can be applied in the transformed domain. If the signal model includes an unknown epoch or phase which varies from realization to realization, no true replications are possible, and the test must be modified. The modified test has reasonable power at acceptably low test levels. However an ad hoc test, based on the asymptotic distribution of averaged two-dimensional periodograms, is shown to be more powerful than the likelihood ratio test under the conditions considered. It requires, however, that the signal components be isolated from each other in wavenumber and in frequency, since it utilizes data from neighboring cells to eliminate the unknown spectral density.

Analysis of variance and methods of multiple comparison have also been applied in the transformed domain. With the model of signals with unknown phase differences, the analysis is applied to the periodograms. The test is found to be robust to the resulting non-normal (i.e., chi-square) population, at least when the spectral density is constant. Non-constant spectral density results in unequal cell variances. In this case, the test with a chi-square population is robust only to very moderate inequality of cell variances; the test with a normal population is considerably more robust. When there are many signal components, analysis of variance and multiple comparison tests are more powerful than the ad hoc test. The latter, which considers each component independently, is less sensitive to non-constant spectral density.

The results of computer simulation of the various tests considered are presented, as is a table comparing their power at test levels α , with $0.5 \geq \alpha \geq 10^{-6}$.